

MEASUREMENT OF DEVELOPMENT LENGTH OF 0.5 INCH AND
0.6 INCH DIAMETER PRESTRESSING STRAND IN
FULLY BONDED CONCRETE BEAMS

by

Bruce A. Lutz, B.S.

THESIS

Presented to the Faculty of the Graduate School of
The University of Texas at Austin
in Partial Fulfillment
of the Requirements
for the Degree of

MASTER OF SCIENCE IN ENGINEERING

THE UNIVERSITY OF TEXAS AT AUSTIN

MAY 1991

TABLE OF CONTENTS

Chapter		Page
1	INTRODUCTION.....	1
	1.1 Background and Definition of Problem.....	1
	1.2 Objective of Research Program.....	4
	1.3 Scope and Objective of Thesis.....	5
	1.4 Thesis Organization.....	6
2	LITERATURE REVIEW	7
	2.1 Burdette and Deatherage.....	8
	2.2 Cousins, Johnston, and Zia.....	10
	2.3 Florida Department of Transportation.....	12
	2.4 Future Readings.....	13
3	TEST PROGRAM	14
	3.1 Specimen Design and Designation.....	14
	3.2 Material Properties.....	16
	3.2.1 Pretensioning Steel.....	16
	3.2.2 Concrete Properties.....	17
	3.3 Specimen Fabrication.....	19
	3.3.1 Pretensioning Setup.....	19
	3.3.2 Pretensioning Instrumentation.....	19
	3.3.3 Pretensioning Procedure.....	23

LIST OF TABLES

Table	Page
3.1 Specimen Numbering Scheme.....	16
3.2 Concrete Mix Design.....	18
3.3 General Test Dimensions.....	45
4.1 Summary of Development Length Test Results....	50
4.2 Summary of Flexural Failures.....	54
4.3 Summary of Bond/Shear Failures.....	54
5.1 Comparison of Development Length Results.....	77

LIST OF FIGURES

Figure	Page
3.1 Specimen Cross Section Detail.....	15
3.2 Pretensioning/Casting Bay (Figure).....	20
3.3 Pretensioning/Casting Bay (Photograph).....	21
3.4 Pretensioning Anchorage (Jacking End).....	24
3.5 Pretensioning Anchorage (Holding End).....	25
3.6 Sequence of Prestress Transfer (Figure).....	31
3.7 Test Setup (Photograph).....	33
3.8 Loading Frame (Photograph).....	35
3.9 Specimen Support (Photograph).....	37
3.10 End Slip Instrumentation (Figure).....	39
3.11 End Slip Instrumentation (Photograph).....	40
3.12 DEMEC Gage Points (Photograph).....	42
3.13 Typical Test Setup (Figure).....	44
3.14 Specimen Support Arrangement for Test A and Test B (Figure).....	47
3.15 Data Acquisition System (Photograph).....	48
4.1 Plot of 0.5 inch specimen Results - Type of Failure vs. Embedment Length.....	52
4.2 Plot of 0.6 inch specimen Results - Type of Failure vs. Embedment Length.....	52
4.3 Load vs. Deflection for FA460-5A.....	56
4.4 Load vs. Extreme Fiber Compressive Strain for FA460-5A.....	56

CHAPTER ONE

INTRODUCTION

1.1 Background and Definition of Problem

Development of prestressed concrete started in France around 1928, by E. Freyssinet, who used high-strength steel wires for prestressing. However, it was E. Hoyer of Germany who first used two buttresses several hundred feet apart to anchor the stretched wires. Hoyer then cast several concrete units, and cut the wires after the concrete had hardened. The application of prestressing was not practical until methods for tensioning and anchoring became more economical and high strength materials became available to overcome the prestress losses over time. In 1939, Freyssinet developed the conical wedges and a special jacking system that tensioned and then thrust male cones into the female cones for anchorage. This method used a frictional

wedging action which is, in principle, similar to the current use of "reusable chuck [10]."

The full acceptance of prestressed concrete occurred in the 1950's, with the development of the high-strength seven-wire strand. The seven-wire strand offered better bonding and higher strength than the high-strength wires previously used. Since there was a global shortage of steel after World War II, the high strength seven-wire strand also proved more economical. The 1/4 to 3/8 inch diameter seven-wire strand became an industry standard [10].

As in most other industries, economics dictated the growth and evolution of prestressed concrete. From an economic view point, using fewer strands to achieve the same prestressing force was advantageous. To use fewer strands, either larger diameter or higher strength strands are required. Since the ultimate strength of the strands was already 250 ksi, the obvious solution was to increase the diameter and ultimate strength. Therefore, the 3/8 inch standard diameter developed into the 7/16 inch diameter and finally into the 1/2 inch diameter, which is the current standard.

Recent advances in high strength concrete, above 10,000 psi, have required another increase in strand size to 0.6 inch diameter. The increase in strand size is needed, since the higher strength concrete can utilize more $\frac{1}{2}$ inch strands. However, since there is only a given amount of space to put the strands in a member, fewer strands of increased diameter are required. The 0.6 inch strand has approximately 40 percent more area than the $\frac{1}{2}$ inch strand.

As with any new material advance, research is required to determine the behavioral characteristics. However, as previously mentioned, economics dictates industry changes, and the use of 0.6 inch diameter strand began before any comprehensive research was conducted. Due to the lack of data supporting the behavior of 0.6 inch strand, the Federal Highway Administration (FHWA) issued a memorandum on October 26, 1988 disallowing the use of 0.6 inch prestressing strand. This memorandum is the single most important factor which influenced the start of the present research program.

1.2 Objective of Research Program

The project undertaken at The University of Texas at Austin, entitled "Debonding of Strands in Pretensioned Prestressed Concrete Beams," was performed in five phases. The research was intended to study the possible use of debonded strands instead of draped strands. The overall project was modified to include the determination of the transfer lengths and development lengths for $\frac{1}{2}$ inch and 0.6 inch diameter strand. The transfer length is defined as the distance from the end of a member for a strand to transfer the prestressing force into the concrete. The development length consists of the transfer length plus the flexural bond length. Flexural bond is the length of bonded strand required to attain a compression failure in the concrete member in flexure, without breaking the strand.

The initial phase was a study of bonded and debonded single strand specimens to investigate transfer length. A study of multistrand transfer length specimens followed as the second phase. Both phases of transfer length research included $\frac{1}{2}$ and 0.6 inch diameter strand in concentric rectangular specimens. The third phase considered the development length of fully bonded

multistrand beams. The fourth and fifth phases investigated the development length of debonded beams under static and fatigue loading, respectively. The development length test specimens were non-standard 'I' sections. All debonded beams contained $\frac{1}{2}$ inch strand.

1.3 Scope and Objective of Thesis

This thesis concludes the third phase of the research program, an investigation of the development length of fully bonded 0.5 and 0.6 inch diameter prestressing strand. The scope of the test series included four beams with 0.5 inch strand and five beams with 0.6 inch strand. Each beam provided an independent test at each end, resulting in a total of nineteen (19) tests (one beam was tested three times). In each test, data on end slip, deflection, and extreme fiber compressive concrete strain were obtained. The development length was then obtained from the results of all nineteen tests.

The objective of this thesis is to provide a better understanding of the flexural behavior in the end regions of prestressed beams under flexural loading and to determine the development length of $\frac{1}{2}$ and 0.6 inch

strand. The $\frac{1}{2}$ inch strand can be thought of as a control group, in that the data can be used to verify the current code provisions. The focus of the research was to help establish behavioral guidelines for using 0.6 inch prestressing strand in common applications. Furthermore, the results and conclusions drawn from the development length tests can further be used for recommendations for possible revisions to the current building code, for the two strand sizes.

1.4 Thesis Organization

The thesis is divided into six chapters. The body of the thesis starts in Chapter Two with a review of previous literature on topics relevant to the research. Chapter Three provides a detailed overview of the specimen design, material properties, specimen fabrication, test setup, instrumentation, and test procedure. The results and discussion are presented in Chapter Four. Chapter Five contains a comparison to past research and current code provisions. The summary and conclusions are presented in Chapter Six.

CHAPTER TWO

LITERATURE REVIEW

The majority of the past research and relevant literature on transfer and development length is from the 1950's and early 60's. The research started with the introduction of the seven-wire strand. However, transfer length, not development length, was the focus of most of the previous research. Furthermore, the strand properties have changed considerably over the last 30 years. The current industry standard for pretensioning strand is the 270 ksi low-relaxation strand, and the earlier studies used 250 ksi stress-relieved strand. There is also very little data on the 0.6 inch strand which has only been available for the last few years. Due to these considerations, there are not many articles available to review.

A detailed review of transfer and development length literature was included in the theses by Raheel Malik

(11) and Ozgür Unay (15). Recently, three studies undertaken after the FHWA memorandum was issued have completed their research. The remainder of this chapter considers these studies, which were not discussed in the prior theses.

2.1 Burdette and Deatherage

The objective of the research conducted by Burdette and Deatherage (2), at The University of Tennessee, was the investigation of transfer and development lengths for pretensioned concrete beams. The study also investigated the lateral spacing requirements of the pretensioned strand. A total of 20 AASHTO Type-I beams were used for the study. The specimens were simple beams tested to give results at both ends. The research included several different strand diameters ($\frac{1}{2}$ inch, $\frac{1}{2}$ inch special, $\frac{9}{16}$ inch, and 0.6 inch), two different lateral spacings (2 inches and 1.75 inches), and different strand surface conditions (mill and weathered). Six concrete prisms with a single concentric strand were also constructed to measure the transfer length. The transfer of prestress was accomplished by flame cutting the strands.

The measured transfer length was approximately 42.75 inches ($85.5d_b$) and 42.25 inches ($70.4d_b$) for the $\frac{1}{2}$ inch and 0.6 inch diameter strand, respectively. The results from this study indicate that the transfer length is longer than current AASHTO or ACI codes predict. This is true for all but the 1.75 inch laterally spaced specimens.

Where 1.75 inches was used for the center to center spacing of the strand, the measured transfer lengths were shorter than the code equation predicts. The lower transfer length for the 1.75 inch lateral spacing is due to the surface condition of the strand. All of the specimens with the 1.75 inch spacing contained strand which was weathered for three (3) days, thereby improving the bond characteristics of the strand.

The development length results demonstrate that the required embedment length is approximately the same as AASHTO/ACI calculations predict. The measured development length was approximately 1.1 times the current code provisions. This data is substantiated by the results found in the current research program at The University of Texas at Austin. The discussion of development length results was not as thorough as the

portion on transfer length, since a more detailed analysis of the development length data is yet to be completed.

2.2 Cousins, Johnston, and Zia

The focus of the recent study by Cousins, Johnston, and Zia (4) was the use of epoxy-coated pretensioning strand to prevent corrosion. The research was conducted at North Carolina State University, and investigated both transfer and development lengths. The series consisted of 35 rectangular, single strand specimens. Each specimen contained one of three different levels of grit on the epoxy surface, to investigate the effect of the epoxy coating on the development length. Uncoated strands were also used as a control group. The three sizes of pretensioning strand used were $3/8$ inch, $1/2$ inch, and 0.6 inch diameter.

The results of the study indicate that the required embedment length is lower for the grit impregnated epoxy-coated strand than for the uncoated strand. The reduction is due to the improved bond the grit creates, compared to the smooth surface of the uncoated strand. The medium and high levels of grit produced a development

length substantially below that obtained using AASHTO/ACI calculations. The low level of grit demonstrated a development length equal to the AASHTO prediction.

Test data reported by Cousins et al. indicate that uncoated strand required 1.9 and 1.7 times the development length predicted by the AASHTO/ACI equation for 0.5 and 0.6 inch diameter strand, respectively. However, flexural failure was never achieved for the specimens containing $\frac{1}{2}$ inch uncoated strand, and only one specimen containing 0.6 inch uncoated strand failed in flexure. The cause for the reported development lengths exceeding the current code provisions may be linked to the size and limited number of the specimens. Since the specimens were rectangular and relatively small, the behavior of a full sized bridge girder may not be accurately represented.

The specimens tested at North Carolina State University also contained only one strand. Current research at The University of Texas at Austin indicates that the use of multiple strands in test specimens may reduce the transfer length (and hence the development length). The multiple strand specimens also showed

significantly less scatter than the single strand specimens.

Since the low level of grit produced behavior similar to uncoated strand, the use of epoxy coatings may be beneficial, other than for corrosion protection. The longer transfer and development lengths reported in Reference (4) for uncoated strand played a major role in the FHWA decision to place a moratorium on the use of the 0.6 inch strand, even though the focus of the test program was epoxy coated strand.

2.3 Florida Department of Transportation

The research program at the Florida Department of Transportation investigated the shear and bond behavior of AASHTO Type-II girders. Both transfer and development lengths were studied. The research parameters included variations in shear reinforcement, strand size, steel confinement, and strand shielding (debonding).

Although the report is not yet complete, the preliminary results have been presented. The data indicates that the transfer length is 30 inches for $\frac{1}{2}$ inch strand, and 45-60 inches for 0.6 inch strand. The

transfer length for the 0.6 inch strand still requires testing to reduce the scatter in the data.

The test results on the development length are more definitive. The preliminary results indicate that the required development length is 1.68 times the length predicted by AASHTO/ACI for both $\frac{1}{2}$ inch and 0.6 inch strand. Until the report is available, the actual cause of the increased development length is unknown.

2.4 Future Readings

Although the research is not yet complete for the project of which this report is a part of, it should be noted that similar studies on the transfer and development length are currently underway at The University of Texas at Austin.

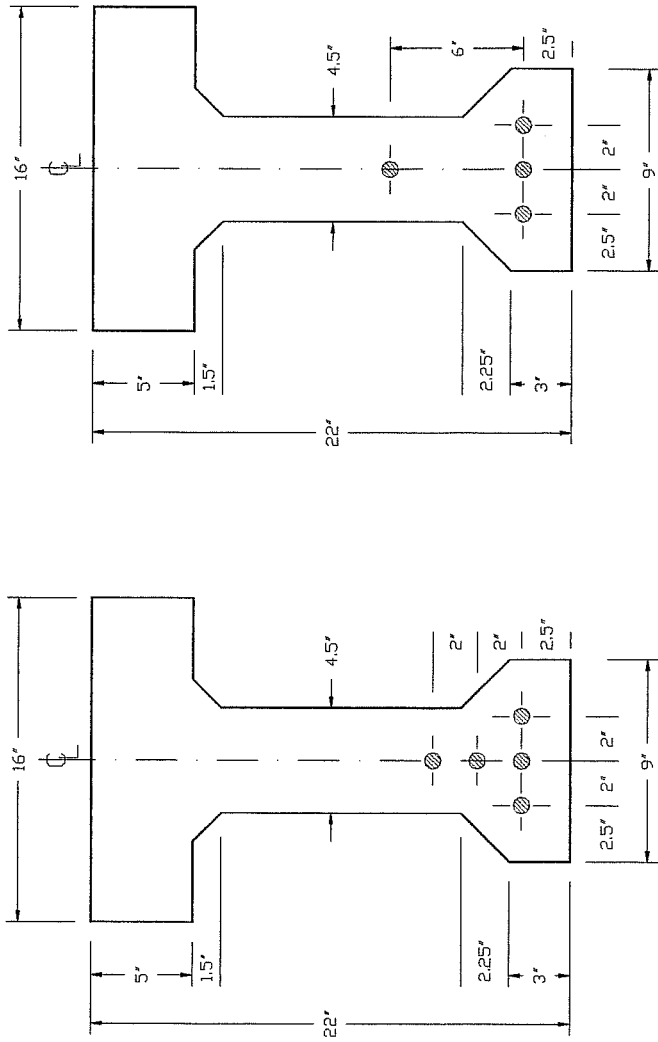
CHAPTER THREE

TEST PROGRAM

The purpose of the tests reported herein is to determine the development length of 0.5 and 0.6 inch strand in fully bonded pretensioned prestressed concrete beams. This chapter presents the specimen design, designation, fabrication, the material properties, the test setup, instrumentation, and test procedure used for this series of specimens.

3.1 Specimen Design and Designation

A total of nine (9) I-shaped prestressed concrete beams were cast at The Phil M. Ferguson Structural Engineering Laboratory of The University of Texas at Austin for this study. Four of the beams contained five (5) - 0.5 inch strands, and the remaining five had four (4) - 0.6 inch strands. The typical cross section for the specimens is shown in Figure 3.1. The test specimens



$$A = 177.3 \text{ sqin}$$

$$Ix = 9194 \text{ in}^4$$

$$y_b = 12.89 \text{ in}$$

Cross Section for 0.6
inch diameter Specimens

Cross Section for 0.5
inch diameter Specimens

Figure 3.1 Cross Section Details

also contained 5-#3 reinforcing bars in the top flange, and varying shear reinforcement.

Since this series of tests was part of a much larger program, a five part specimen designation was used to identify each end of a beam. An example of the numbering scheme is FA 550-1 A, and is explained in Table 3.1.

Table 3.1 Specimen Numbering Scheme

F	Fully Bonded (D = Debonded)
A	Cross Section 'A' (B = Cross Section B)
5	Five Strands (4 = Four Strands, etc.)
5	0.5 inch Strand (6 = 0.6 inch Strand)
0	2 inch Spacing (2 = 2.25 inch Spacing)
1	Number of Specimen
A	First Test of Specimen (B = Second Test)

3.2 Material Properties

3.2.1 Pretensioning Steel

The pretensioning strand used in this research program was donated by Florida Wire and Cable Company (FWC). The strand was seven-wire, low-relaxation prestressing strand with a specified ultimate tensile stress of 270 ksi. The breaking strength reported by FWC

consolidation and workability were encountered during the first placement due to the hot and dry conditions. Subsequent casts replaced the 3/8 inch MSA with 5/8 inch MSA. The slump was maintained between 4 and 6 inches for ease of placement. Concrete was also placed into plastic cylinders (6 inches in diameter and 12 inches high) and then moist cured. The concrete cylinders provided an accurate measure of the concrete strength gain over time. Appendix B contains graphs of the concrete compressive strength versus time for the beams tested (based on cylinder strength).

Table 3.2 Concrete Mix Design

<u>Material</u>	<u>Quantity</u>
Type I Cement	611 lb/cuyd
Water	290 lb/cuyd
Course Aggregate (Gravel)	1680 lb/cuyd
Fine Aggregate (Sand)	1355 lb/cuyd
Master Builders 761-N Admixture	37.0 oz/cuyd

3.3 Specimen Fabrication

All the beams required for this research project were fabricated at The Phil M. Ferguson Structural Engineering Laboratory. Careful attention to detail was taken to simulate standard practice in the prestressing industry. The fabrication of a beam included building the shear reinforcement "cage," stressing the strands, setting the formwork, casting the concrete, and transfer of the prestress force to the concrete. The following sections describe the specimen fabrication in detail.

3.3.1 Pretensioning Setup

The pretensioning was accomplished between two steel abutments. The steel abutments were used to anchor the strands once they were tensioned. The steel abutments were 76 feet apart, and there were a total of three (3) pretensioning bays. Figures 3.2 and 3.3 show the setup for pretensioning and casting the beams.

3.3.2 Pretensioning Instrumentation

To assure proper pretensioning, instrumentation for the pretensioning setup was required. The data collected

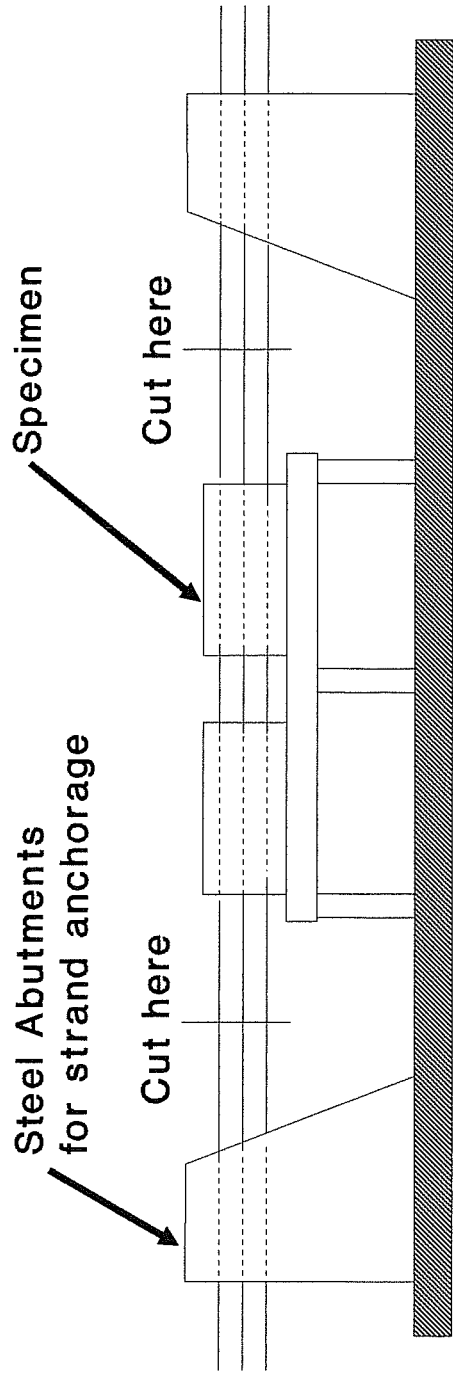


Figure 3.2 Pretensioning/Casting Bay

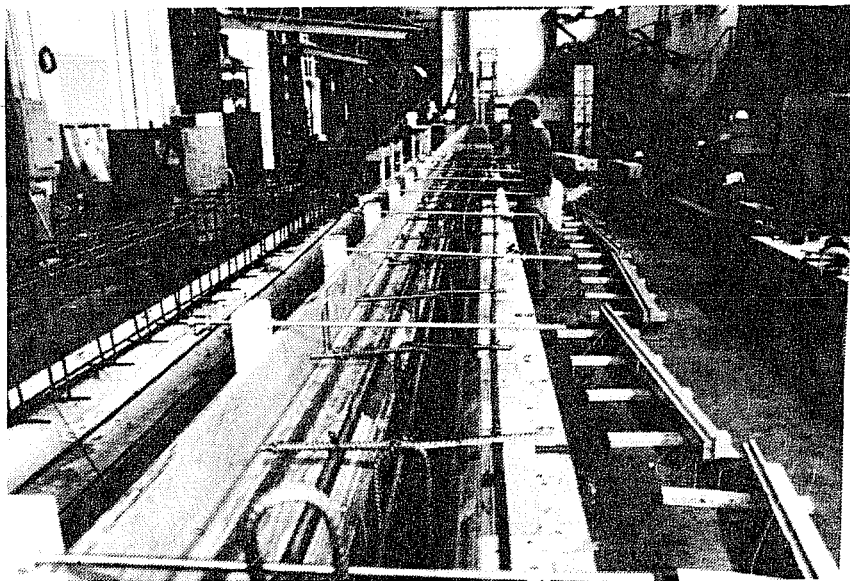


Figure 3.3 Pretensioning/Casting Bay

included: 1) electrical resistance strain gages to measure the steel strain, 2) a pressure indicator and a pressure transducer to measure the pressure in the stressing system, 3) a load cell at one end of the stressing bed, and 4) a linear variable displacement transducer (LVDT) to measure strand elongation.

The strain in the strand was monitored using electrical resistance strain gages. Four gages were applied to each end of the specimen. Two of the gages were applied to the bottom center strand, and one on each of the other bottom strands, respectively.

To verify the actual prestress force in the system, two pressure measurements were made. A pressure indicator adjacent to the pump was used to determine the stress on the strand while jacking, and a pressure transducer was used as a more accurate check. The top strand instrumented with strain gages also had a load cell at the holding end of the stressing bed for further confirmation of the applied pretension.

The final method of instrumentation to verify the prestress force was to measure the elongation of the strand. The elongation of the strand equipped with the load cell was measured with a LVDT. A steel rule was

used for the other strands. A data acquisition system, as described in Section 3.5, was used to record the readings from the strain gages, pressure transducer, load cell, and LVDT.

3.3.3 Pretensioning Procedure

Before the actual stressing of the strands, a reinforcing cage was built using #3 reinforcing bars as stirrups. After the reinforcing cage was fabricated, the strands were passed between the two abutments. Once the strands were in the proper position, approximately 10.4 ksi was applied to each strand requiring instrumentation. The initial 10.4 ksi was used to align the respective strand, and also set one end relative to the other for the purpose of instrumenting the specimen.

After the strands were instrumented, the initial 10.4 ksi was removed. Each strand was then stressed with a double cylinder Velzy hydraulic ram. The hydraulic ram reacted directly against the chuck, which had its bearing against the steel abutment. The chuck used to anchor the tensioned strand were "American Multi-Chux" (utilizing the male conical wedges and female cylindrical chuck body). Figures 3.4 and 3.5 are photographs of the strand

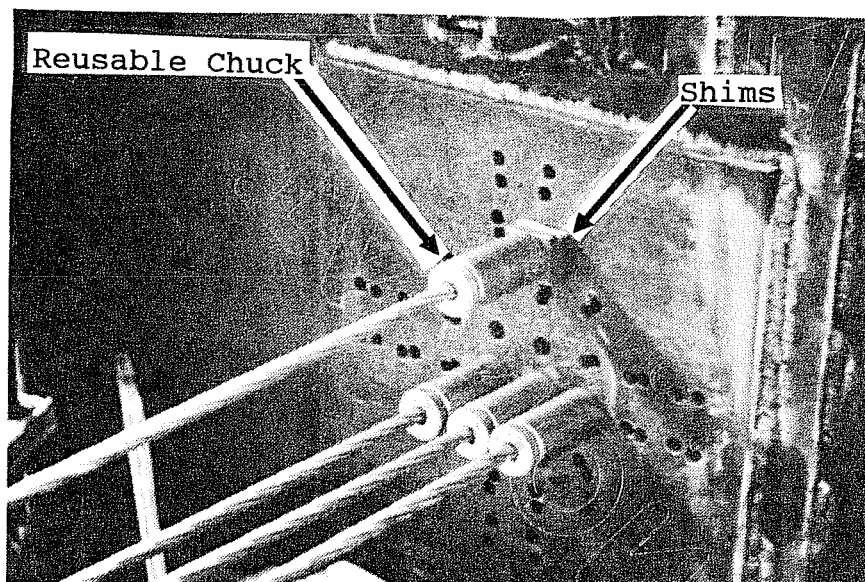


Figure 3.4 Strand Anchorage (Jacking End)

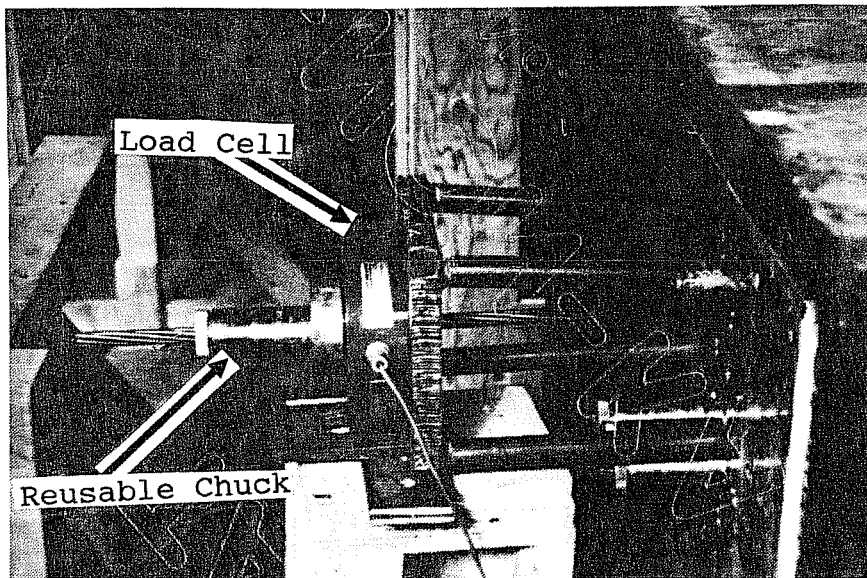


Figure 3.5 Strand Anchorage (Holding End)

anchorage at the stressing end and holding end. To allow for data readings to be taken during stressing, the actual application of the pretensioning force occurred in several steps. The sequence of pretensioning was to stop the ram at predetermined stress levels (10.4 ksi, 26 ksi, 104 ksi, 197.6 ksi, and 202.5 ksi) and take the required data readings at each stress level. At each stress level the pressure, elongation, load, and strain were recorded. The final target prestress of 202.5 ksi corresponds to $0.75f_{pu}$.

Two $\frac{1}{2}$ inch shims were placed between the abutment and the chuck on the top strand, as shown in Figure 3.4. The shims were later removed during the transfer of pretension to allow gradual detensioning of this one strand. The transfer procedure is covered later in Section 3.3.6. All other strands were suddenly detensioned (flame cut).

The ram allowed for the jacking force to be transferred into a seating force. The seating force thrust the male conical wedges into the female chuck body, while the ram held the strand in place. This method of seating the wedges yielded only a 5 percent

seating loss. The average final pretension stress, as measured by the strain gages, was on average 189 ksi.

3.3.4 Formwork

The last step before casting the specimen was to set the formwork. Two tables which served as the bottom form for the beams between steel abutments (see Figures 3.2 and 3.3). Each two (2) foot wide table was considered an individual bay, and was approximately 56 feet long in the north-south direction of the laboratory. Depending on the desired specimen length, either one 40 foot or two 27 foot beams were cast in each bay. The top of the tables were clad with Plexiglass to reduce the friction between the table and the concrete member at transfer of the prestressing force.

Wooden forms were bolted to the table, and tied together at the top of the form to maintain the desired cross-sectional dimensions. To prevent the possibility of damaging the bond characteristics of the strand, form oil was not used. However, after each beam was cast the forms were scraped clean and lacquered to extend the life of the forms and aid in form removal. The same forms were used to fabricate all the third phase beams in this

test program. The pretensioning procedure was performed one day prior to the concrete placement.

3.3.5 Concrete Placement

The concrete was placed in the forms using a bucket to carry the material from the ready mixed truck to the forms. The bucket held approximately three quarters of a cubic yard of concrete. The concrete was placed in two lifts. Before the second lift was placed, the first lift was consolidated using an internal vibrator and external form vibrator. The second lift was consolidated in a similar manner. The top of the specimen was then screeded, floated, and finally troweled to provide the desired finish. The average placement took approximately forty-five (45) minutes to complete. After the concrete was cast, the specimens were cured in the form for 48 hours. To prevent excessive evaporation and maintain a moist curing environment, plastic sheets were used to cover the top of the specimens.

3.3.6 Transfer of Pretension Procedure

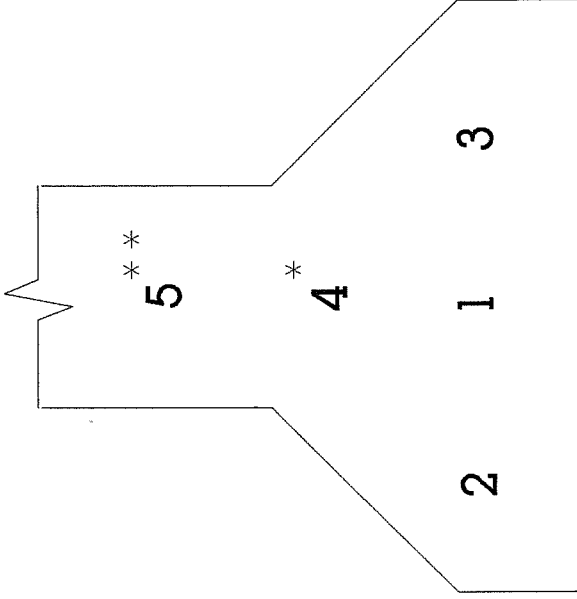
The transfer of the pretension force to the concrete, or detensioning, was performed approximately 48

hours after completing the concrete placement. A cylinder strength test was performed before transfer, to assure that the desired 4500 psi initial concrete strength (f_{ci}) had been reached. The strands were flame cut with a acetylene torch. Flame cutting the strands at transfer simulates the worst case scenario. The gradual detensioning was performed to reduce the total prestress, since the sudden release of pretension would collapse the tables the specimens were cast on.

Each strand was fitted with a three foot segment of strand in the region at the end of the beam where the strands were cut. The short segments of strand were held in place with two cable clamps. The purpose of the clamps was to prevent the wires in the strand from unraveling during and after the cutting procedure. A band of tape was also wrapped around each strand at both ends of the specimen as a reference point to detect any slippage of the strand into the beam at transfer. The strands were then flame cut with an acetylene torch. In order to follow industry practice, strands were flame cut at each end of the pretensioning bay. A sequence of cutting was adopted to emulate standard industry procedures.

To simplify the description of the transfer procedure, the strands will be referred to by number, as shown in Figure 3.6. The sequence of cutting the strands started at the north end of the bay with the cutting of strand 1 (bottom center). The same strand on the south end of the bay was cut next. Strand 2 (west of center) was then cut on the north end, followed by the cutting of the same strand on the south end. The strand east of center (strand 3) was then cut on the north end. The sequence continued, going from north to south until only the top middle strand remained.

The last strand cut was the top center. The shims between the abutment and the chuck, as shown in Figure 3.4, were removed prior to the transfer of pretension. The same hydraulic ram used for pretensioning was used to jack the strand just enough to dislodge the shims, and then release the strand. By withdrawing the shims, approximately half of the initial tension in the exposed strand was eliminated. The gradual detensioning was used as a safety precaution, since flame cutting produces a violent release of the energy in the strand. After the shims were removed, the strand was flame cut. When flame cut, the strand actually failed by yielding due to the



- * Strand 4 is four (4) inches higher in 0.6 inch Specimens
 - * * Strand 5 is not used in 0.6 inch Specimens
- Note: See Figure 3.1 for a detail of strand positions

Figure 3.6 Sequence of Prestress Transfer

loss of strength from the applied heat. Necking of the strands was visible.

The data acquisition system was used to scan the strain gages after each strand was cut and after the gradual detensioning procedure. The slippage of the strands, if any, was measured with a steel rule after the transfer procedure was complete. The specimens were then cured in the laboratory under ambient conditions until the desired compressive strength was attained. The average stress in the strands after the transfer procedure was approximately 175 ksi.

3.4 Test Setup

3.4.1 Test Setup

The test setup consisted of a loading frame, a spreader beam, and two support beams. Figure 3.7 shows the test setup. The test setup was constructed next to the pretensioning bays where the specimens were fabricated. Since the object of the research was to determine the development length, the test setup was arranged to accommodate a variety of embedment lengths and support conditions.

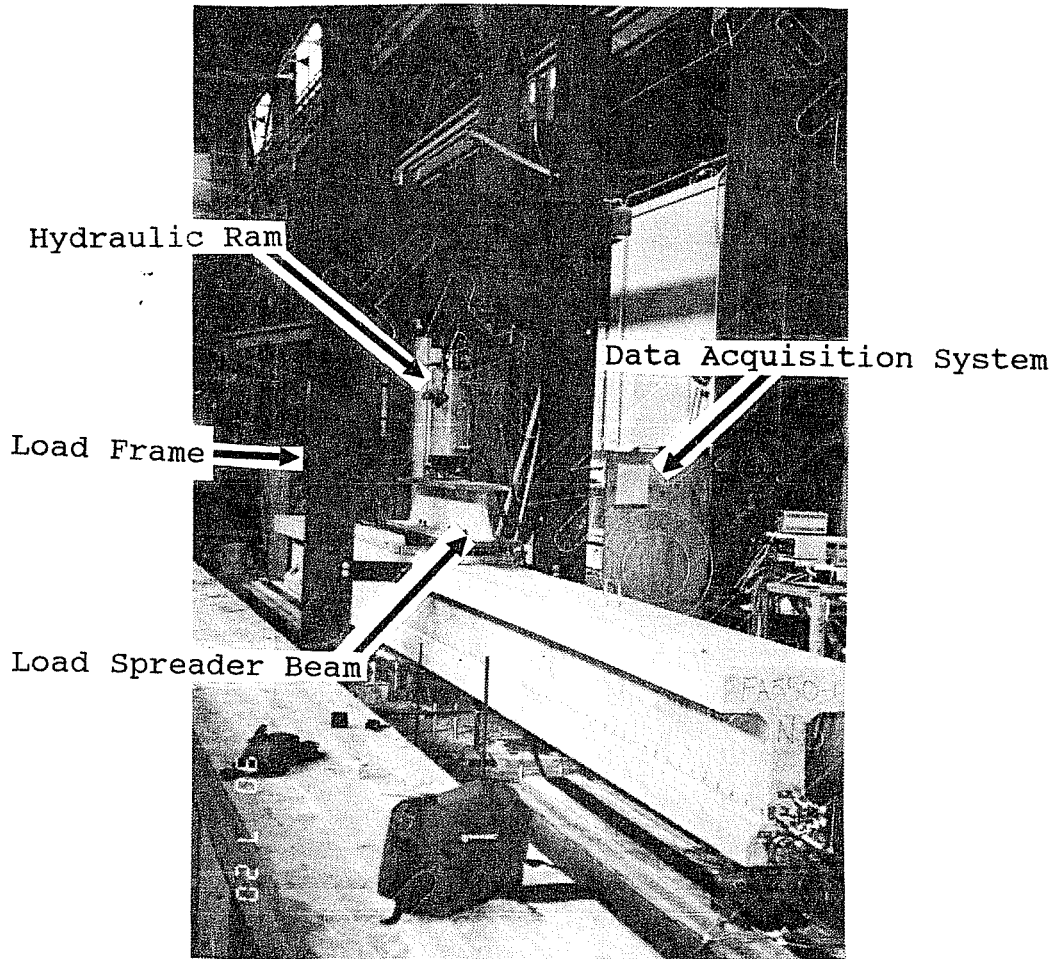


Figure 3.7 Test Setup

The load was applied by jacking a hydraulic ram against the loading frame, as shown in Figure 3.8. The loading frame was constructed using two steel columns, and a cross beam between the columns to load against. The ram rested on a ball and socket support. The ball and socket support then sat on top of a spreader beam, which provided two point loads from a single ram. This two point loading provided a constant moment region between the load points. A load cell was placed between the top of the ram and the load frame. The spreader beam consisted of a 5 foot section of a W10x88 steel section. A plate with 1 inch diameter round stock welded in place was then bolted to the bottom of the spreader beam, simulating a point load. Load points were 24 inches apart. Plates, 12 inches x 6 inches x 1 inch, were used to distribute the bearing stresses. This allowed the round stock to bear against the plate. The plates were leveled with a 2 foot bubble level and shims, using hydrostone to seat them on the top flange of the test specimen. Two pieces of steel angle were also attached to the loading frame as guides to prevent excessive lateral deflections.

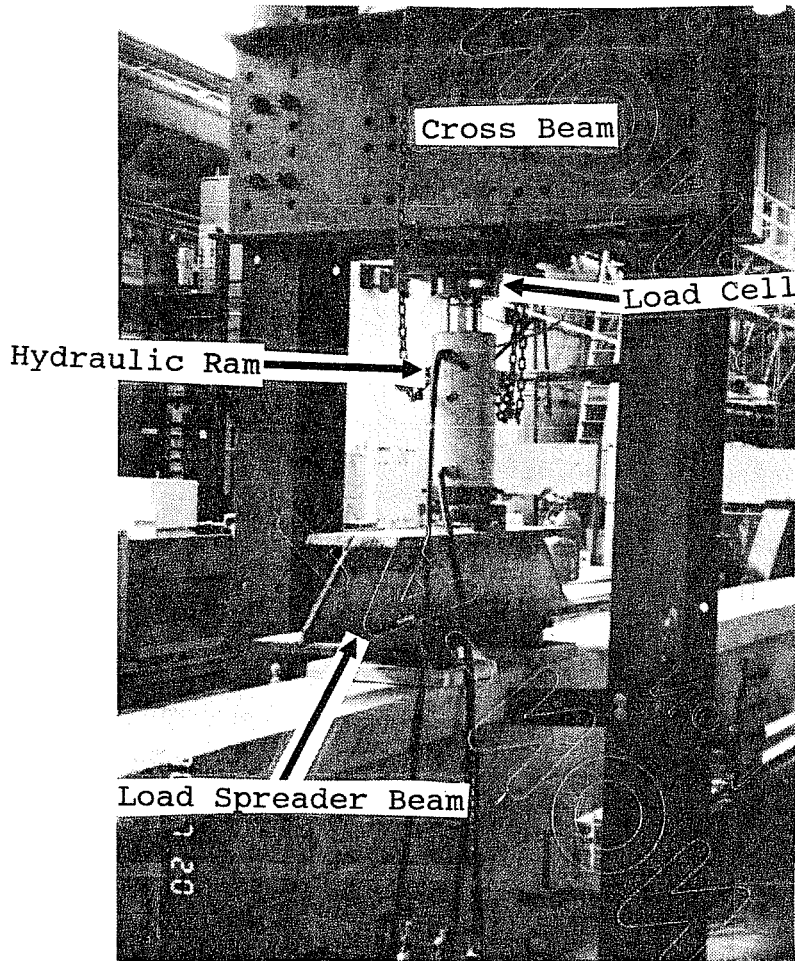


Figure 3.8 Load Frame

The ability to vary the embedment length was accomplished through the use of two steel support beams. The support beams were also embedded in hydrostone on the laboratory floor, to prevent movement. A four inch wide steel plate was shimmed and leveled with an engineering level (Autolevel), and grouted onto the top of the support beams. This provided a level surface for the specimen supports.

The actual specimen supports were comprised of a $1\frac{1}{2}$ inch thick plate, a load cell, and a roller arrangement. Figure 3.9 shows the specimen support arrangement. The $1\frac{1}{2}$ inch plates rested on the shimmed four inch wide plate. The load cells (one at each support) were sandwiched between the $1\frac{1}{2}$ inch plate and another steel plate. The second plate was attached to the load cell, providing complete bearing on the load cell surfaces. This plate also had a piece of round stock welded in position. Another plate rested on top of the round stock, and directly below the concrete specimen. Since the top plate was not attached to the round stock, end rotation and horizontal movement were not restrained. This method of support simulated a simple roller support. The entire support arrangement could then be moved to

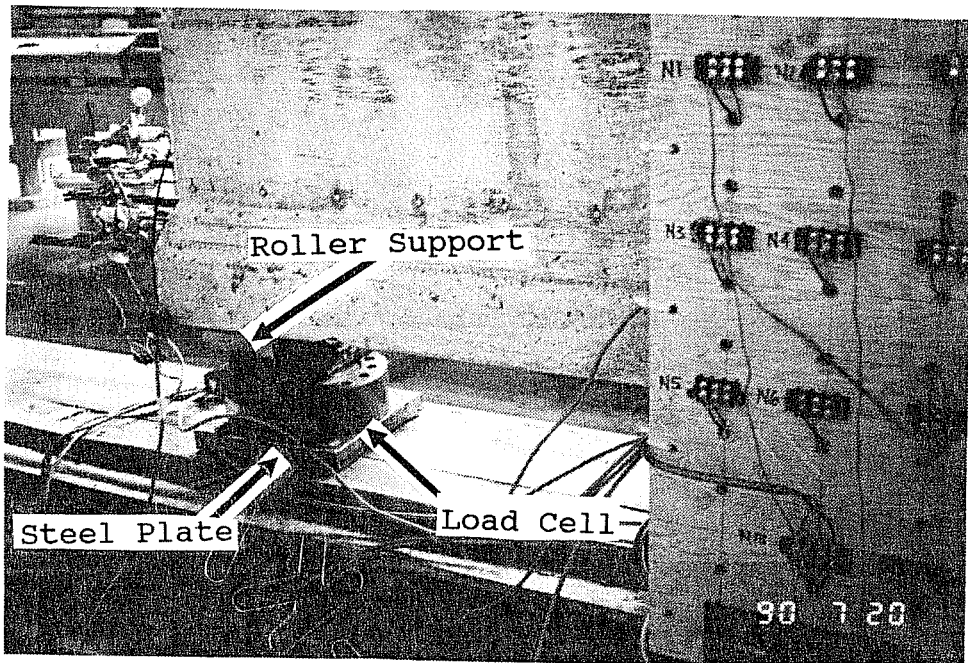


Figure 3.9 Specimen Support

match the span for the test with the desired embedment length.

3.4.2 Testing Instrumentation

The instrumentation for the actual testing of a specimen involved measurements for end slip, strain in the prestressing strands, applied load, deflection, and top fiber compressive strain. The end slip, applied load, deflection, and strand strain data were taken with the data acquisition system.

Each strand on the end being tested had a LVDT clamped in place to detect any slippage of the strand, which is associated with loss of bond. LVDT's were also used to measure the deflection of the specimen. By placing two LVDT's between the load points (one on each side of the lower flange), an average deflection was obtained. Figures 3.10 and 3.11 illustrate the end slip instrumentation. The strand strain data was also taken using the strain gages applied before the concrete was cast.

The load was applied using a center hole hydraulic ram. The pressure in the loading system was induced using a hand pump, and regulated by a pressure indicator

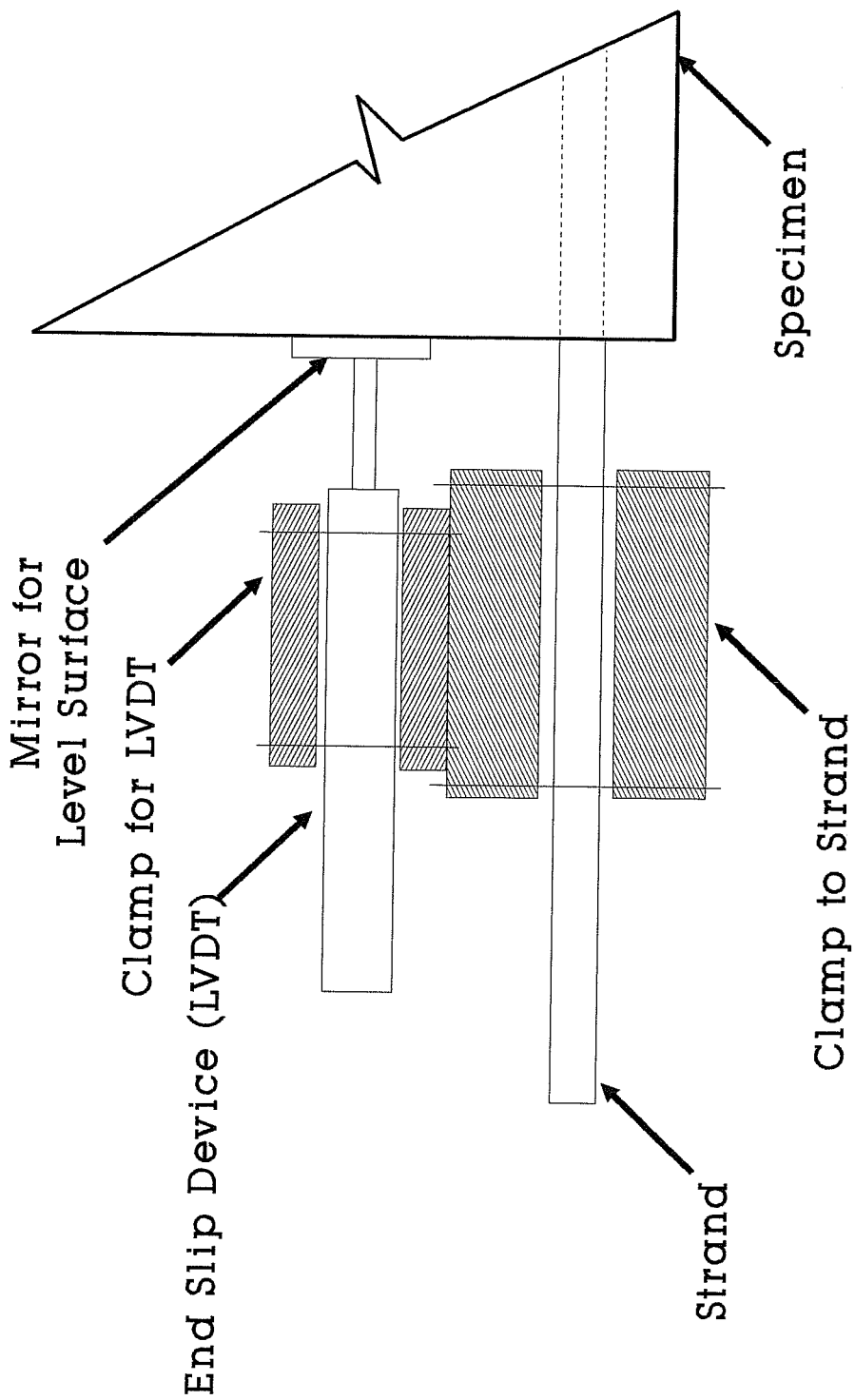


Figure 3.10 End Slip Instrumentation



Figure 3.11 End Slip Instrumentation

and pressure transducer. The pressure indicator gave a visual reading at the pump to know how much load was being applied. The pressure transducer provided a secondary source for verification of the applied load, and was recorded on the computer for each sweep of data during the test. Three load cells were used to measure the applied load. One load cell was placed under each support, and the third was placed at the point of loading.

The last type of instrumentation was four pairs of DEMEC gage points to measure the extreme fiber compressive concrete strain. The DEMEC system consists of a mechanical dial gage and stainless steel disks for gage points. The DEMEC gage points were bonded to the beam with a two (2) inch lateral spacing and an eight (8) inch gage length. The gage points were placed $1\frac{1}{2}$ inches from the edge of the top flange, as shown in Figure 3.12. Both sides of the flange were instrumented.

The DEMEC system was developed to measure concrete strains, and has been successfully used at The Phil M. Ferguson Structural Engineering Laboratory before this project. The accuracy of the DEMEC system is approximately ± 20 microstrains. The DEMEC gage points

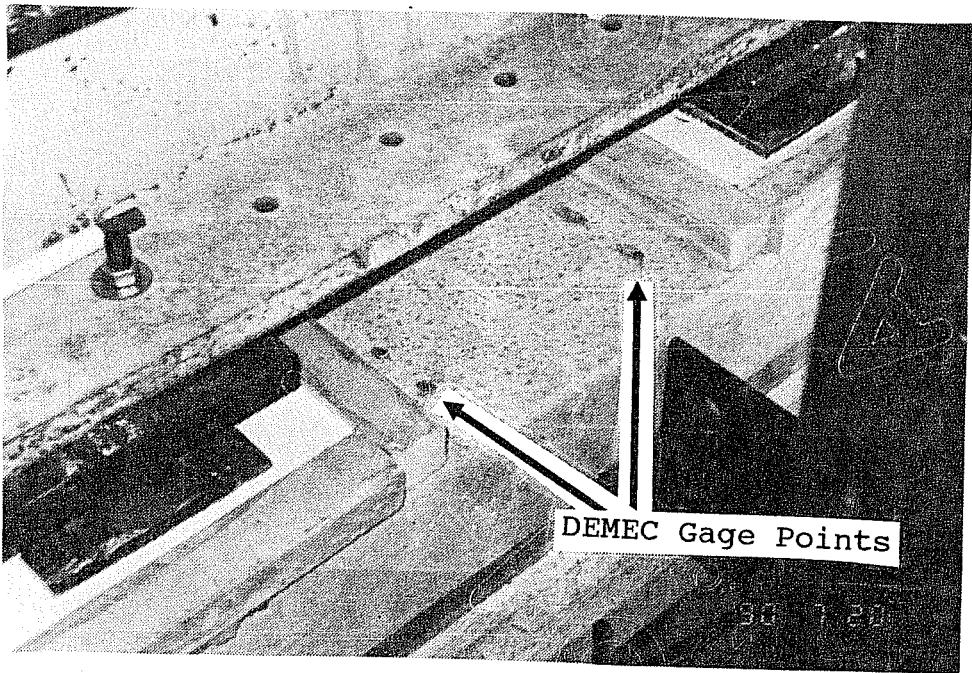


Figure 3.12 DEMEC Gage Points

have a hole punched in the center to receive the DEMEC gage, and were attached to the concrete surface with an epoxy adhesive. The dial gage on the DEMEC strain indicator measured the relative change in length between the points. The strain between the points was therefore known, since the points were at a known distance apart.

3.4.3 Test Procedure

The sequence of testing included incrementally applying a load and taking data readings. Beams were loaded statically, with each test taking approximately two (2) hours. A typical test setup is shown in Figure 3.13. Figure 3.13 also shows the important variable test dimensions. The test dimensions shown in Figure 3.13 are presented in Table 3.3. Failure occurred when either (1) the concrete on the top flange crushed or (2) significant end slip occurred. Slip failure was characterized by a drastic drop in load carrying capacity due to loss of prestress. The specimens were placed in the test setup in the same orientation (north-south) as they were cast and cured.

The specimens were designed to provide an independent test at each end. As shown in Figure 3.14,

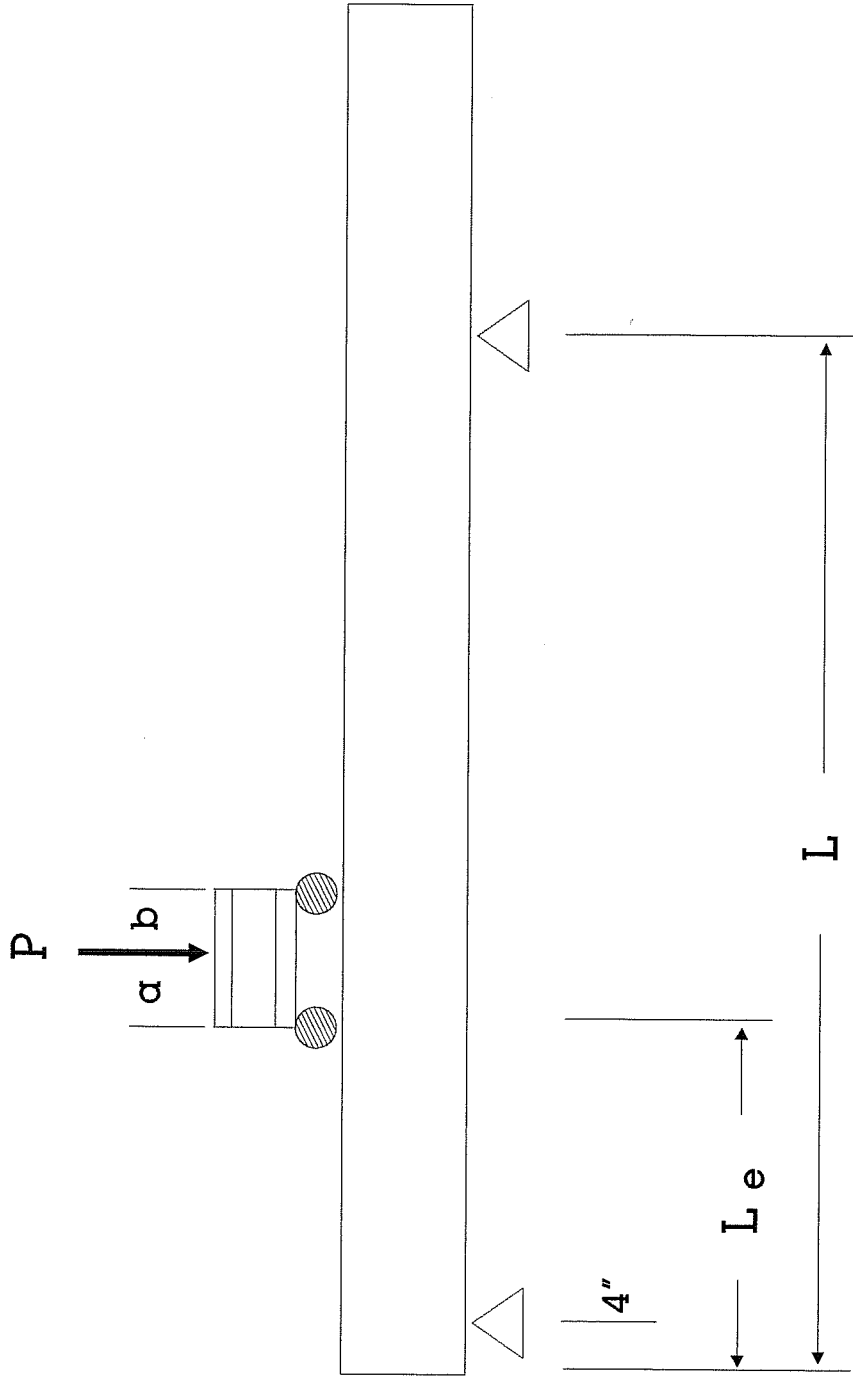


Figure 3.13 Typical Test Setup (see Table 3.3)

Table 3.3 Typical Test Dimensions

Beam Number	a (in.)	b (in.)	Le (in.)	L (in.)
FA550-1A	14	10	140	264
FA550-1B	8	16	60	196
FA550-1C	12	12	100	220
FA550-2A	7 5/8	16 3/8	72	216
FA550-2B	11	13	92	220
FA550-3A	11	13	92	220
FA550-3B	9	15	76	224
FA550-4A	8	16	68	220
FA550-4B	7 5/8	16 3/8	72	216
FA460-1A	12 5/8	11 3/8	167.5	340
FA460-1B	12	12	128	276
FA460-2A	10 1/4	13 3/4	86	220
FA460-2B	12	12	96	212
FA460-3A	12	12	100	220
FA460-3B	12	12	92	204
FA460-5A	9 1/2	14 1/2	80	220
FA460-5B	10	14	84	220
FA460-6A	10 1/2	13 1/2	88	220
FA460-6B	10	14	84	220

the specimen supports were moved after the first test ('Test A') to accommodate the second test ('Test B').

The load was applied in 5 kip increments. At each load increment, data for the strand strain, load cells, end slip, jacking pressure, deflections, and concrete compressive strain were taken. Important observations about beam performance were also noted. Visible cracks were marked with an ink marker at each load increment. When unanticipated behavior occurred, loading was stopped for observations and readings. After flexural cracking occurred, the load increment was decreased to 2.5 kips. Loading was continued until failure occurred.

3.5 Data Acquisition System

Data was acquired electronically on a computerized data acquisition system. To simplify the reading of data, all electrical instrumentation was wired into a central circuit panel. The data which was recorded electronically included the end slip gages, deflection gages, a pressure transducer, and the strain gages on the strand. The central panel was then wired to a Hewlett

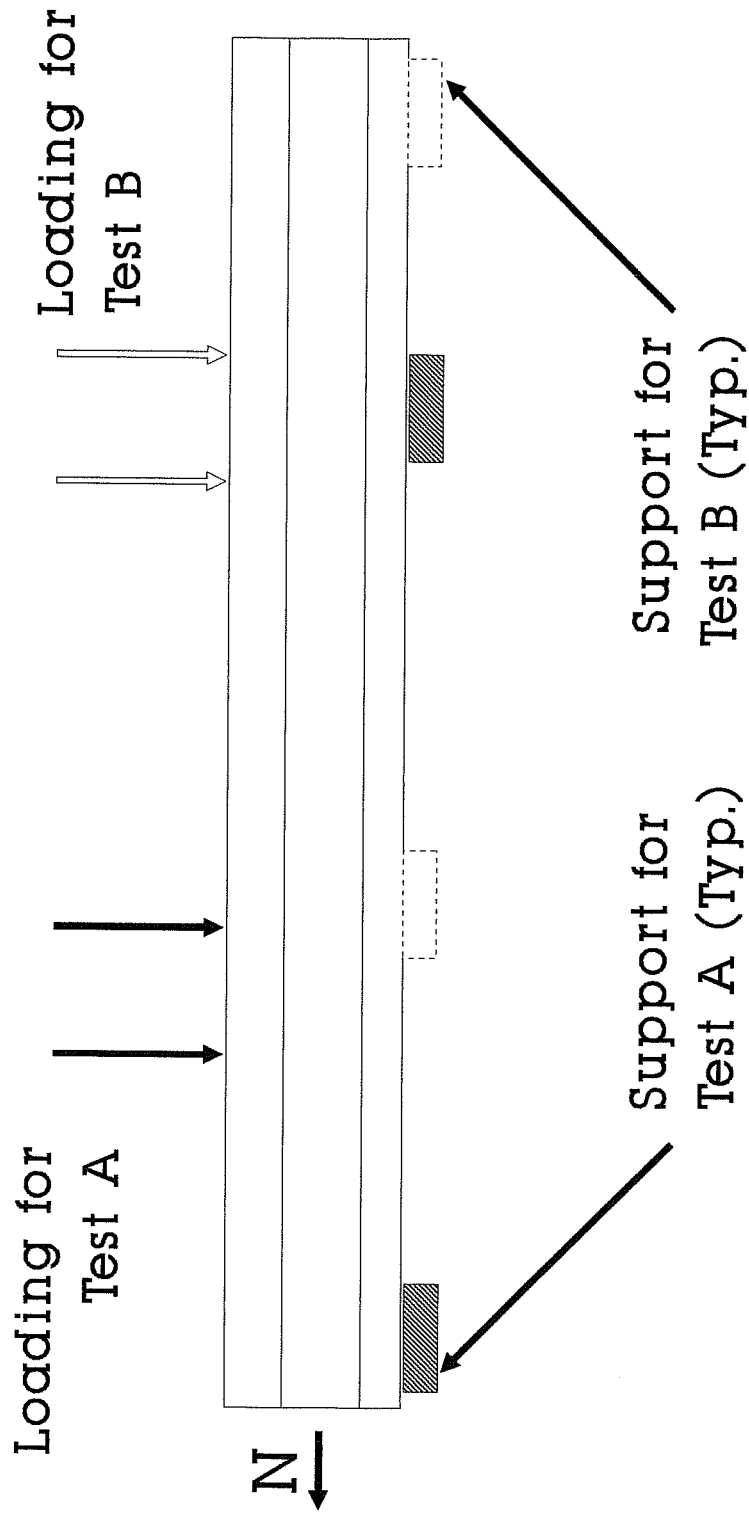


Figure 3.14 Support and Loading Arrangement

Packard scanner. An IBM personal computer was used with software written by Alex Tahmassebi (HPDAS2), to scan the necessary channels. The data was recorded as a change in voltages and stored in a file for future use. The data file was later converted from voltages to engineering units, and formatted for use in a spread sheet. Other non-computer orientated data was also taken, as required. Figure 3.15 is a photograph of the data acquisition system.



Figure 3.15 Data Acquisition System

Packard scanner. An IBM personal computer was used with software written by Alex Tahmassebi (HPDAS2), to scan the necessary channels. The data was recorded as a change in voltages and stored in a file for future use. The data file was later converted from voltages to engineering units, and formatted for use in a spread sheet. Other non-computer orientated data was also taken, as required. Figure 3.15 is a photograph of the data acquisition system.



Figure 3.15 Data Acquisition System

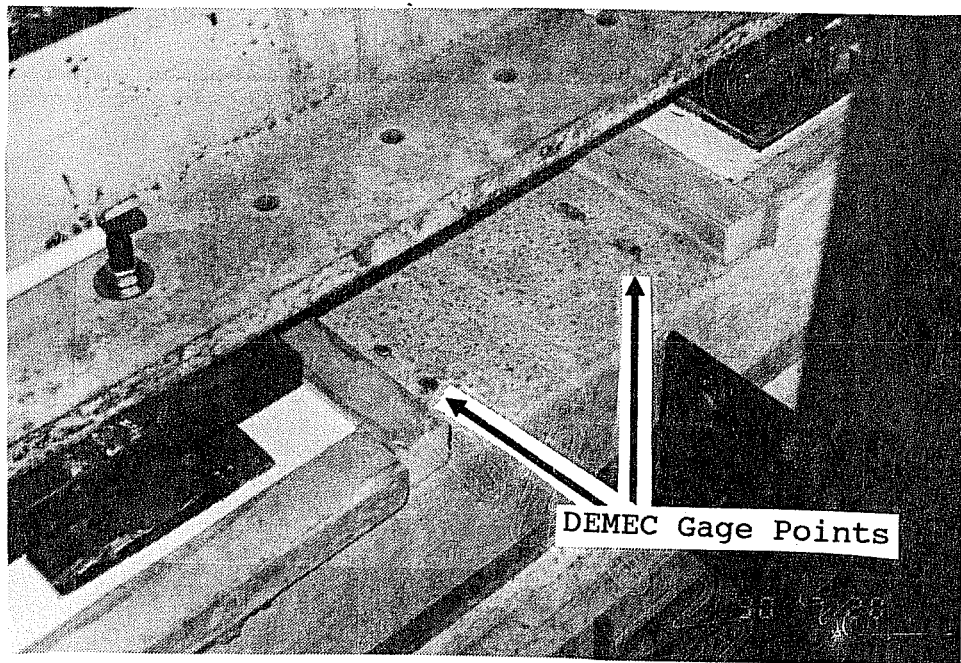


Figure 3.12 DEMEC Gage Points



Figure 3.11 End Slip Instrumentation

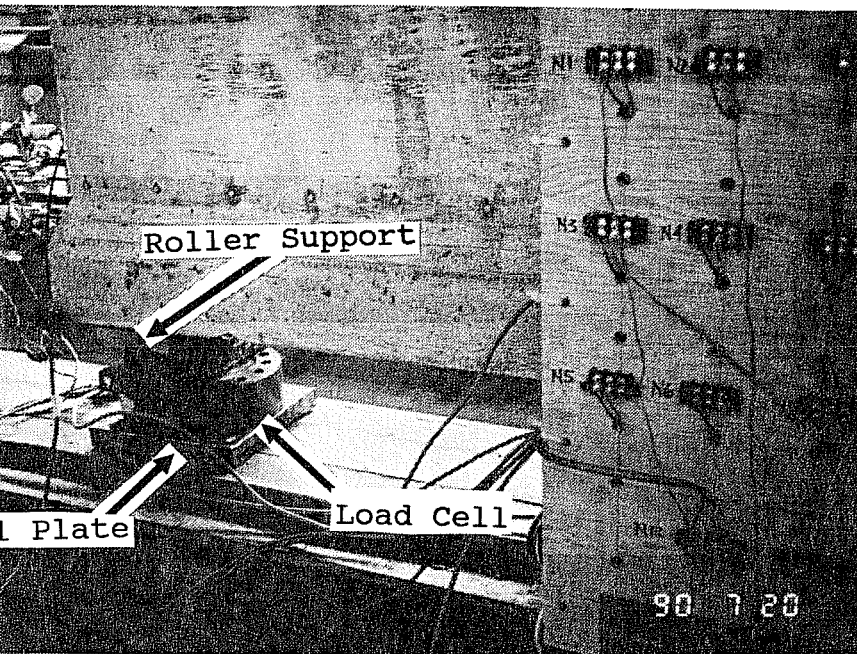


Figure 3.9 Specimen Support

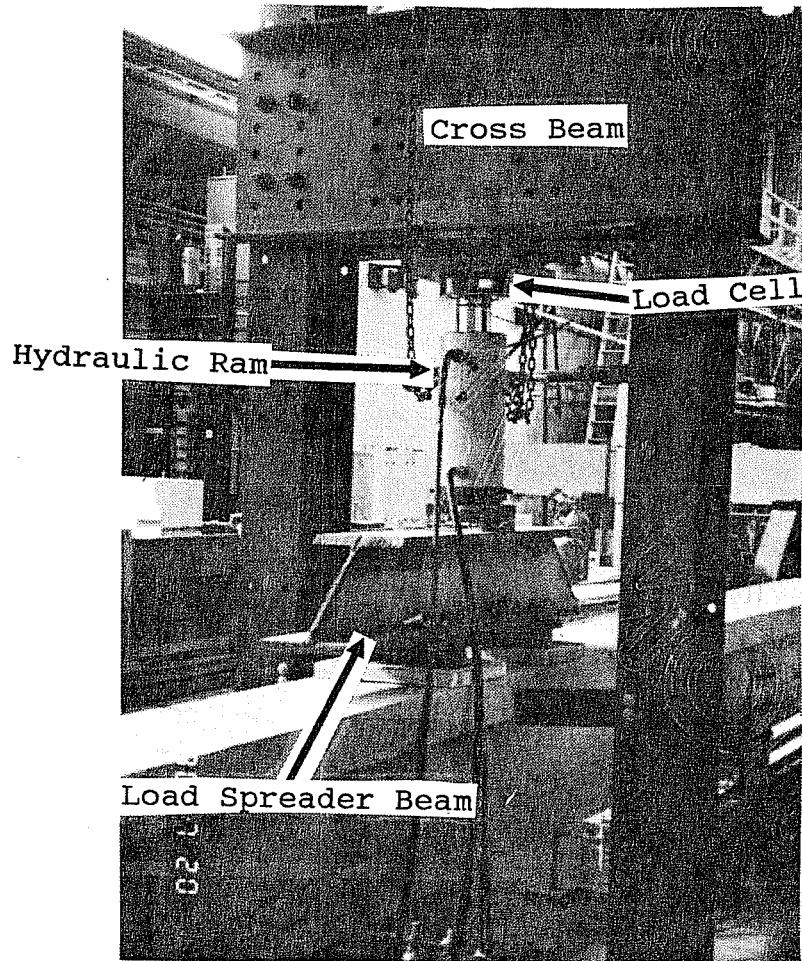


Figure 3.8 Load Frame

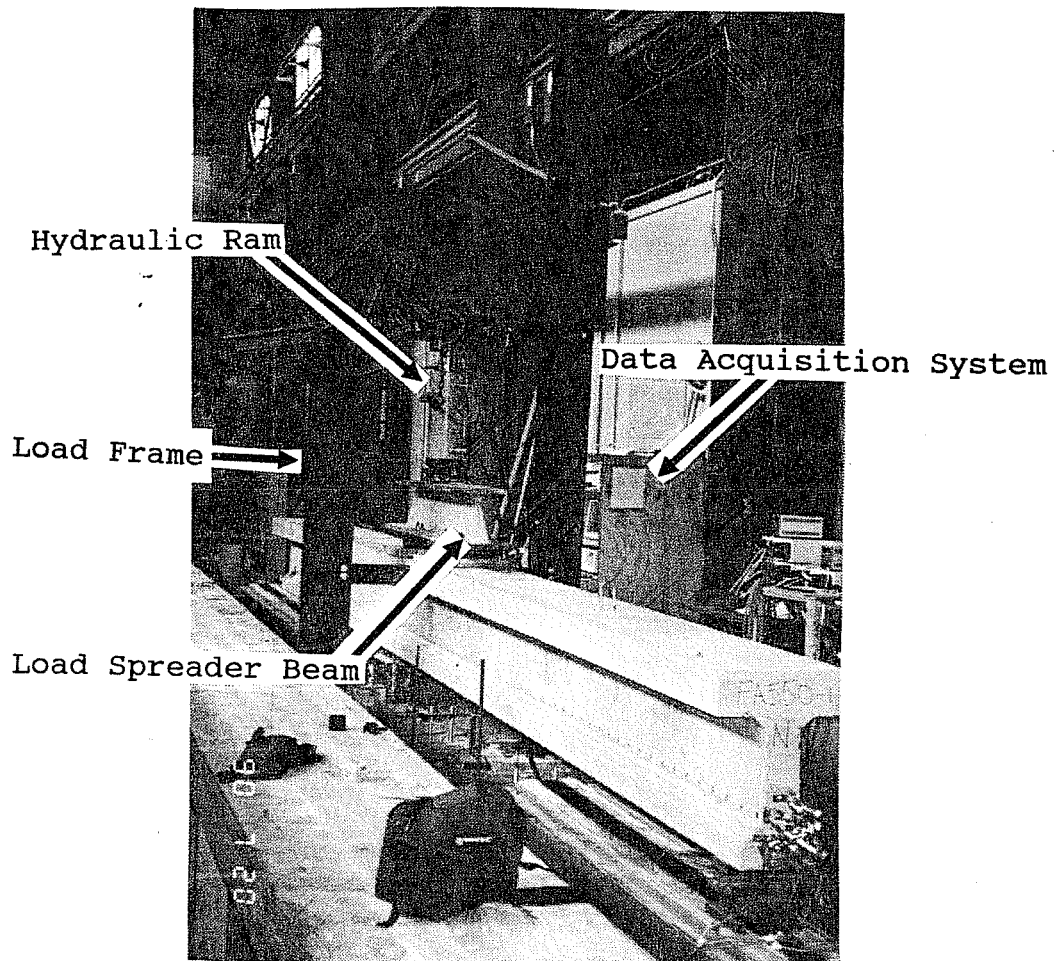


Figure 3.7 Test Setup

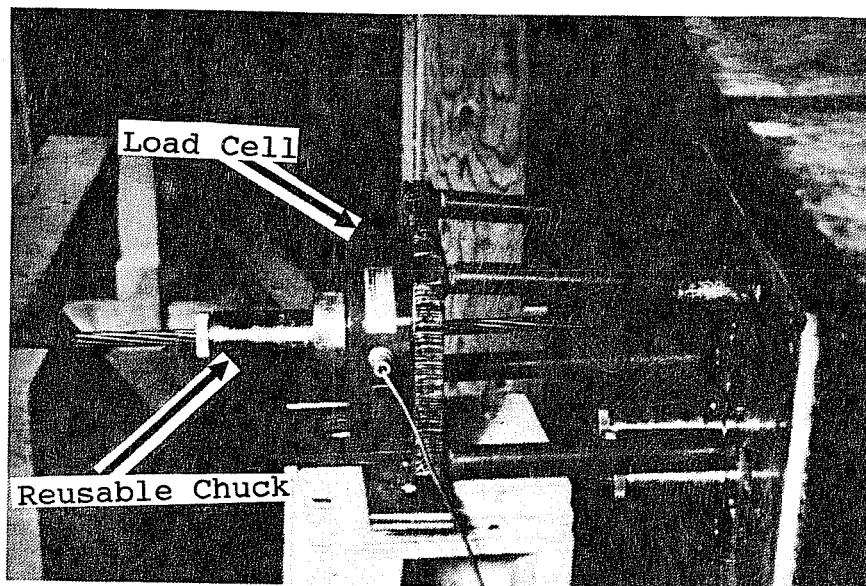


Figure 3.5 Strand Anchorage (Holding End)

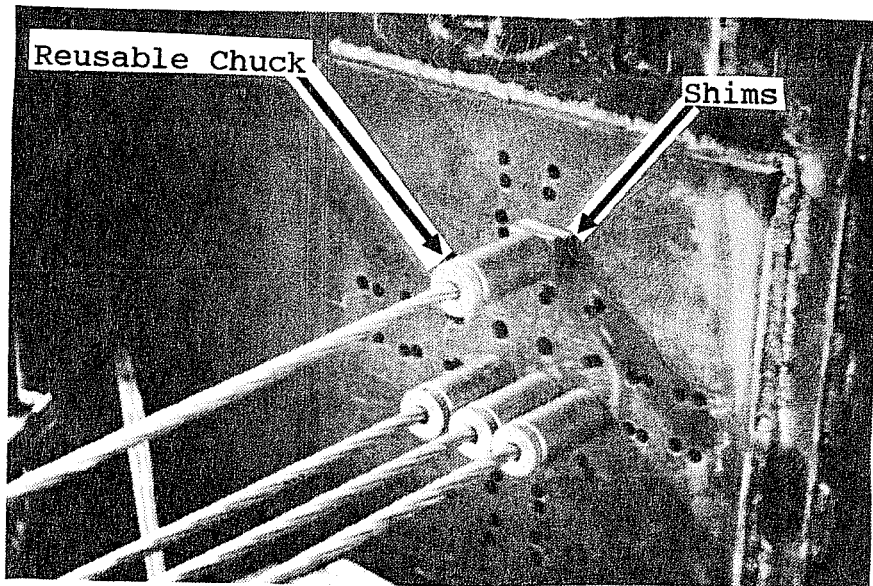


Figure 3.4 Strand Anchorage (Jacking End)

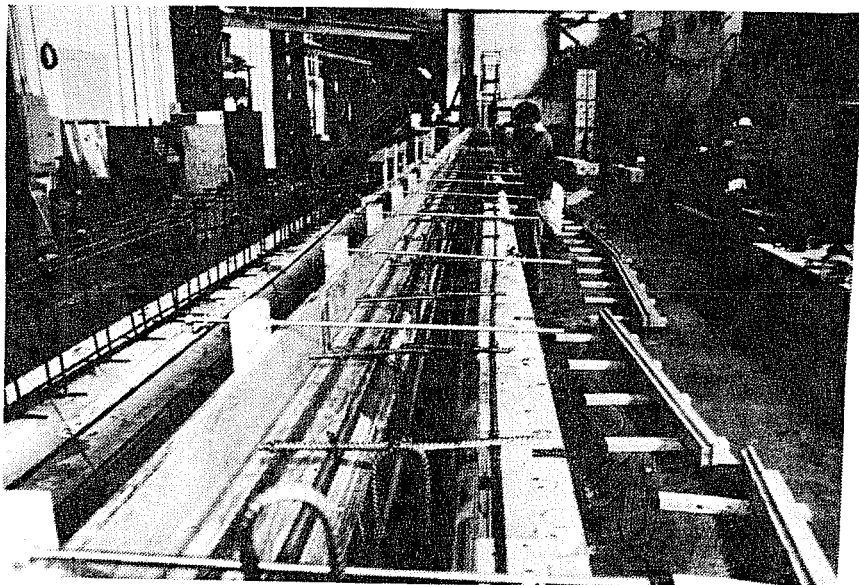


Figure 3.3 Pretensioning/Casting Bay

CHAPTER FOUR

TEST RESULTS

4.1 Test Results

Each specimen was tested at both ends as described in Section 3.4.3, Test Procedure. The test results are presented in Table 4.1. For each test the concrete strength, embedment length, ultimate concrete compressive strain, cracking and ultimate moments, and the mode of failure are tabulated. The moments at cracking and ultimate were calculated based on the measured load. The cracking moment corresponds to the point at which visible cracking first occurred.

Unlike transfer length, the development length cannot be directly measured. The determination of the actual development length was obtained by loading beams with different embedment lengths. The embedment length is defined as the length of bonded strand from the end of the member to the point of maximum moment. There are only two possible types of failure which could occur: 1) flexural bond failure, as indicated by end slip, or 2)

Table 4.1 Summary of Development Length Results

BEAM NUMBER	f'c (psi)	EMBEDMENT (in)	% of AASHTO Ld*	MEASURED (kip*ft)		Ultimate Concrete Strain (*10 ⁻⁶ in/in)	MODE OF FAILURE
				Mcr	Mult		
FA550-1A	5107	140	1.75	179.6	292.1	4424	FLEXURAL
FA550-1B	5107	60	0.75	156.3	311.1	2146	BOND
FA550-1C	5107	100	1.25	159.5	301.4	2756	FLEXURAL
FA550-2A	5107	72	0.9	197.1	286.1	1938	BOND/SHEAR
FA550-2B	5107	92	1.15	198.8	306.9	2382	BOND/SHEAR
FA550-3A	5426	92	1.15	201.6	307.8	4148	FLEXURAL
FA550-3B	5426	76	0.95	192.2	302.6	3724	FLEXURAL
FA550-4A	5846	68	0.85	194.1	298	1731	BOND/SHEAR
FA550-4B	5846	72	0.9	195.1	338.2	3142	FLEXURAL
FA460-1A	6362	167.5	1.708	202.1	315.2	3016	FLEXURAL
FA460-1B	6362	128	1.33	214.5	344	3113	FLEXURAL
FA460-2A	6852	86	0.9	210.8	338.3	3538	FLEX/BOND
FA460-2B	6852	96	1	213.6	320.3	2228	BOND/SHEAR
FA460-3A	6852	100	1.04	209.6	335	3192	FLEXURAL
FA460-3B	6852	92	0.96	219	337.3	3454	FLEXURAL
FA460-5A	7020	80	0.833	216	298.5	1646	BOND/SHEAR
FA460-5B	7020	84	0.875	212.4	296.8	1488	BOND/SHEAR
FA460-6A	7439	88	0.92	213.6	336.4	3198	FLEXURAL
FA460-6B	7439	84	0.875	211.4	325.8	3106	FLEXURAL

* Ld is defined in Section 4.2.1

** Mcalc is based on strain compatibility

flexural failure, as indicated by yielding of the strand and eventual crushing of the concrete in the extreme compression fibers (one beam failed in shear because inadequate shear reinforcement was provided). If the embedment was inadequate to develop the stress in the strands before crushing the concrete, bond/shear failure occurred. However, if adequate embedment was provided, the failure was crushing of the concrete in the top flange or a flexural failure.

If a bond failure occurred, the embedment length was increased for the next test. If a flexural failure occurred, the following specimen was tested with a shorter embedment length. This iterative procedure continued until the development length was determined for the particular size of strand. The test results are also plotted in Figures 4.1 and 4.2, which show the iterative testing sequence used to determine the development length. Figures 4.1 and 4.2 clearly show the break point between flexural failures and bond/shear failures. Figures 4.1 and 4.2 also show the low degree of scatter obtained in test data.

4.2 Discussion of a Typical Failure

The mode of failure for the specimens tested could be categorized as either a flexural or bond failure. However, regardless of the failure mode, the specimens exhibited linear behavior up to cracking. A discussion of a typical bond/shear failure and a typical flexural failure follow, with references to graphs of load vs. deflection and load vs. concrete strain which were measured. The load vs. deflection curves and load vs. concrete strain curves for all of the tests in this study are provided in Appendix C and D, respectively. The development length results are also summarized by type of failure, and are presented in Tables 4.2 and 4.3.

The load vs. deflection graphs contain two curves, "actual" and "predicted." The "actual" curve corresponds to the data taken during the test. The "predicted" curve is based on a strain compatibility analysis. The points plotted correspond to the predicted cracking, yield ($f_{ps}=0.9f_{pu}$), and ultimate loads. As the load vs. deflection curves show, the behavior of prestressed concrete beams is predictable. The predicted curves assume that the ultimate flexural load can be attained (adequate embedment provided). The predicted curves were

Table 4.2 Summary of Flexural Failures

BEAM NUMBER	f'c (psi)	EMBEDMENT (in)	% of AASHTO Ld*	MEASURED (kip*ft)		M _{ult} /M _{calc} **		Ultimate Concrete Strain (*10 ⁻⁶ in/in)
				M _{cr}	M _{ult}	M _{ult}	M _{calc} **	
FA550-1A	5107	140	1.75	179.6	292.1	0.99		4424
FA550-1C	5107	100	1.25	159.5	301.4	1.02		2756
FA550-3A	5426	92	1.15	201.6	307.8	1.04		4148
FA550-3B	5426	76	0.95	192.2	302.6	1.02		3724
FA550-4B	5846	72	0.9	195.1	338.2	1.15		3142
FA460-1A	6362	167.5	1.708	202.1	315.2	0.96		3016
FA460-1B	6362	128	1.33	214.5	344	1.05		3113
FA460-3A	6852	100	1.04	209.6	335	1.02		3192
FA460-3B	6852	92	0.96	219	337.3	1.03		3454
FA460-6A	7439	88	0.92	213.6	336.4	1.02		3198
FA460-6B	7439	84	0.875	211.4	325.8	0.99		3106

Table 4.3 Summary of Bond/Shear Failures

BEAM NUMBER	f'c (psi)	EMBEDMENT (in)	% of AASHTO Ld*	MEASURED (kip*ft)		M _{ult} /M _{calc} **		Ultimate Concrete Strain (*10 ⁻⁶ in/in)
				M _{cr}	M _{ult}	M _{ult}	M _{calc} **	
FA550-1B	5107	60	0.75	156.3	311.1	1.05		2146
FA550-2A	5107	72	0.9	197.1	286.1	0.97		1938
FA550-2B	5107	92	1.15	198.8	306.9	1.04		2382
FA550-4A	5846	68	0.85	194.1	298	1.01		1731
FA460-2B	6852	96	1	213.6	320.3	0.98		2228
FA460-5A	7020	80	0.833	216	298.5	0.91		1646
FA460-5B	7020	84	0.875	212.4	296.8	0.90		1488

* Ld is defined in Section 4.2.1

** M_{calc} is based on strain compatibility

also used during the actual tests to identify anticipated changes in specimen behavior. The strain compatibility calculations are presented in Appendix E.

4.2.1 Bond Failure

Specimen FA 460-5 A exhibited a typical bond failure. The specimen was set up with the embedment length of $0.83L_d$, where L_d is the calculated development length from the AASHTO/ACI equation (1,14):

$$L_d = (f_{ps} - 2/3f_{se}) * d_b$$

Figures 4.3 and 4.4 illustrate the load vs. deflection and load vs. concrete strain, respectively. As shown in the figures, the beam behaved in a linear-elastic manner up to cracking, followed by a loss of stiffness. The deflection per increment of load then increased, as expected. End slip was observed at approximately 76 kips from the data readings. Immediately after end slip was detected, web shear and new flexural cracks formed.

The end slip for test FA 460-5 A occurred on the top strand first. The test continued as shown in Figure 4.3, and failure occurred at 78 kips (298.5 kip*ft) when the

end slip was between 0.24 and 0.42 inches in all of the strands. An attempt was made to apply additional load, but the specimen only deflected and showed more end slip. The extra end slip was accompanied by additional web shear cracking forming closer to the load point. The failure could be considered gradual, since the cracks at the end of the beam formed, followed by the propagation of new flexural shear cracks towards the center of the beam as more load was applied. The new cracks were caused by the loss of prestress due to end slip.

The failure was not accompanied by the crushing of concrete. As Figure 4.4 shows, the ultimate compressive concrete strain was 1650 microstrains. This corresponds to just over half of the code assumed ultimate concrete strain (3000 microstrains). The graph also shows a strain reversal at the ultimate load (78.01 kips), which indicates evidence of end slip or loss of prestress. The strain reversal was accompanied by a drop in load carrying capacity.

4.2.2 Flexural Failure

The specimen designated FA 460-1 B demonstrated a typical flexural failure. This specimen was set up with

an embedment of $1.33L_d$. Figures 4.5 and 4.6 show the load vs. deflection and load vs. concrete strain, respectively. As expected, the beam showed linear-elastic behavior up to cracking. After the flexural cracks formed, the flexural stiffness decreased, as evident by the large increase in deflection per load increment. The failure occurred when the concrete crushed between the load points on the top flange.

The flexural failure exceeded the code assumed ultimate concrete strain of 3000 microstrains, as shown in Figure 4.6. The specimen continued to carry the applied load as the concrete began to crush. No end slip occurred during the test.

4.3 Observed Crack Patterns

The formation of the first flexural crack occurred between the load points. The following cracks formed progressively toward the supports. Figure 4.7 illustrates the crack pattern on Specimen FA 550-2 B. The numbers next to the cracks are the loads corresponding to the given level of cracking. As shown in the figure, the cracks begin at the bottom of the flange between load points (due to tension in the

concrete), and continue to grow vertically toward the top of the specimen. However, the cracks between the load point and the supports became inclined as they propagated. The difference occurs since concrete between the load points is in bending with almost no shear, causing vertical flexural cracks, while the concrete between the load points and the supports is in combined bending and shear, causing inclined cracks.

A significant difference in the number of cracks was observed between the $\frac{1}{2}$ inch and 0.6 inch strand. Figure 4.8 shows the crack pattern for specimen FA 460-2A. The specimens containing 0.6 inch strand exhibited a wider crack spacing than the $\frac{1}{2}$ inch beams, as seen by comparing Figures 4.7 and 4.8. The average crack spacing was 8.4 inches for $\frac{1}{2}$ inch specimens and 14.1 inches for 0.6 inch specimens. The specimens with 0.6 inch strand also showed more branching of cracks.

Possibly the reason for the difference in crack patterns can be attributed to the difference in strand size. Another possible cause for the difference in crack patterns could be the number of strands, since the 0.6 inch specimens had one less strand than the $\frac{1}{2}$ inch specimens. The last possible cause for the difference in

crack patterns is the difference in concrete strengths. Table 4.1 contains the compressive strength of the concrete at the time of testing, and the difference in concrete strengths between the $\frac{1}{2}$ inch and 0.6 inch beams can readily be seen. The 0.6 inch diameter strand specimens had consistently higher concrete strengths than those with $\frac{1}{2}$ inch diameter strand. The average compressive strength was 5342 psi and 6905 psi for the $\frac{1}{2}$ inch and 0.6 inch specimens, respectively.

4.4 Effect of Cracking on Beam Capacity

The cracking phenomenon is more complex in prestressed concrete than in reinforced concrete. As reported by Janney (7), when a beam is loaded in flexure, tension is induced below the neutral axis and steel stress increases. As the concrete cracks, the bond stress in the immediate vicinity of the crack increases to a limiting value. When the limiting bond stress is attained, local slip between the strand and the concrete occurs along the length of strand adjacent to the crack. After the local slip occurs, the bond stress is relieved, and the stress is reduced to a lower level. Figure 4.9 illustrates the typical strand behavior as cracking

occurred. The steel strain was obtained with the strain gages, and confirms that the steel strain (and hence stress) in the vicinity of a crack drastically increases, followed by a sharp drop to a lower value.

The increase in bond stress can be thought of as a "wave," moving towards the supports as new cracks form. The general slip of the strand occurs when the wave of bond stress reaches the transfer zone (distance from the end of the beam to the point where the pretensioned force is transferred from the strand to the concrete). Since the concrete is not fully prestressed in the transfer zone, flexural shear cracking in the transfer zone, as shown in Figure 4.10, can cause bond slip. However, since cracking does not usually occur under service load conditions, the flexural behavior of a given beam should not be affected by flexural cracking.

When cracking does cause bond slip, the slip causes an increase in stress, and hence a decrease in the strand diameter due to Poisson's Ratio. As the strand diameter decreases, the frictional resistance is reduced, causing a general bond slip. Evidence that a general bond failure occurred is shown in Figure 4.11, where the end slip gages have all rotated. This would indicate a

twisting of the strand, caused by a loss of the frictional and mechanical resistance.

4.5 Effect of Slip on Beam Capacity

The occurrence of bond slip, as described above, has an important influence on the ultimate flexural capacity of a beam. The result of end slip in a pretensioned beam is not necessarily a sudden failure. Since the mechanical interlock still exists, the beam will continue to carry some load. However, the beam may undergo a gradual failure, starting with end slip and ending in a shear failure.

The end slip in a pretensioned beam results in a loss of some of the initial prestress. This is due to the relaxation of the strand caused by the slip. As the level of prestress is reduced, the member becomes more susceptible to web shear. In most of the tests where end slip occurred, web shear cracking was also observed at the same load increment that first slip was detected. Although it was difficult to tell which happened first, the web shear due to loss of prestress is probable. The web shear cracks in turn produce further end slip, by damaging the bond between the strands and the concrete in

the end regions of the beam. Increased slip in the transfer zone finally results in a bond/shear failure. Current research at The University of Texas at Austin is investigating the relationship between bond slip and web shear.

All of the beams which failed in bond underwent considerable web shear cracking. Figure 4.12 shows a picture of the end region of a specimen which failed in bond/shear. The progression of web shear cracking is shown in Figure 4.13. The sequence of cracking began with the development of several small web shear cracks, as shown in Figure 4.13a. The cracks began near the top of the web and propagated toward the bottom of the specimen. After more load was applied, branching of existing cracks and new cracks formed closer to the load point (Figure 4.13b). The existing cracks also continued to propagate toward the bottom of the specimen. An attempt to apply additional load was accompanied by the propagation of the cracks into the upper and lower flanges, as shown in Figure 4.13c. A bond/shear failure occurred when the specimen was not able to carry the applied load due to the "hinge" formed by the shear cracking.

Nonetheless, the occurrence of end slip does not always result in a shear failure. Specimen FA 460-2 A had end slip and web shear cracking occur near the predicted ultimate load. However, the beam was able to carry additional load. As the load was increased, further end slip occurred. Even though the final end slip ranged from 0.04 to 0.18 inches, the failure mechanism was crushing of the concrete (flexural). Therefore, the result of end slip is the possible formation of web shear cracking, which can precipitate a gradual collapse if the mechanical interlock is not strong enough to resist further slip.

4.6 Moment Capacity

The minimum embedment of the strands to develop the predicted moment capacity of a beam is 72 inches and 86 inches for the $\frac{1}{2}$ and 0.6 inch diameter pretensioning strand, respectively. These development lengths correspond to approximately 144 times the strand diameter ($144d_b$) or 90 percent of the current code provision ($0.9L_d$) for both strand sizes. However, if a design constraint of "no slip at flexural failure" is imposed, the embedment lengths would be considerably

longer. The condition of "no slip at flexural failure" is important since it is possible to have a flexural failure with some end slip. Since the load range in which the flexural behavior changes from a flexural failure to a bond/shear failure is very narrow, the problem occurs in defining the amount of end slip which is acceptable.

The ratios of measured ultimate moment to the calculated ultimate moment are also tabulated for each test in Table 4.1. All of the tests which ended with a flexural failure were within 5 percent of the nominal moment capacity predicted by a strain compatibility analysis. Specimens FA 550-1A, FA 460-1A, and FA 460-6B were the only tests which did not attain the predicted nominal moment capacity. However, the specimens still failed in flexure, since failure was accompanied by the crushing of concrete in the upper flange.

Even the tests which ended in a bond failure were able to reach at least 90 percent of the theoretical moment capacity. This further illustrates the narrow load range between a flexural failure and a bond/shear failure. As shown in Table 4.3, half of the specimens which failed in bond (FA 550-1B, FA 550-2B, and FA 550-

4A) exceeded the predicted moment capacity. Therefore, the nominal moment capacity of the specimens was not drastically affected by the failure mode.

4.7 Concluding Remarks

Although the moment capacity is not greatly affected by the mode of failure, the flexural behavior is drastically different for both modes of failure. All of the specimens behaved similarly up to approximately 85 percent of the predicted moment capacity. The specimens which failed in flexure continued to carry load, and exhibited a ductile failure (large deformations and crushing of concrete). However, the specimens which failed in bond/shear abruptly lost ductility and load carrying capacity with the occurrence of bond slip.

The change in behavior between a flexural failure and a bond/shear failure occurred in a very narrow load range. The sudden change in behavior took place when web shear cracking and bond slip occurred. Since a ductile type of failure is desirable, the code should assure that a ductile flexural failure occurs, in addition to adequate moment capacity. This would prevent an

unexpected and possibly catastrophic failure. General observations for each test are contained in Appendix F.

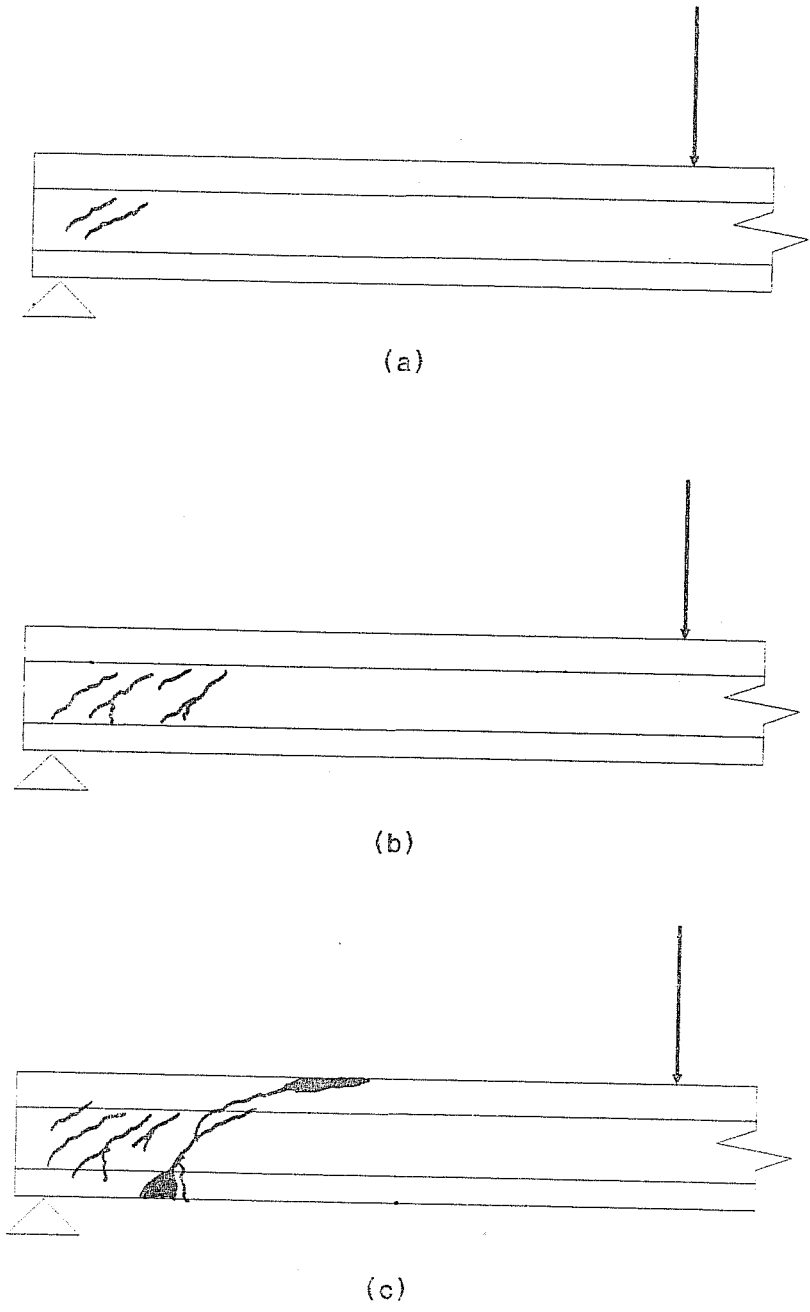


Figure 4.13 Sequence of Web Shear Cracking

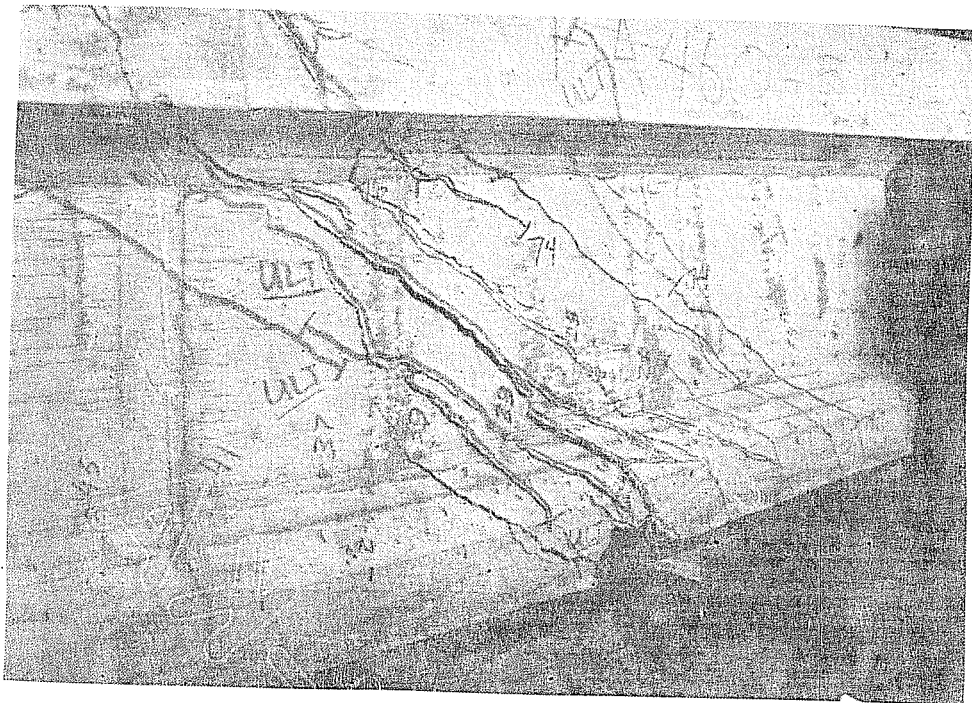


Figure 4.12 End Region After Bond/Shear Failure

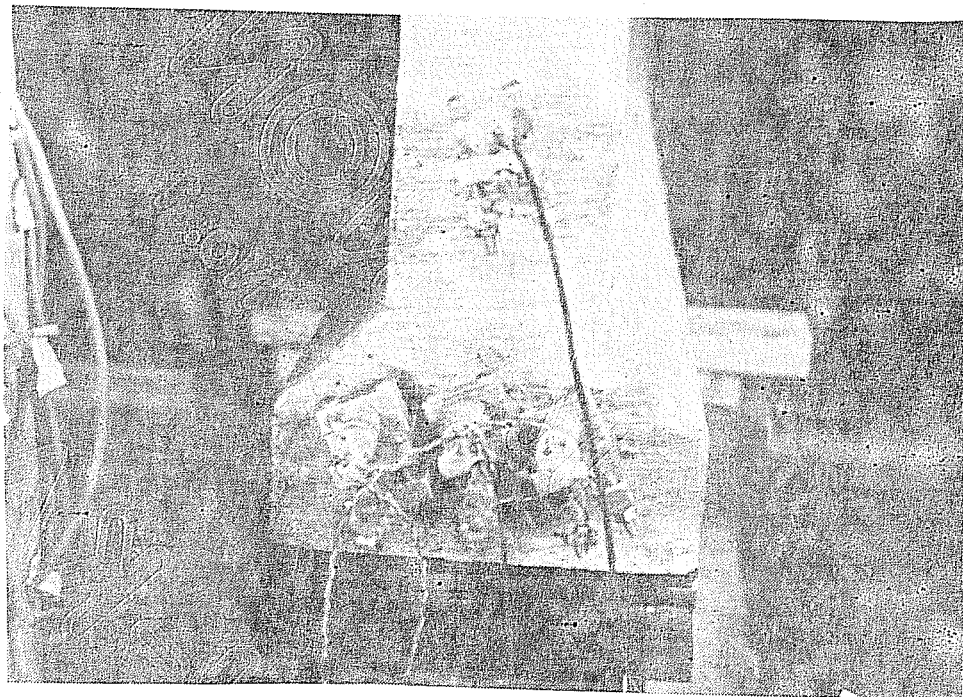
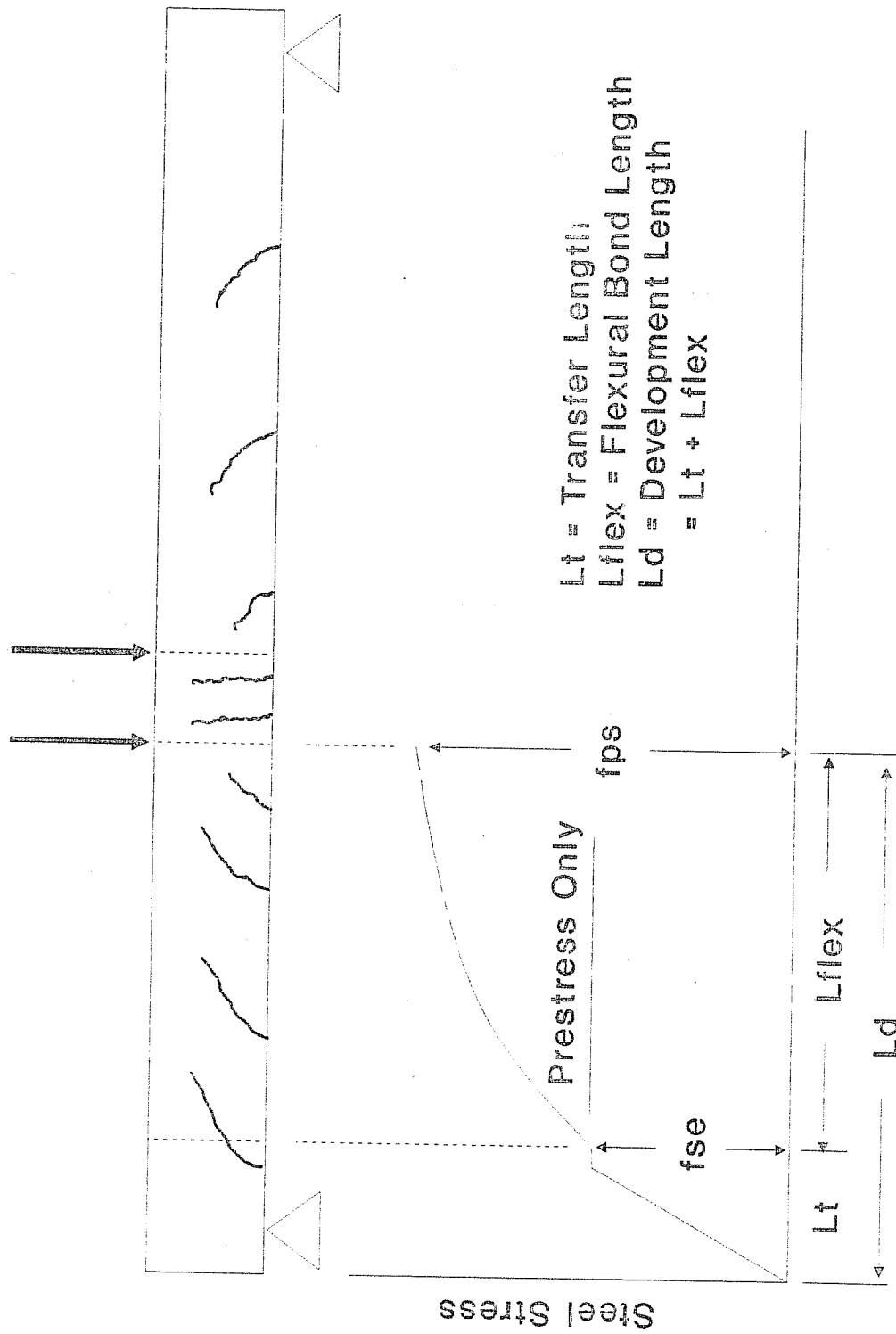


Figure 4.11 Rotation of End Slip Gages



Distance from free end of strand

Figure 4.10 Cracking Along Length of Specimen

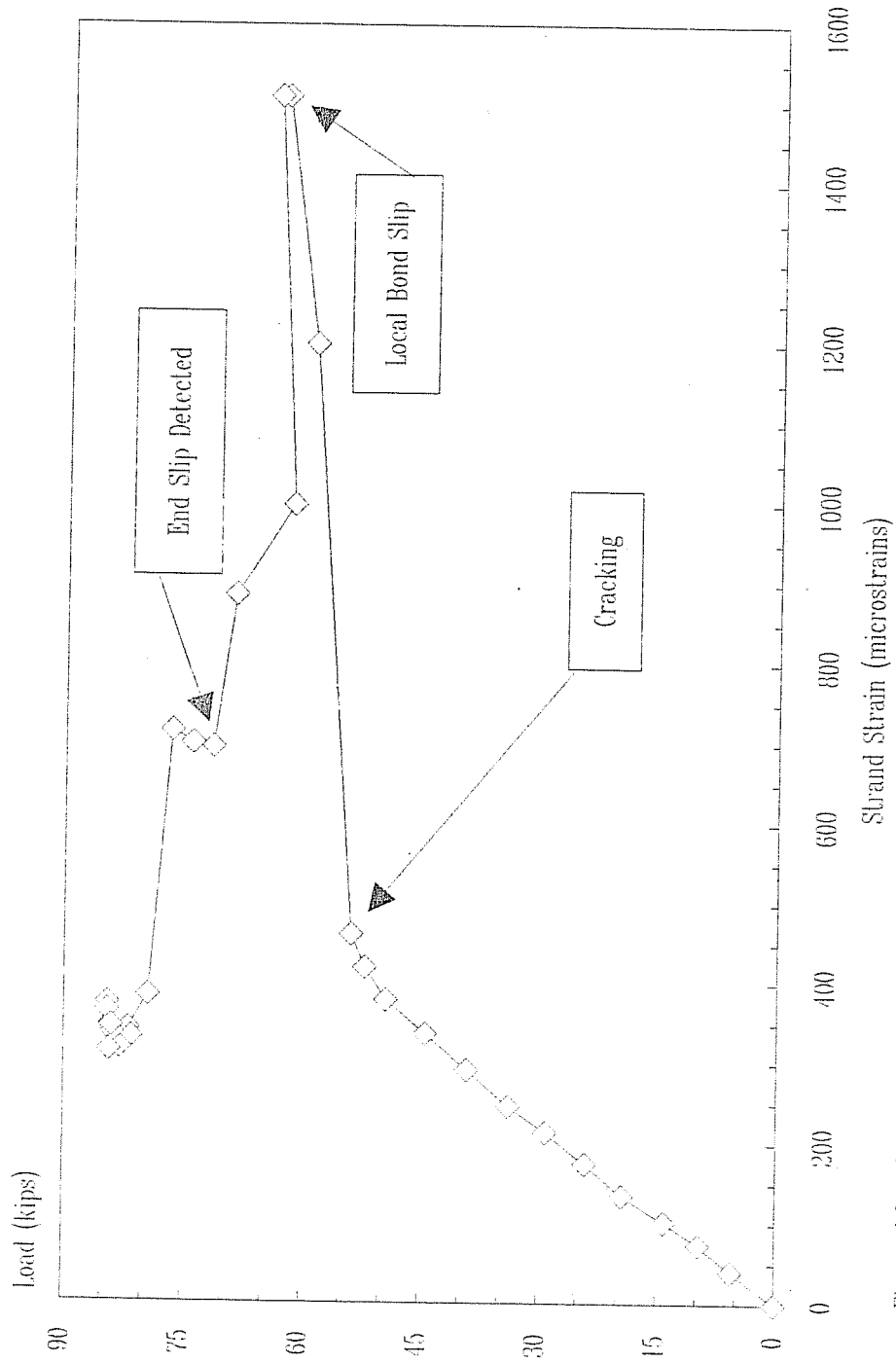


Figure 4.9 Load vs. Steel Strain

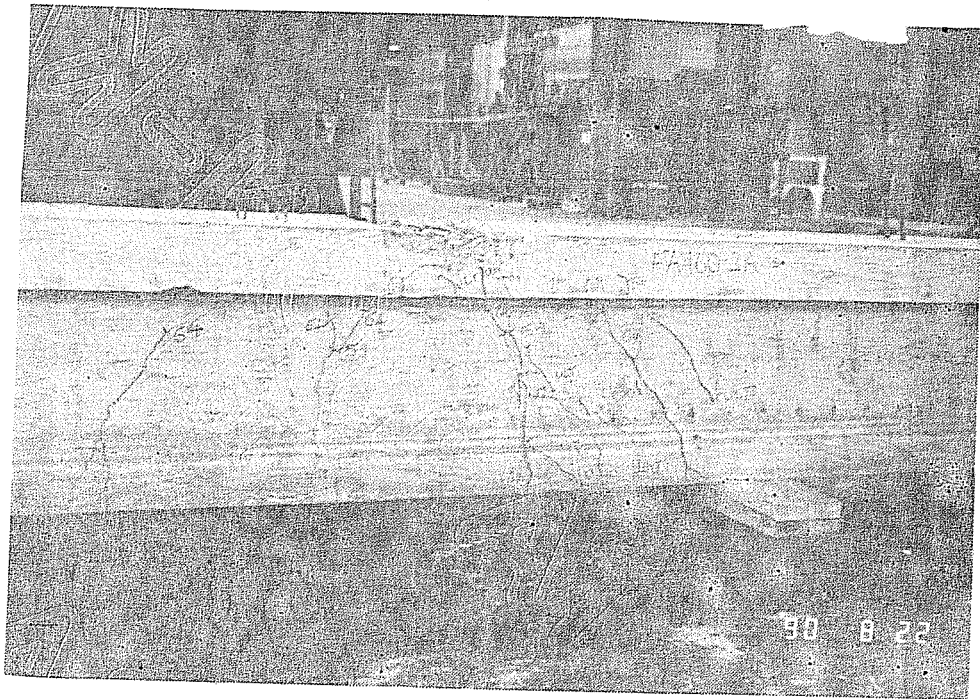


Figure 4.8 Crack Pattern for FA460-2A

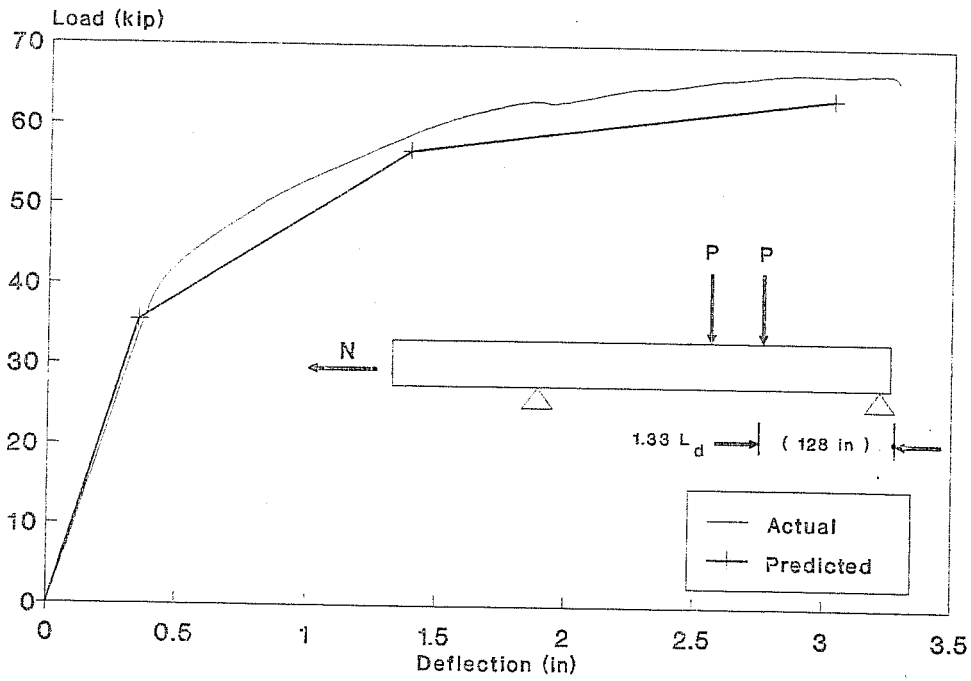


Figure 4.5 FA 460-1 Test B - Load vs. Deflection

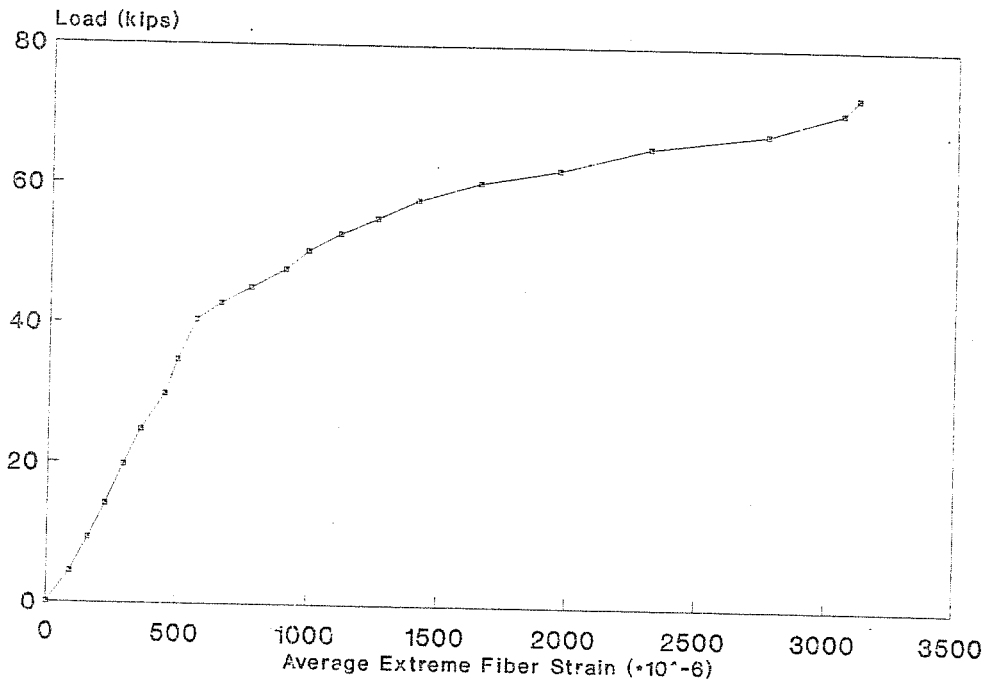


Figure 4.6 FA 460-1 Test B - Load vs. Extreme Fiber Strain

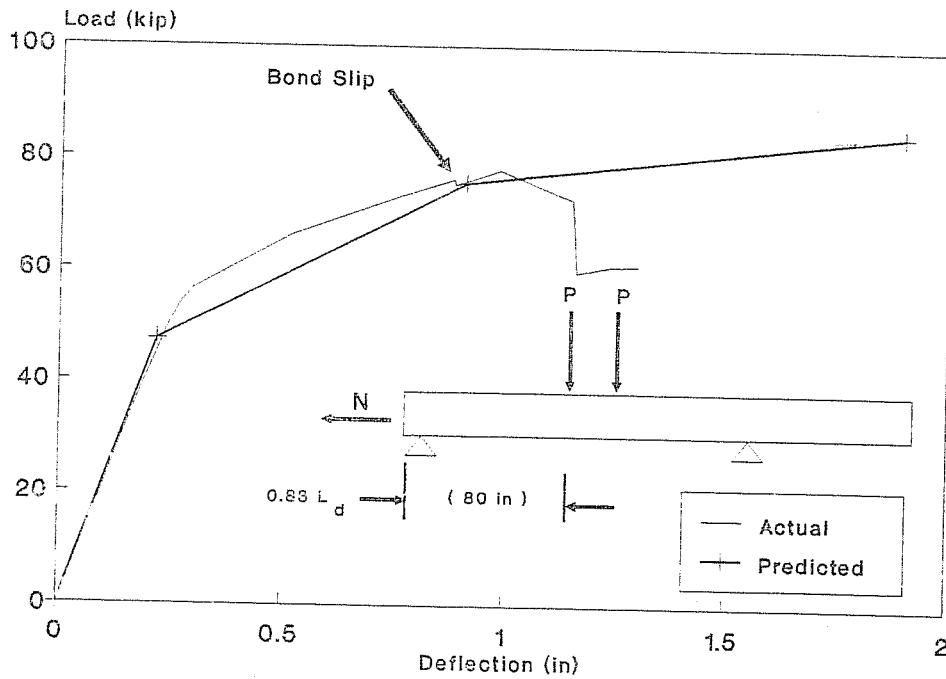


Figure 4.3 FA 460-5 Test A - Load vs. Deflection

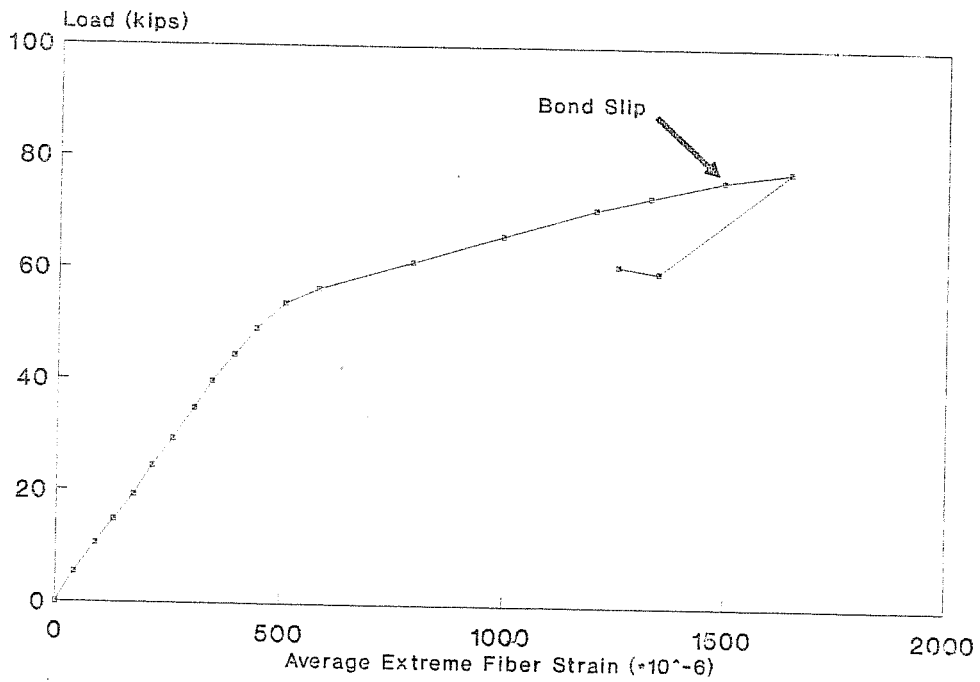


Figure 4.4 FA 460-5 Test A - Load vs. Extreme Fiber Strain

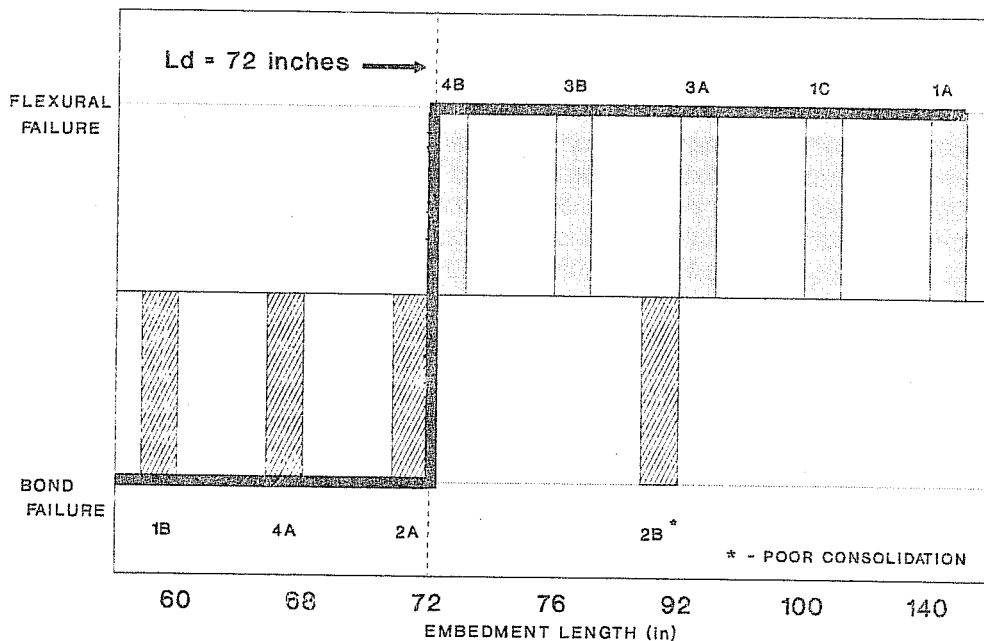


Figure 4.1 Plot of Development Length Results for 0.5 inch Specimens

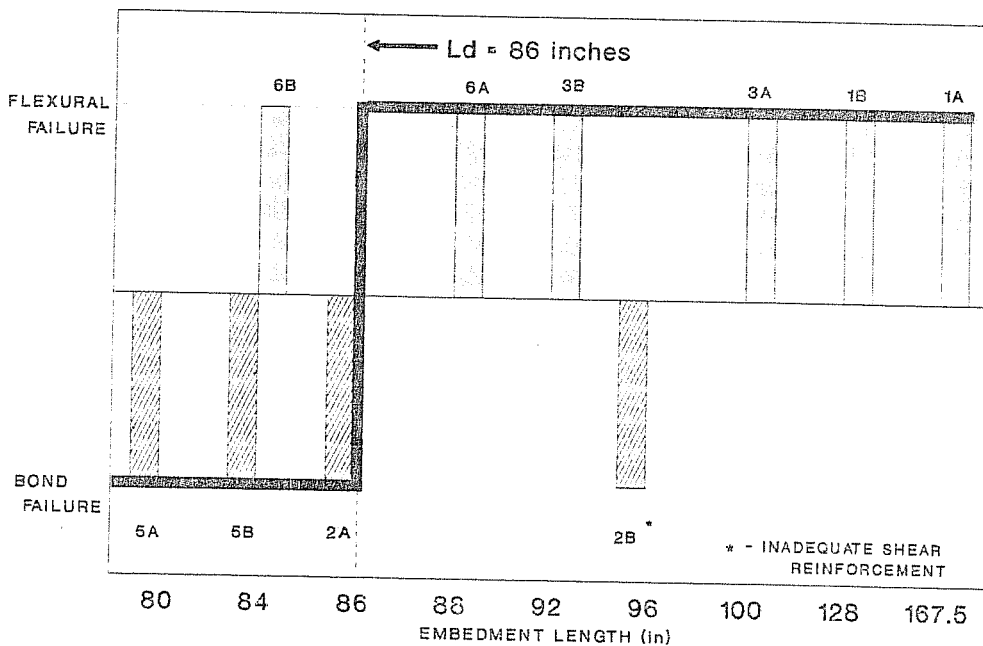


Figure 4.2 Plot of Development Length Results for 0.6 inch Specimens

CHAPTER FIVE

COMPARISON TO OTHER RESULTS

The past research on the development length of pretensioned strand is very limited. One of the main problems in testing for the development length is the considerable amount of scatter in the results. Another problem is the large number of specimens required to obtain conclusive results. The studies conducted in the 1950's and 60's will not be covered, since the strand size, concrete strength properties, and the method of pretensioning have all significantly changed since then. Table 5.1 presents the results from the current research program compared to the previous studies.

5.1 AASHTO/ACI Equation

The current code provisions for the development length of pretensioned strand are in Section 9.27.1 of the AASHTO code (14). The equation for fully bonded strand is:

$$(f_{ps} - (2/3)f_{se}) * d_b$$

This expression is also used by ACI. By using the average values of steel stress obtained from the strain gages, the code predicts a development length of $160d_b$. This corresponds to 80 inches and 96 inches for the $\frac{1}{2}$ inch and 0.6 inch strand, respectively.

5.2 Burdette and Deatherage

The research conducted at The University of Tennessee, by Burdette and Deatherage (2), was recently completed. Although the final report has been submitted to the Prestressed Concrete Institute, the detailed discussion of the development length results has not been presented yet. Of the 39 tests run, four were on beams containing unweathered $\frac{1}{2}$ inch strand, and eight with 0.6 inch unweathered strand.

The size of the beams and test methods used were comparable to those used in this research program. The main difference is that The University of Tennessee specimens were slightly larger and were produced at a precasting plant. As Table 5.1 illustrates, the results

for the development of the $\frac{1}{2}$ inch and 0.6 inch strand are similar to those obtained in this study.

5.3 Cousins, Johnston, and Zia

Cousins, Johnston, and Zia (4) have also completed their research on the development length of pretensioned strand. The focus of the study was on epoxy-coated strand, and used uncoated strand as the control group. There were six $\frac{1}{2}$ inch and four 0.6 inch uncoated strand tests. The specimens were single strand, and had a rectangular cross section. The study was performed at North Carolina State University.

Test data reported by the investigators indicate a required embedment length of 1.9 and 1.7 times the predicted AASHTO/ACI value for the $\frac{1}{2}$ inch and 0.6 inch strand, respectively. These are considerably higher than the results from this study and those from Burdette and Deatherage.

One possible reason for the difference between the test results is the size of the specimens at North Carolina State. The relatively small cross sections (5"x8" for $\frac{1}{2}$ inch strand and 6"x10" for 0.6 inch strand) tend to generate more errors than the larger specimens.

This is apparent from the first two phases of the research at The University of Texas at Austin. The small, single strand specimens yielded a longer transfer length than the multistrand specimens. After further comparison, the multistrand results were substantiated by other research programs. The use of the multiple strands and larger specimen size more accurately simulates current practice, since multiple strands are used in relatively deep beams.

I believe that another reason for the difference is degree of scatter obtained in the data. The test results presented for this investigation show that none of the $\frac{1}{2}$ inch specimens failed in flexure. Furthermore, only one 0.6 inch specimen failed in flexure. This provides a very wide range of possible development lengths, due to the small number of tests performed.

The development length reported for the uncoated $\frac{1}{2}$ inch specimens was based on the results from the test at $1.9L_d$. This test failed in bond at a moment greater than the average ultimate moment of the other specimens tested in the same series. Therefore, I believe that the results reported by Cousins, Johnston, and Zia are inconclusive.

5.4 Florida Department of Transportation

The research program at the Florida Department of Transportation (FDOT) also used relatively large, multistrand specimens (AASHTO Type-II girders). Details of the test procedure are not available, since a report has not yet been completed. The preliminary results for the research indicate a development length of 1.68 times the length predicted by AASHTO/ACI.

The basis for the difference in measured development length is unknown. The size of the specimen did not pose any potential problems, since the specimens were slightly larger than those used at The University of Tennessee. Perhaps a possible reason for the difference is the scatter in the development length data. Until a preliminary report is available, the explanation of the results obtained at FDOT is only speculative.

5.5 Concluding Remarks

The results obtained by this study and that of Burdette and Deatherage are within 10 percent of the code prediction. Although the current code provisions for the development length of prestressing strand date back to the 1963 edition (ACI 318-63), they appear to be adequate based on the results from Burdette and Deatherage and those reported herein. Even though the material properties have changed and a new strand size is available since 1963, results from this research program indicate that the current code is satisfactory for both $\frac{1}{2}$ inch and 0.6 inch diameter pretensioning strand.

Although I am confident of the results obtained in this study, future testing is needed on full scale girders. The additional tests are necessary to identify any differences in flexural behavior due to the size of the specimen. The future testing will hopefully clarify the differences in the development length results obtained from other research programs, reported herein.

CHAPTER SIX

SUMMARY AND CONCLUSIONS

6.1 Summary

The use of 0.6 inch pretensioning strand was prohibited by FHWA due to the lack of data supporting the behavior of the new size of strand. With the current trend towards high strength concrete and 0.6 inch strands, a definitive study of the transfer and development length was required.

This thesis presents the summary of the results from the third phase of the current research program at The University of Texas at Austin. This phase focused on the development length of $\frac{1}{2}$ inch and 0.6 inch fully bonded strand. The tests were conducted on 22 inch deep 'I' sections, containing either five (5)- $\frac{1}{2}$ inch strands or four (4)-0.6 inch strands. The specimens were fabricated and tested at The Phil M. Ferguson Structural Engineering Laboratory.

The development length was obtained by varying the embedment length of each test. To allow for the inherent scatter in development length data, some of the specimens were set up to fail in either flexure or bond/shear. Since there is very little past research on the development length of prestressing strand, the nineteen (19) tests conducted in this study will greatly contribute to the data base of results.

The required data was obtained using load cells, strain gages, linear variable displacement transducers (LVDT), and a DEMEC mechanical strain gage (for concrete strains). After evaluating the data, a discussion of the results followed. The factors influencing the moment capacity of a specimen were also presented. A comparison to other research and current code provisions were also offered.

6.2 Conclusions

The following conclusions were drawn from the test results:

- 1) The development length of the $\frac{1}{2}$ inch and 0.6 inch diameter strand is approximately 72 inches and 86 inches ($144d_b$), respectively.
- 2) The AASHTO/ACI equation for the development length of pretensioning strand is adequate for $\frac{1}{2}$ inch and 0.6 inch diameter strand based on this study.
- 3) The occurrence of end slip does not always result in a complete bond failure. However, end slip can reduce the web shear capacity and flexural capacity of a beam due to a loss of prestress.
- 4) The 0.6 inch strand exhibits a wider crack spacing than the $\frac{1}{2}$ inch strand. The average flexural crack spacing was 8.4 inches and 14.1 inches for the $\frac{1}{2}$ inch and 0.6 inch diameter strand, respectively.
- 5) Although the moment capacity is not significantly affected by bond slip, the occurrence of slip drastically changes the flexural behavior of a prestressed concrete beam. The ductility and load

carrying capacity of a member is greatly reduced when bond slip occurs.

- 6) Since the change in flexural behavior occurs in a narrow load range, a code provision should be made to assure a ductile failure. This would prevent an unexpected and possibly catastrophic failure due to bond slip.
- 7) Further testing is recommended on full scale beams to identify any possible differences in behavior due to the size of the specimen.

APPENDIX A

STRESS-STRAIN RELATIONSHIP FOR PRETENSIONING STRAND

This appendix contains the stress-strain relationship provided by Florida Wire and Cable Company for the $\frac{1}{2}$ inch and 0.6 inch pretensioning seven-wire strand.

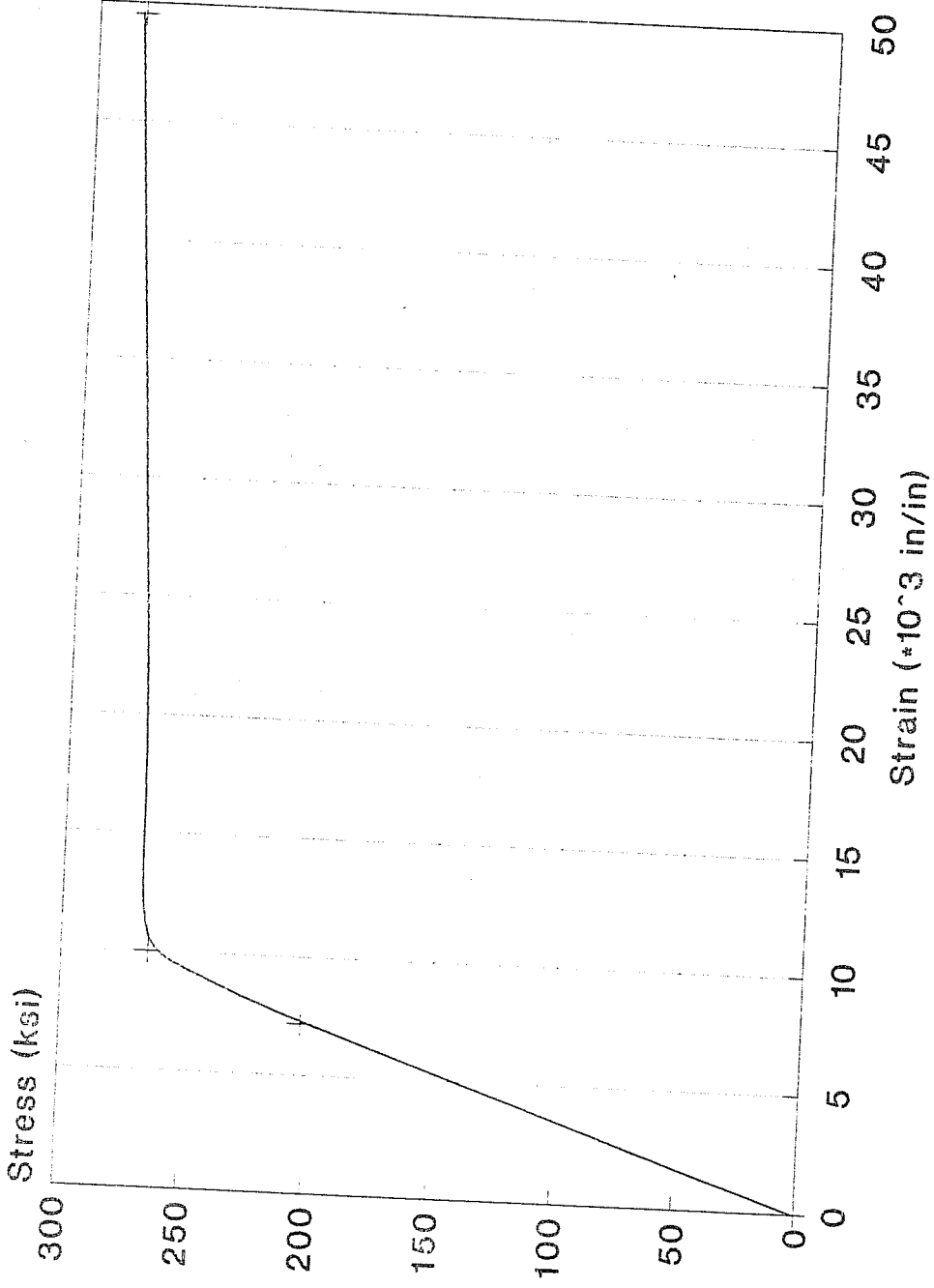


Figure A1: 0.5 inch Diameter Strand

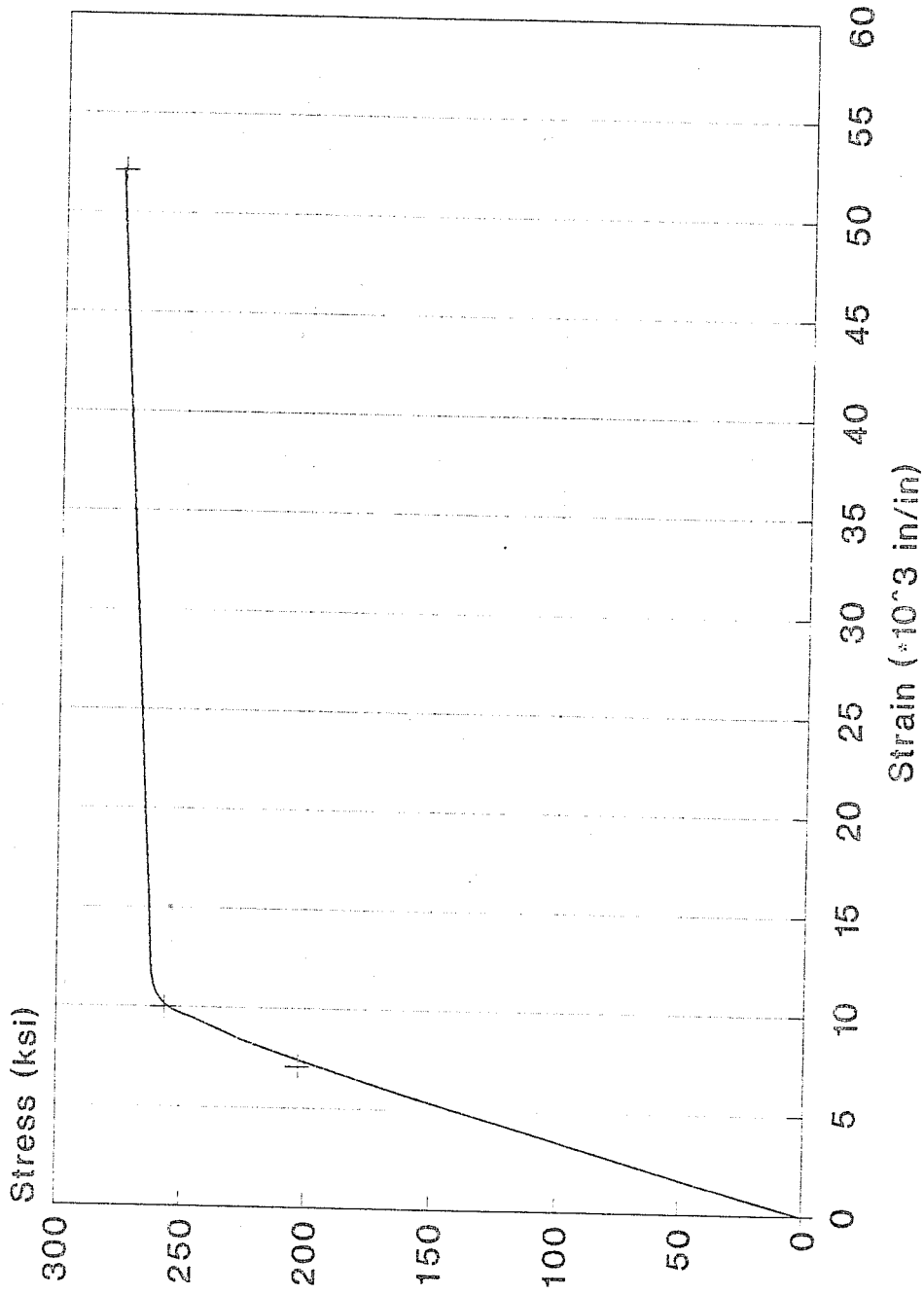


Figure A2: 0.6 inch Diameter Strand

APPENDIX B

CONCRETE STRENGTH vs. TIME

This appendix contains the concrete compressive strength vs. time plots for all nine (9) beams cast. The compressive strength is based on the average of three concrete cylinders.

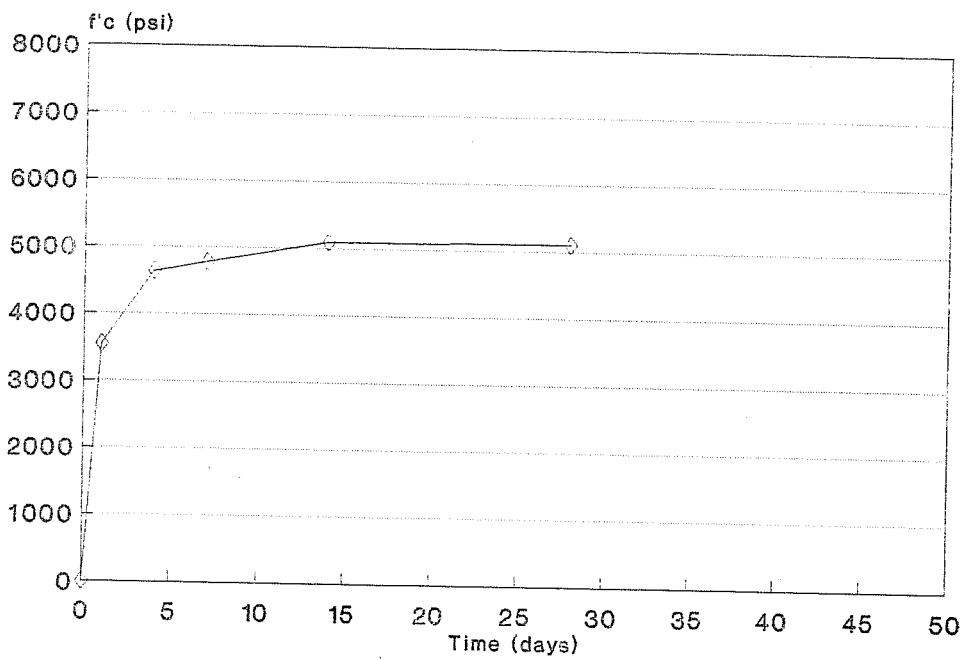


Figure B1: BEAMS FA 550-1 AND 2

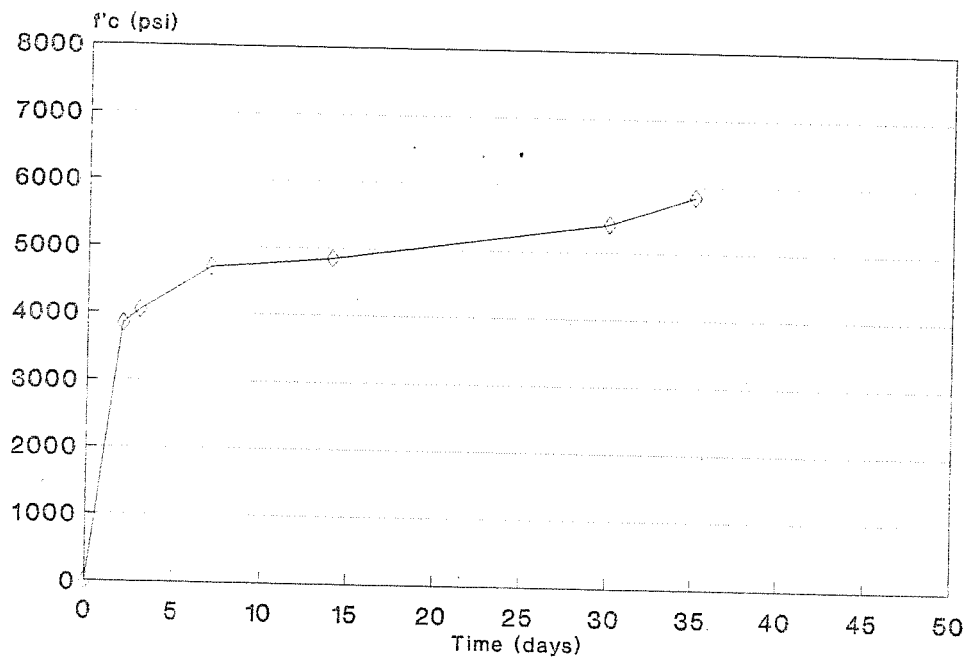


Figure B2: BEAMS FA 550-3 AND 4

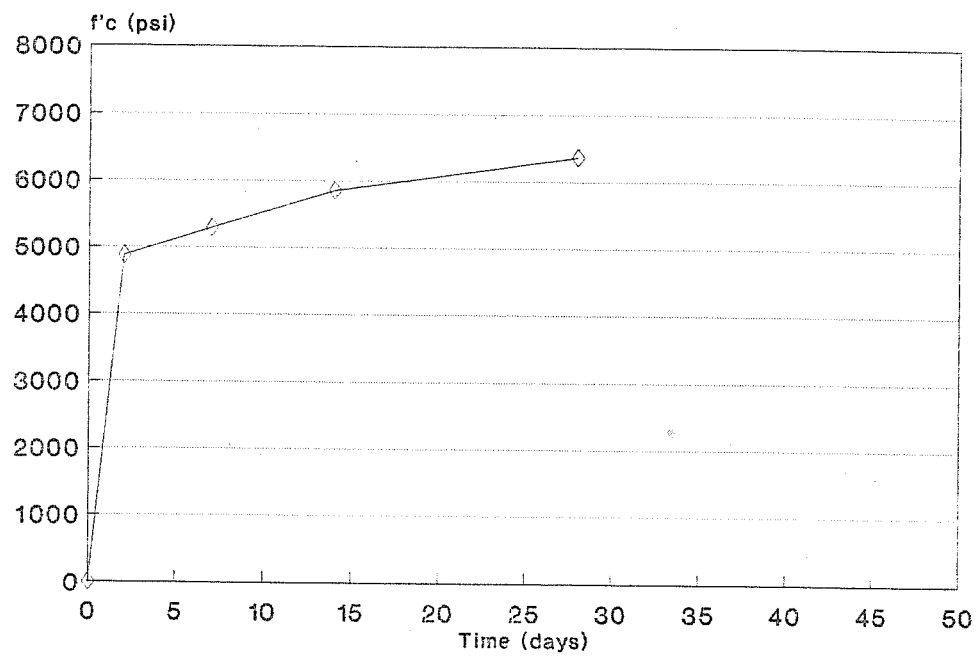


Figure B3: BEAM FA 460-1

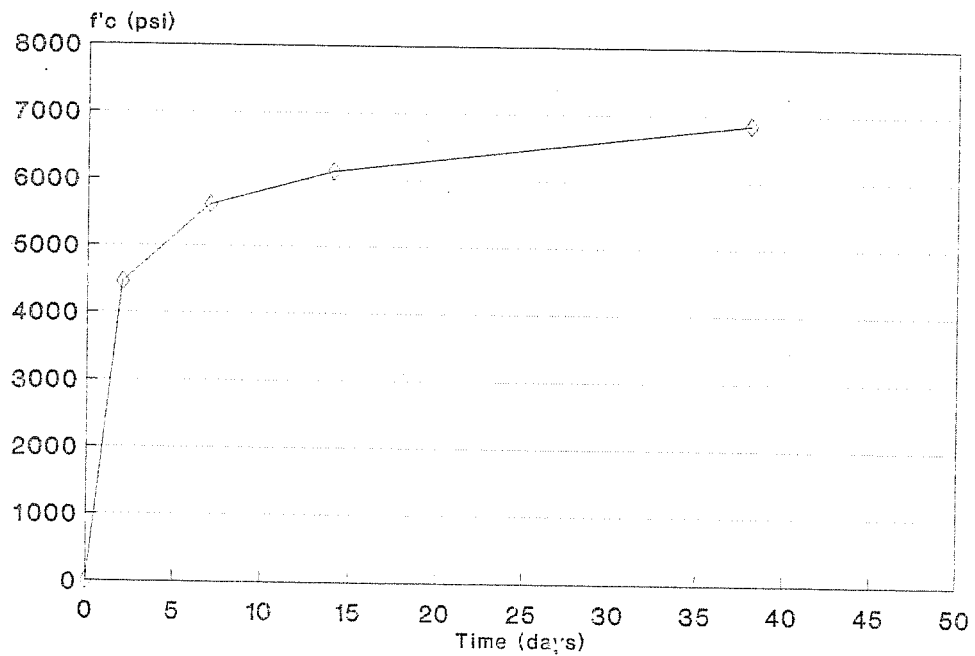


Figure B4: BEAMS FA 460-2 AND 3

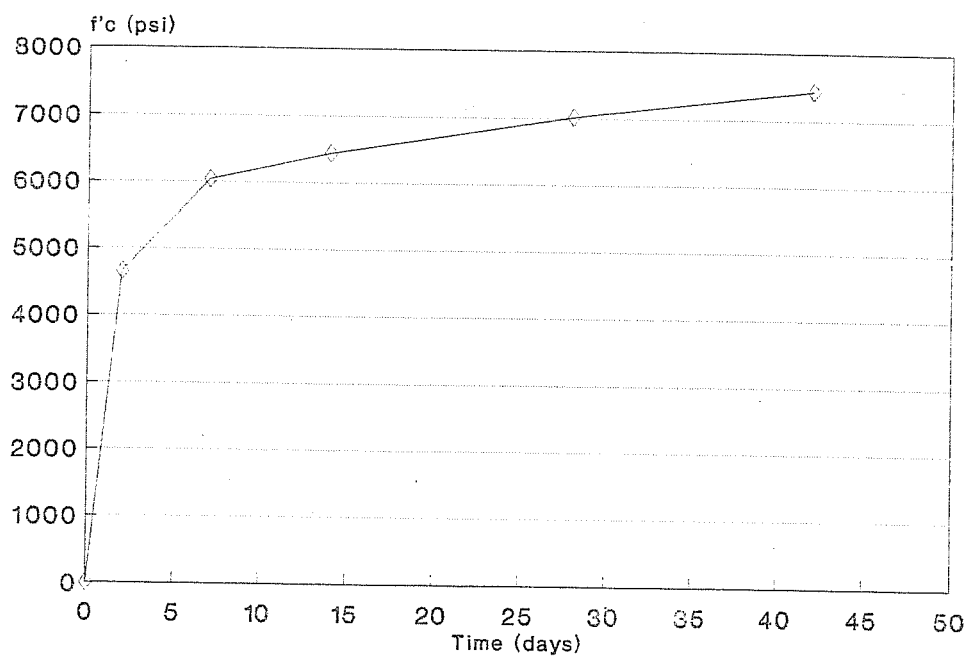


Figure B5: BEAMS FA 460-5 AND 6

APPENDIX C

LOAD vs. DEFLECTION

The load vs. deflection curves for all nineteen (19) tests are contained in this appendix. The deflection is measured between the two load points, and the load corresponds to total load on the system. The predicted curves were calculated using the moment-curvature relationships presented in Appendix E.

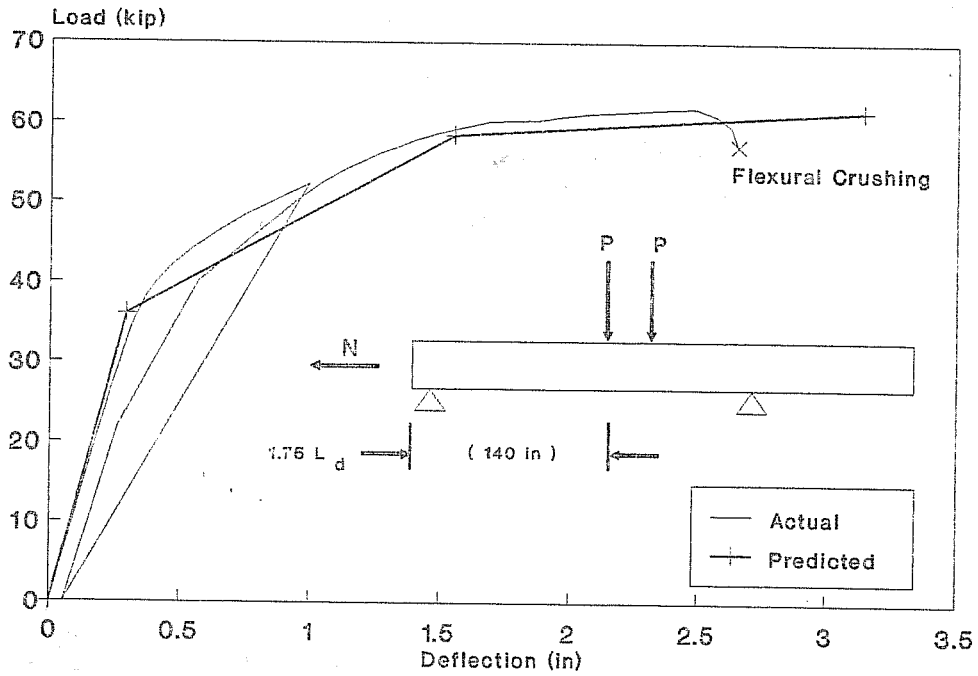


Figure C1: FA 550-1 Test A

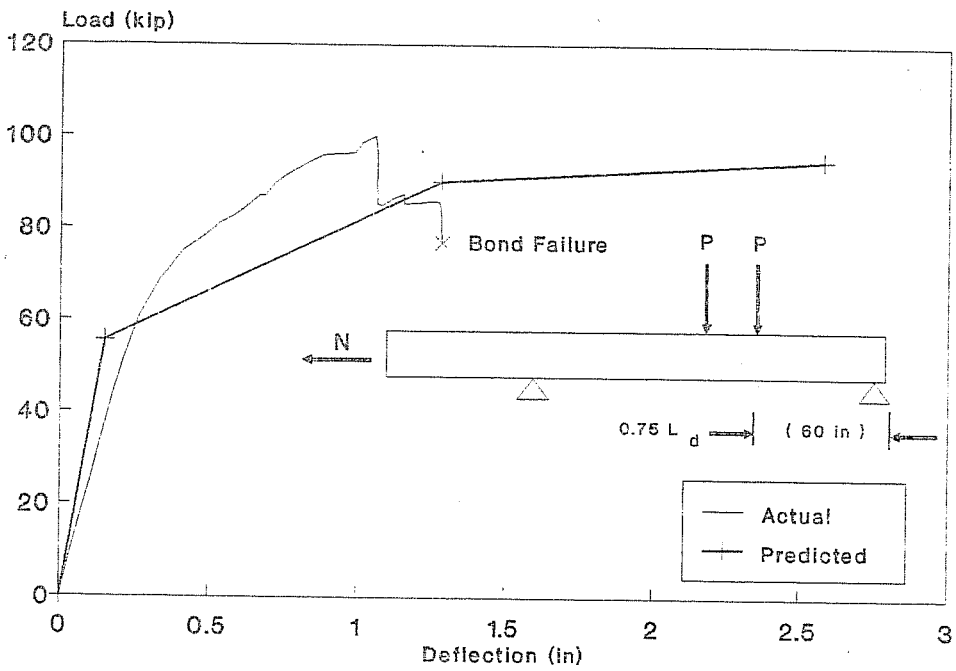


Figure C2: FA 550-1 Test B

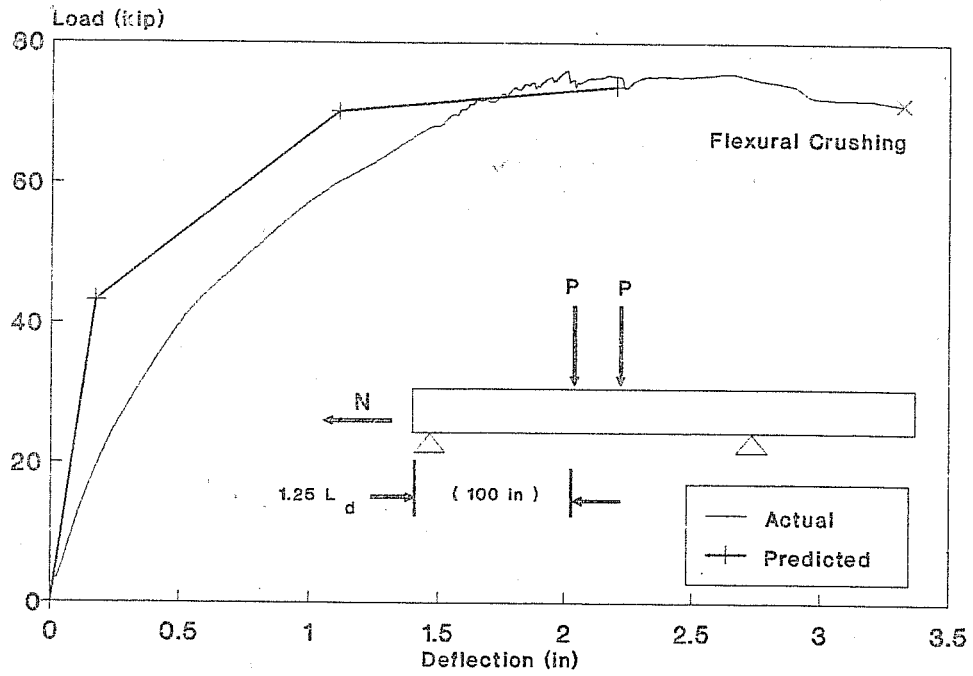


Figure C3: FA 550-1 Test C

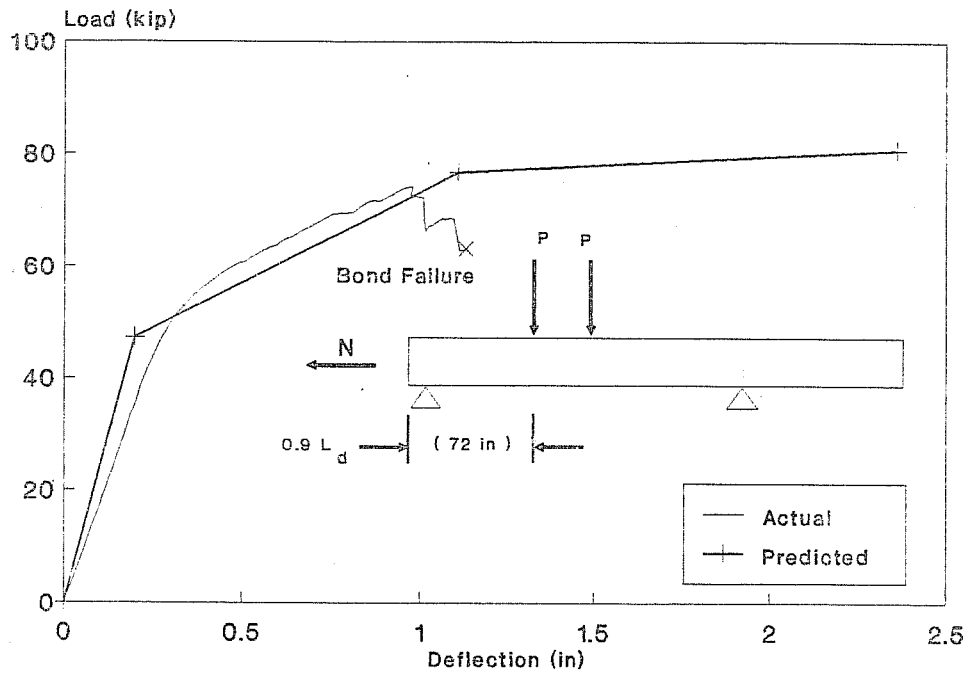


Figure C4: FA 550-2 Test A

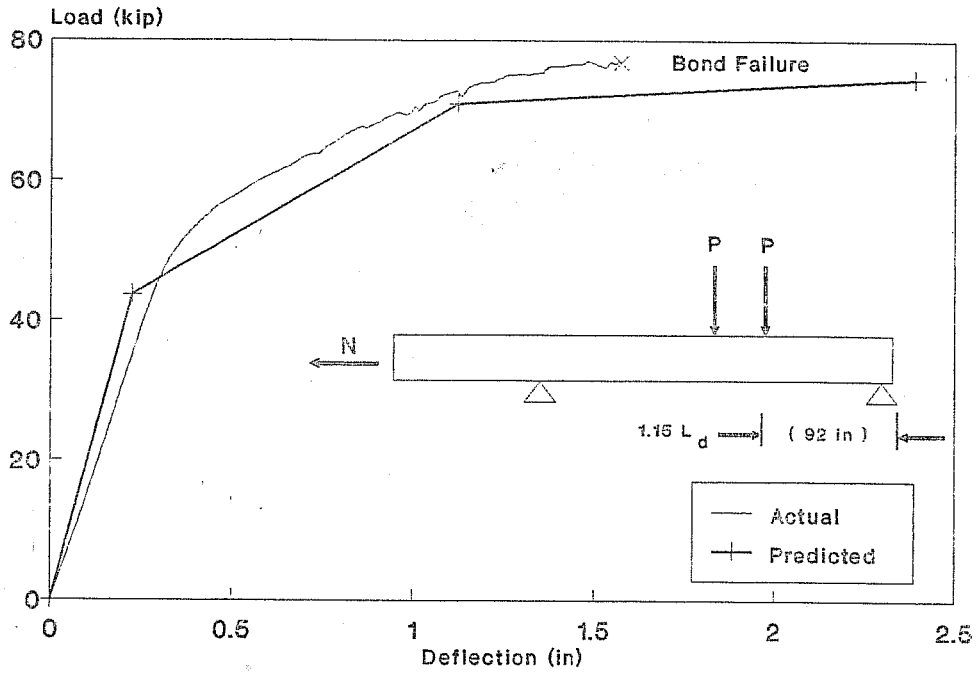


Figure C5: FA 550-2 Test B

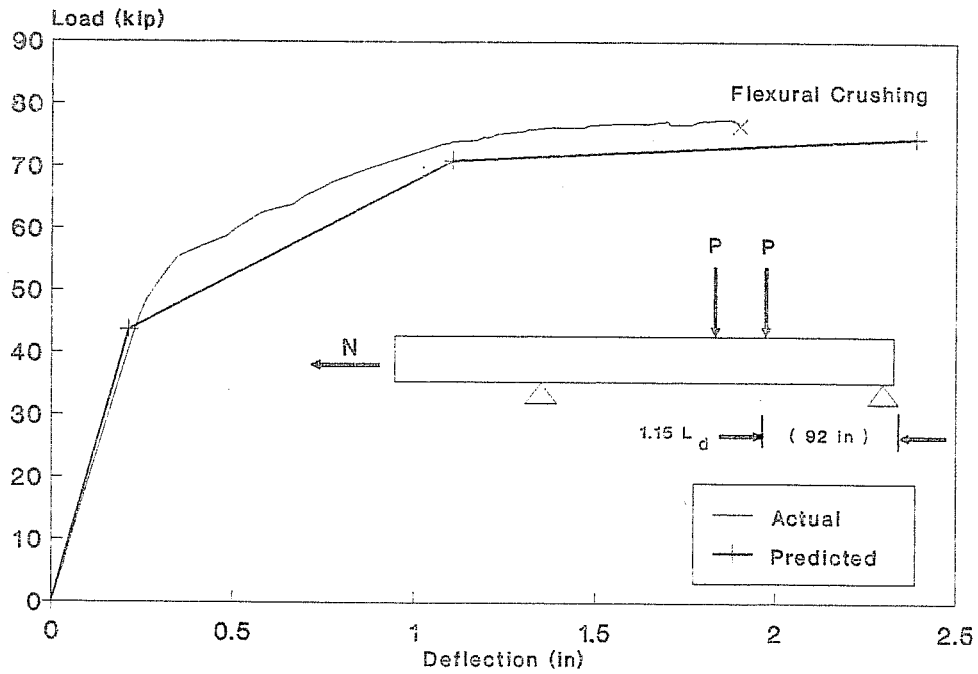


Figure C6: FA 550-3 Test A

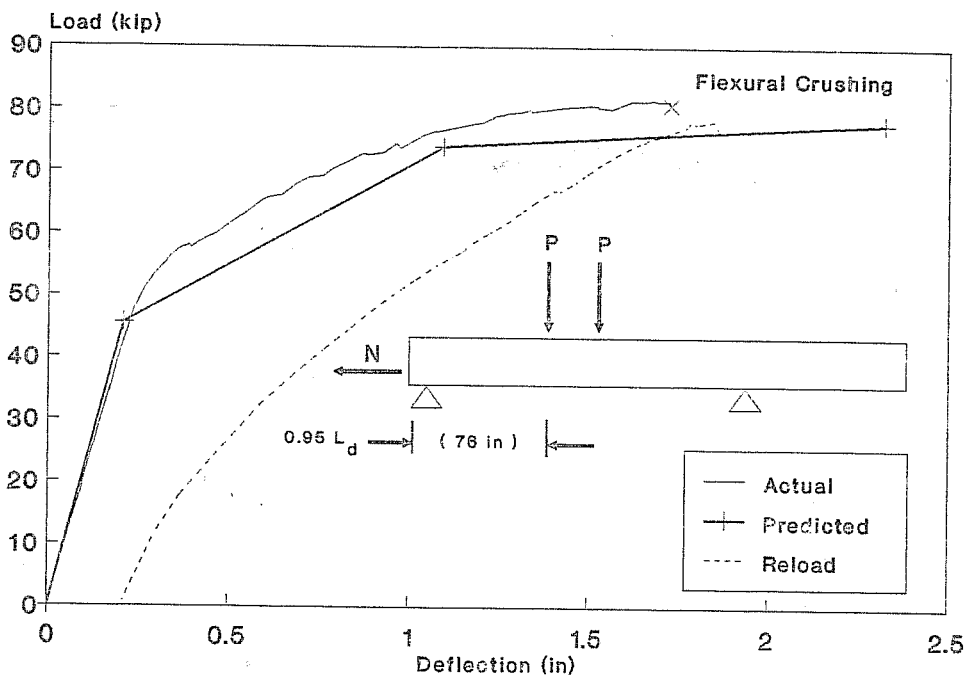


Figure C7: FA 550-3 Test B

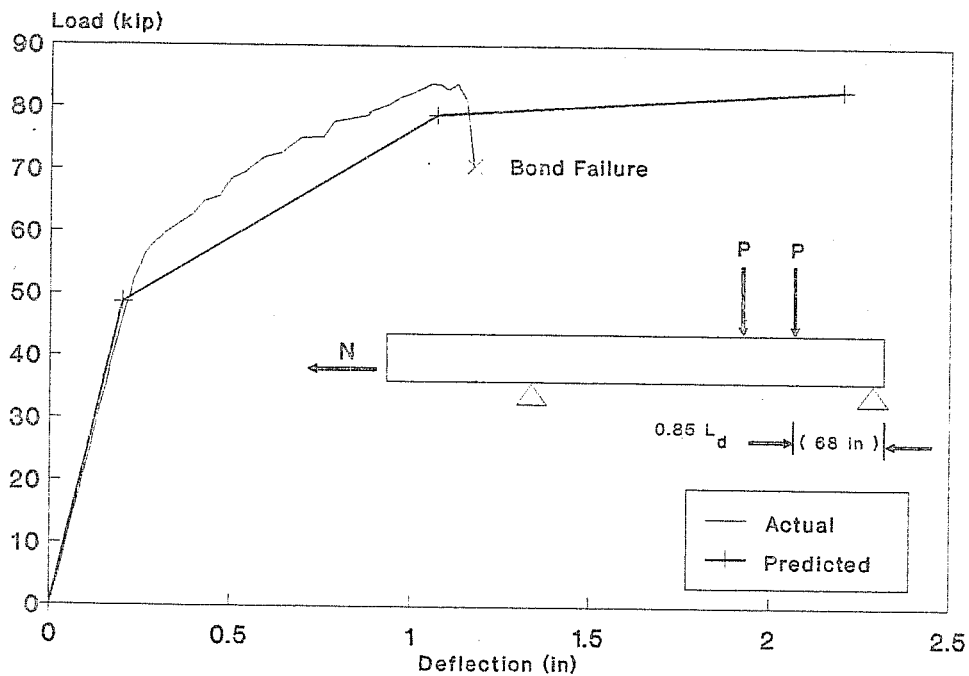


Figure C8: FA 550-4 Test A

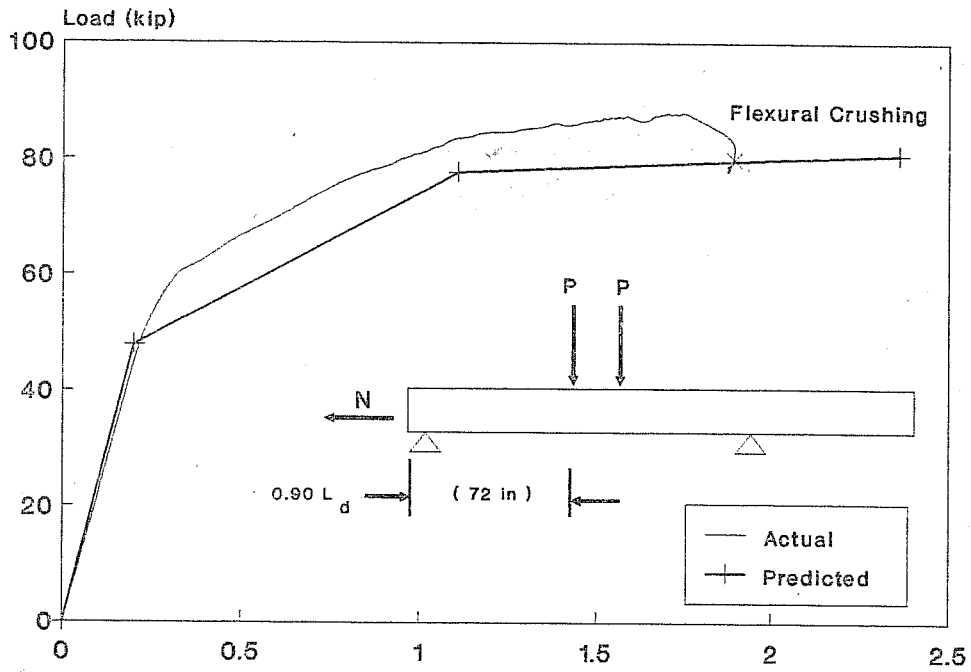


Figure C9: FA 550-4 Test B

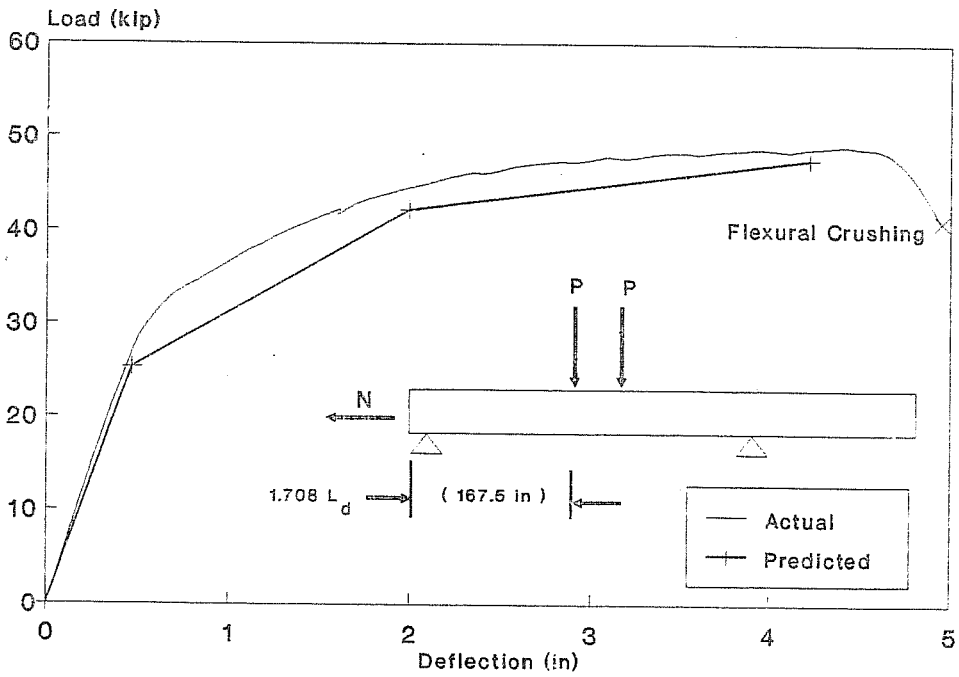


Figure C10: FA 460-1 Test A

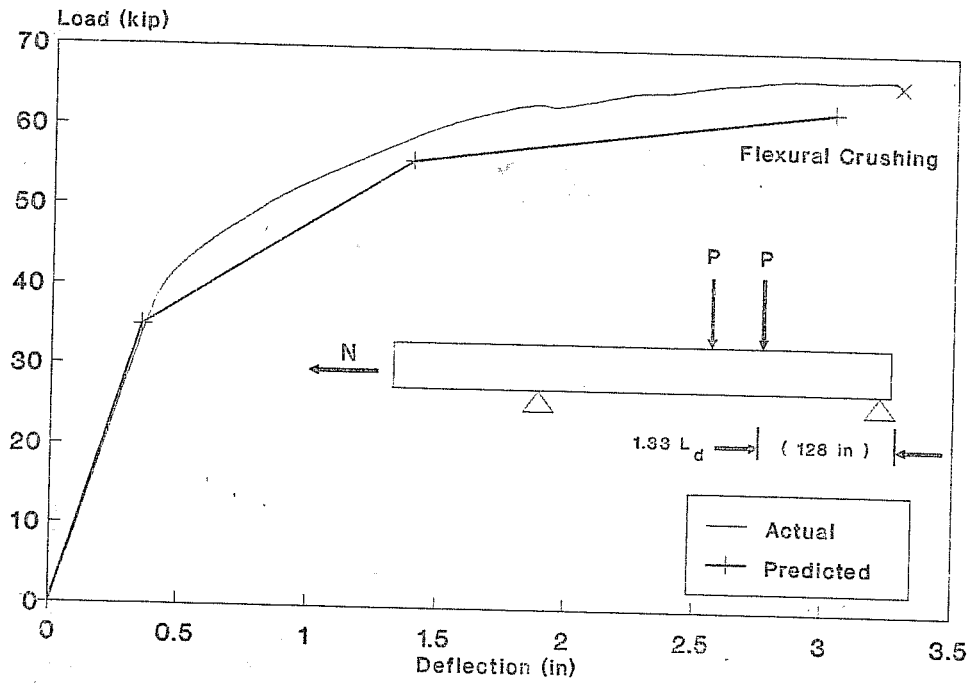


Figure C11: FA 460-1 Test B

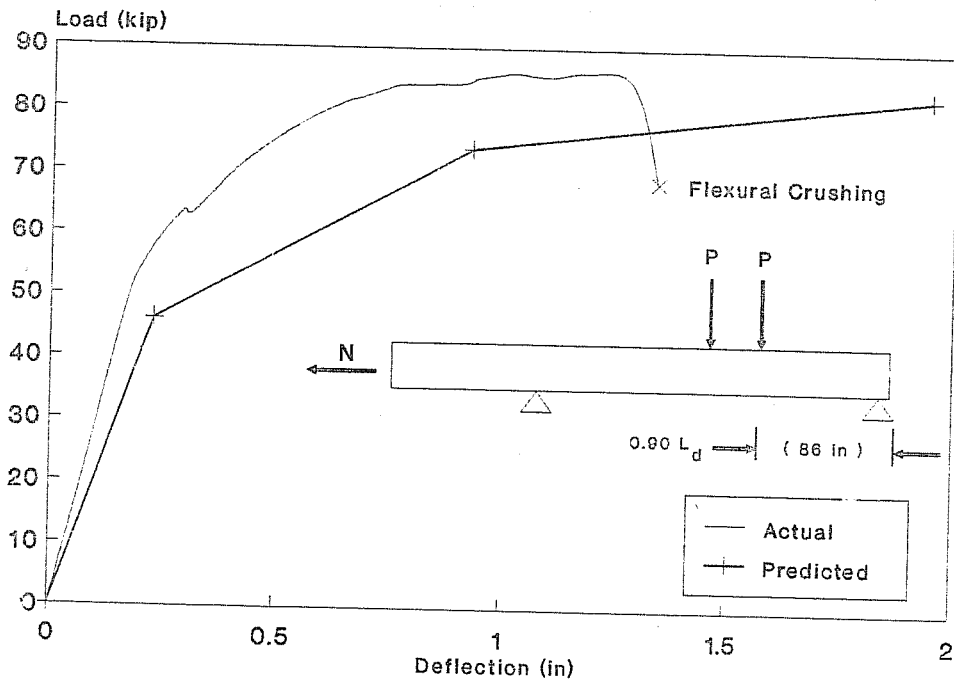


Figure C12: FA 460-2 Test A

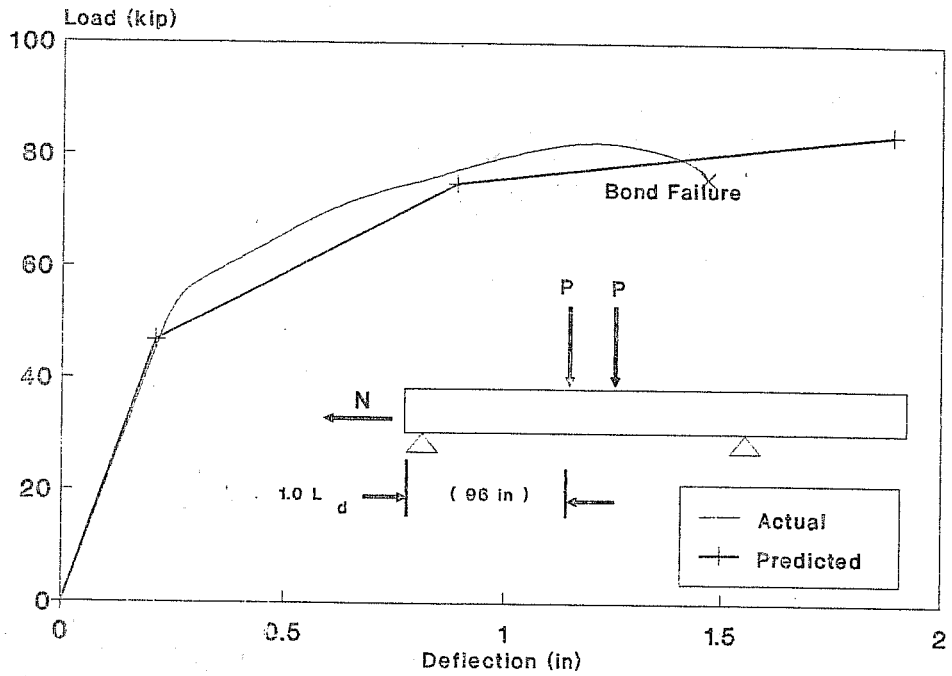


Figure C13: FA 460-2 Test B

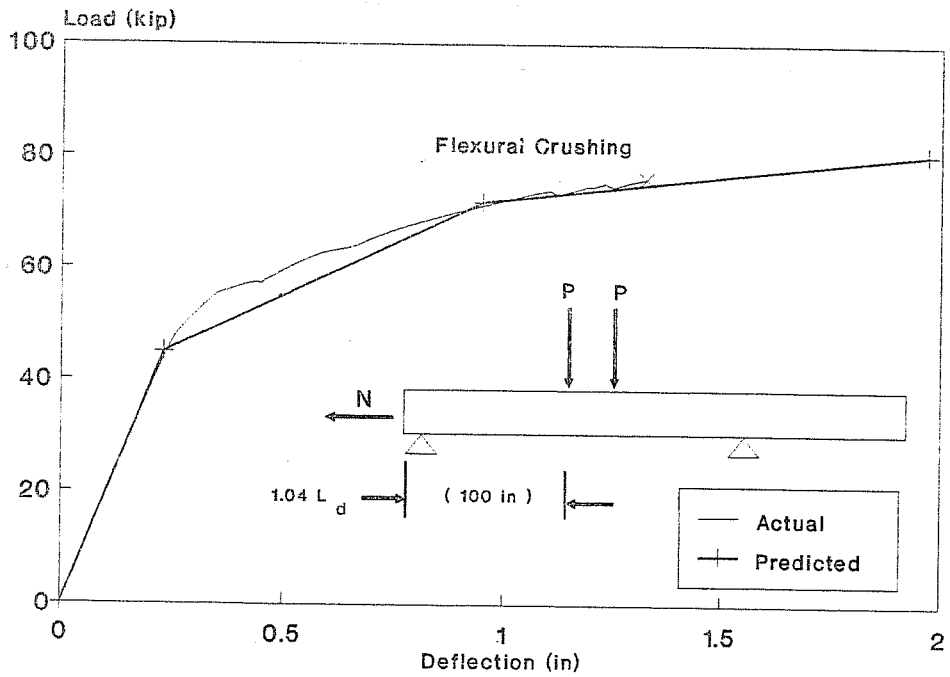


Figure C14: FA 460-3 Test A

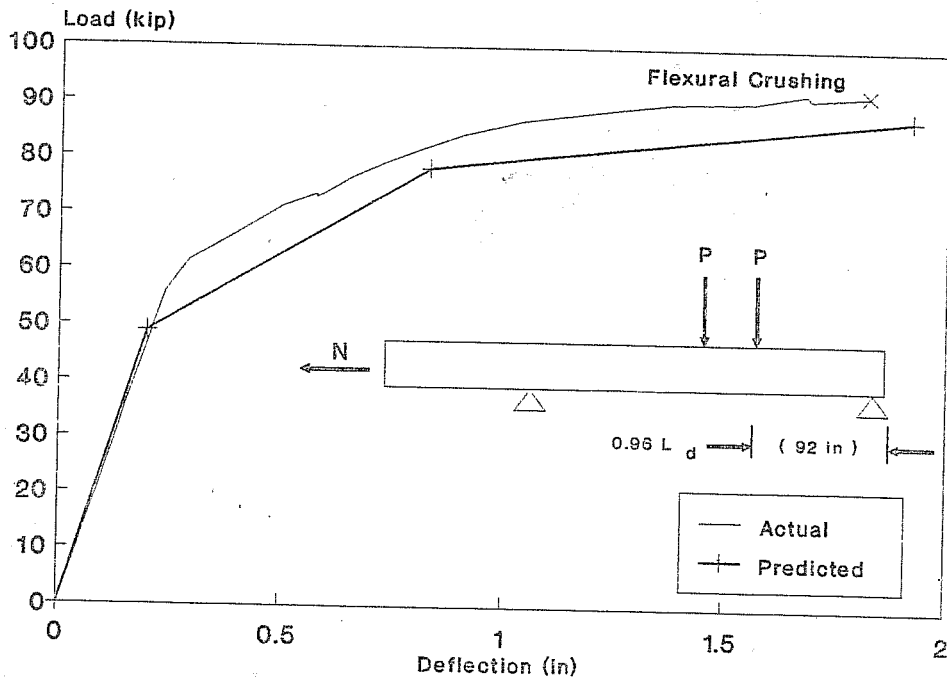


Figure C15: FA 460-3 Test B

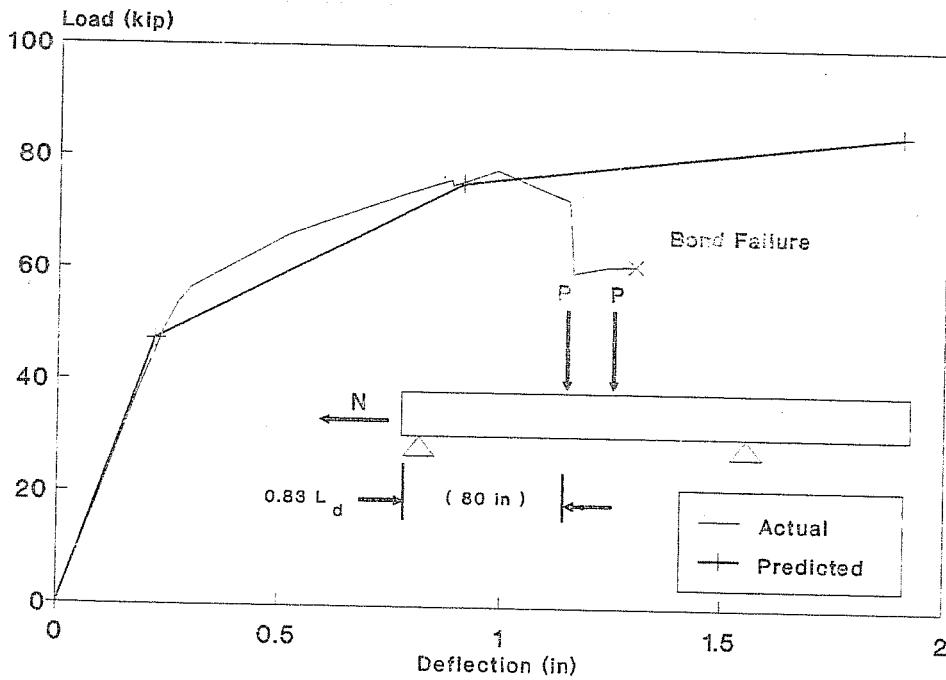


Figure C16: FA 460-5 Test A

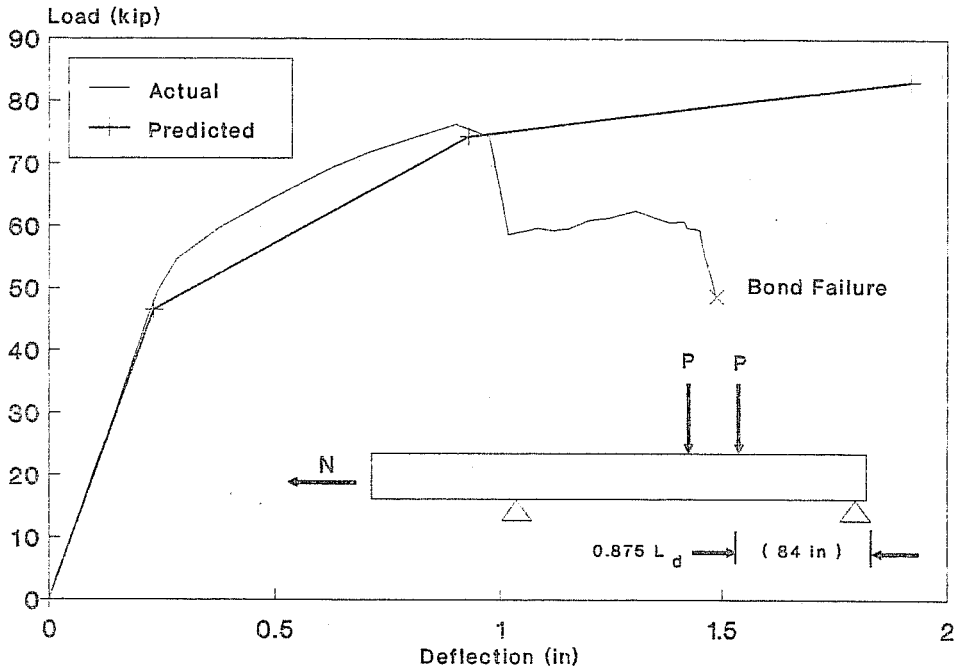


Figure C17: FA 460-5 Test B

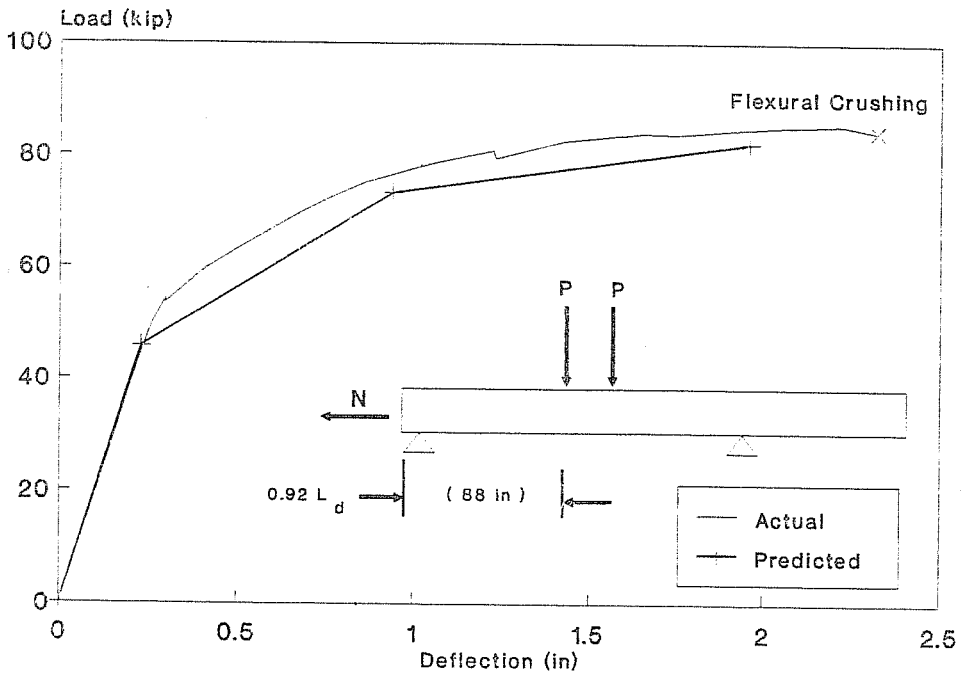


Figure C18: FA 460-6 Test A

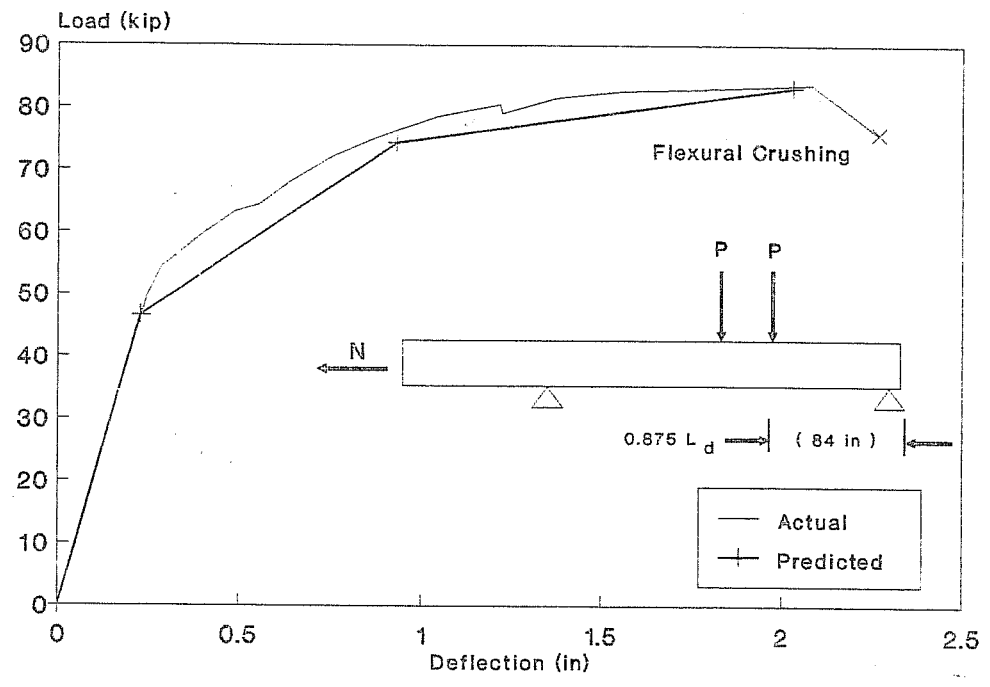


Figure C19: FA 460-6 Test B

APPENDIX D

LOAD vs. CONCRETE COMPRESSIVE STRAIN

The extreme fiber concrete compressive strain is plotted vs the applied load for all nineteen (19) tests in this appendix. The strain was obtained using the DEMEC mechanical gage, and represents the average strain over of four (4) - eight (8) inch gage lengths.

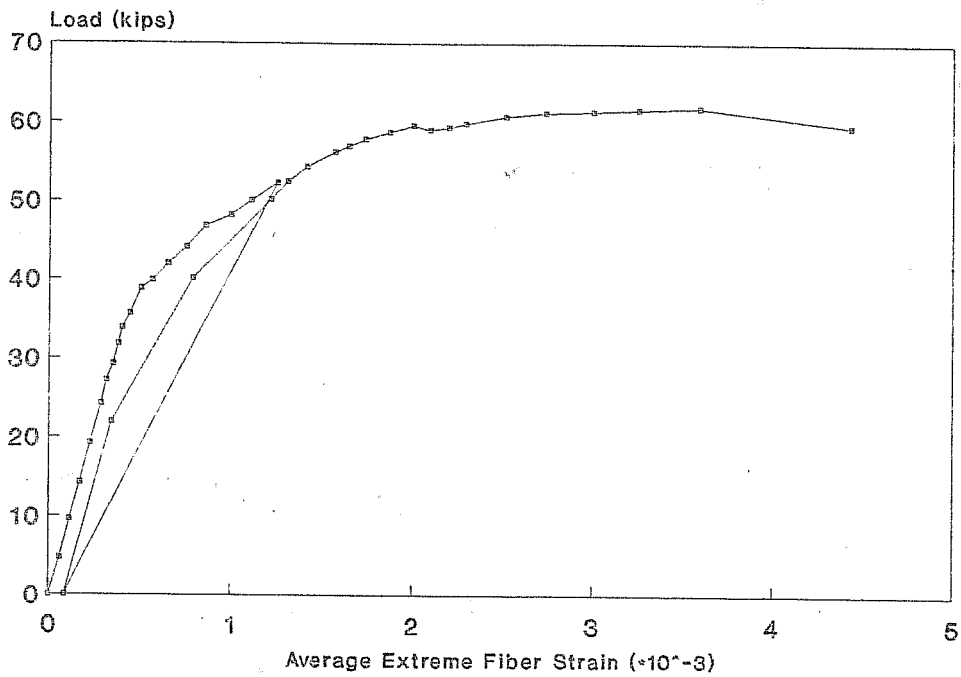


Figure D1: FA 550-1 Test A

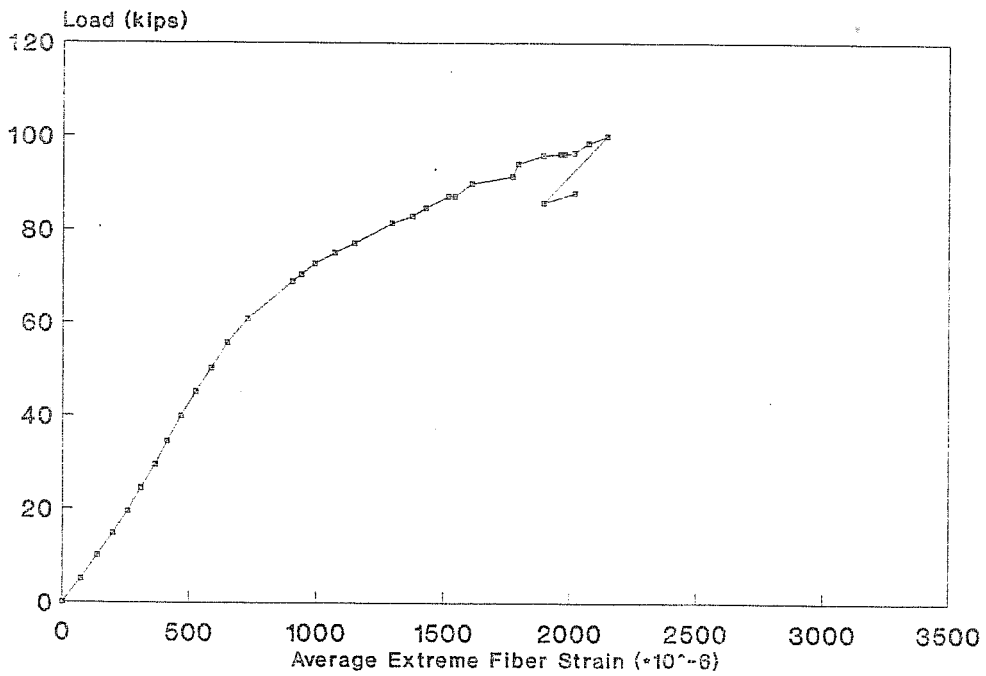


Figure D2: FA 550-1 Test B

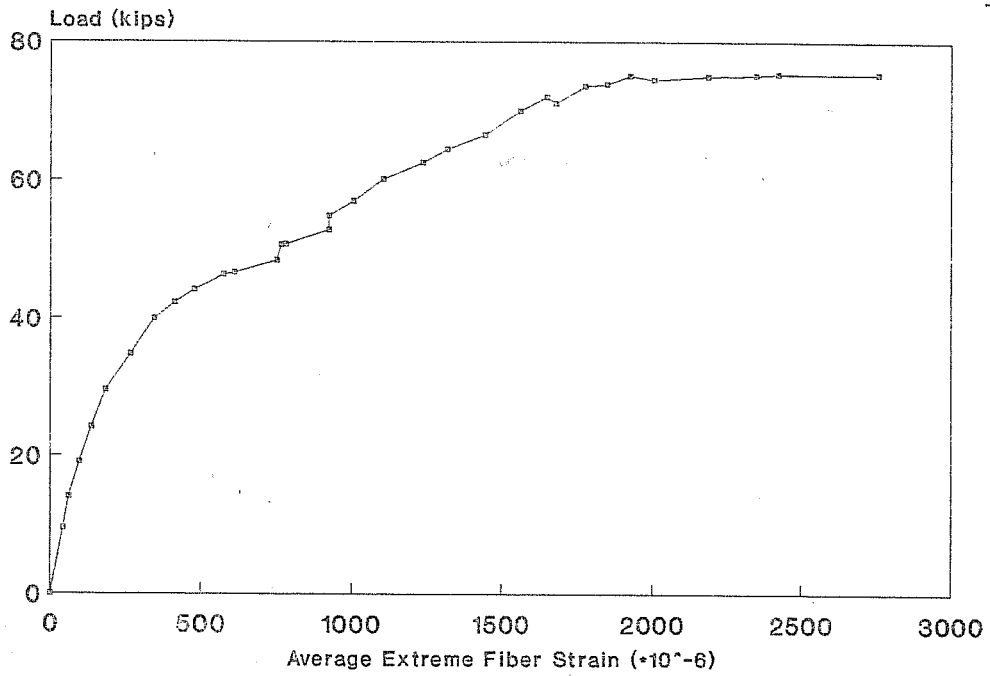


Figure D3: FA 550-1 Test C

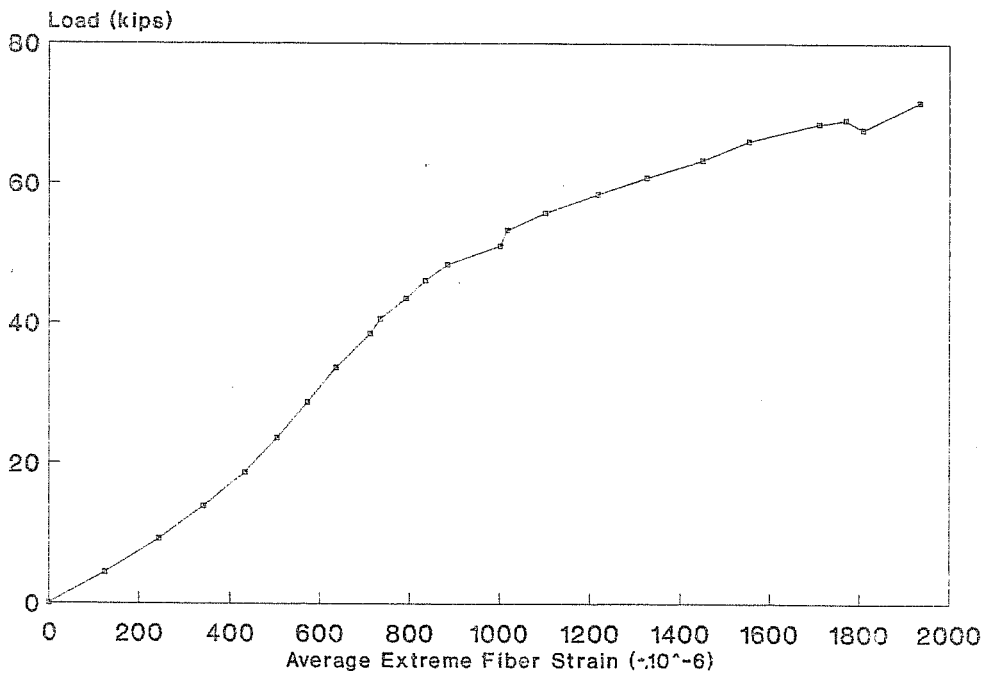


Figure D4: FA 550-2 Test A

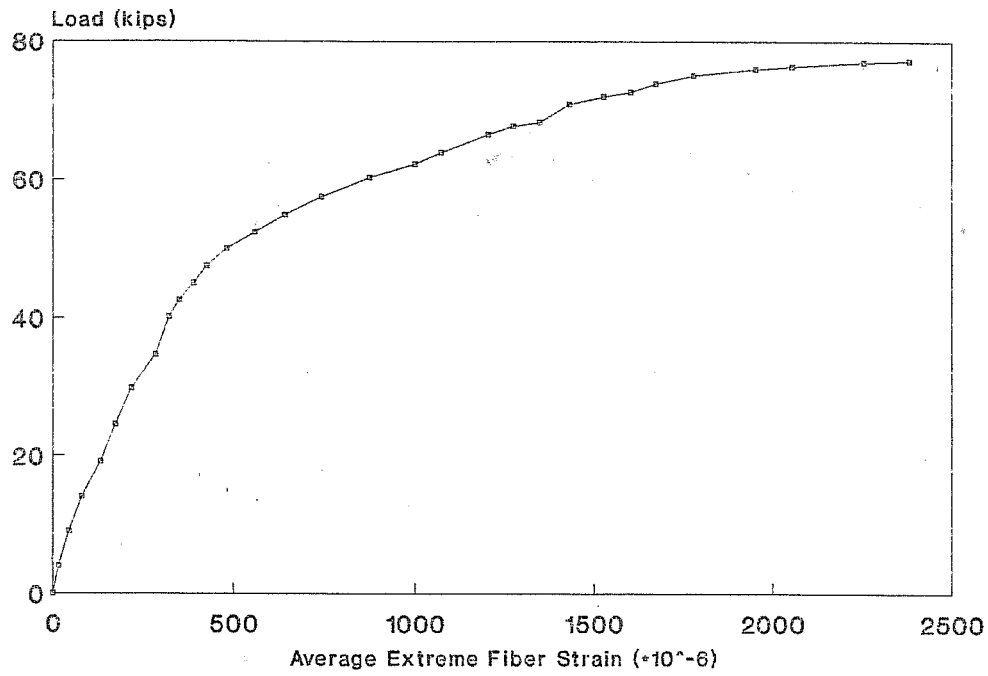


Figure D5: FA 550-2 Test B

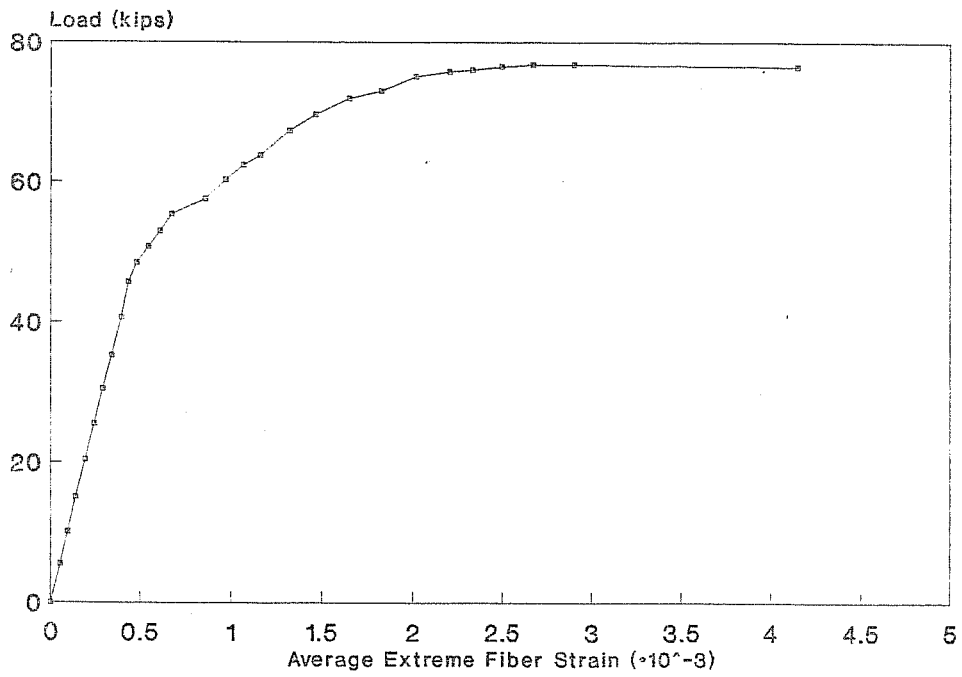


Figure D6: FA 550-3 Test A

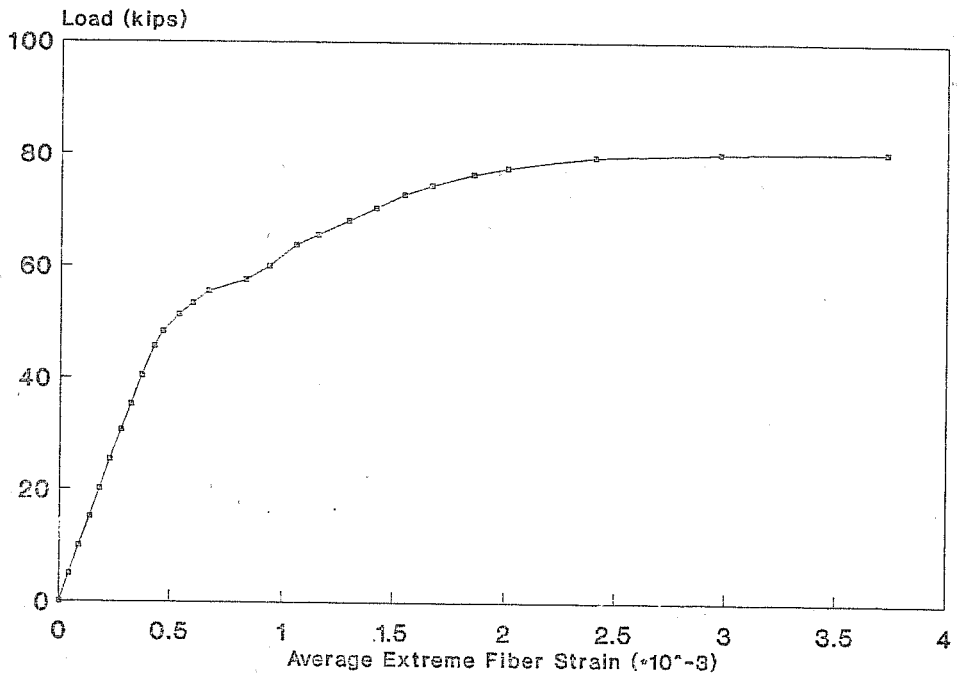


Figure D7: FA 550-3 Test B

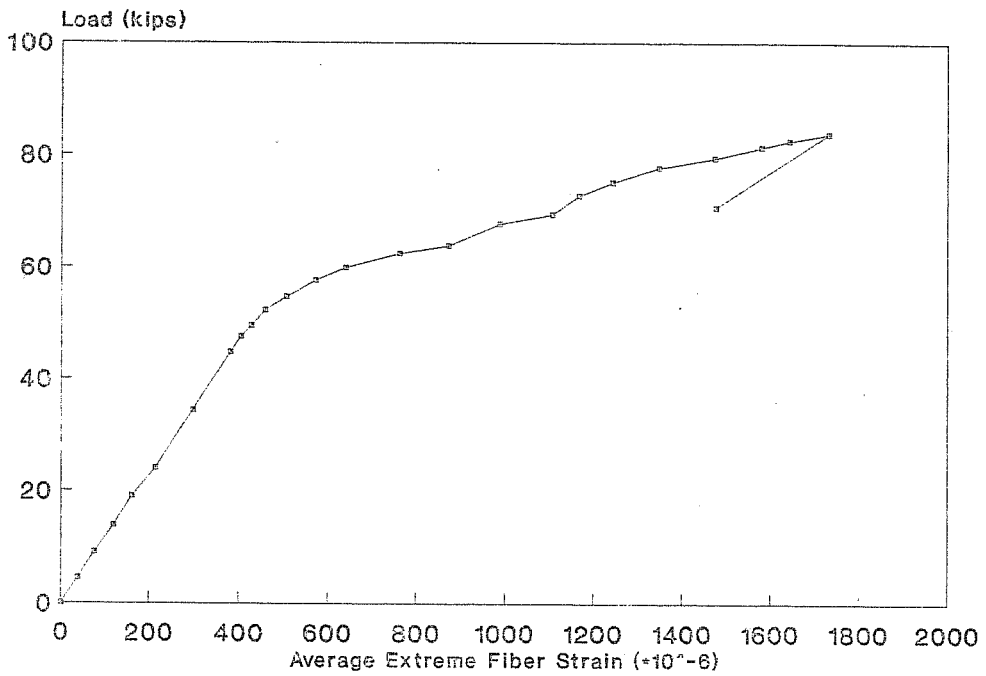


Figure D8: FA 550-4 Test A

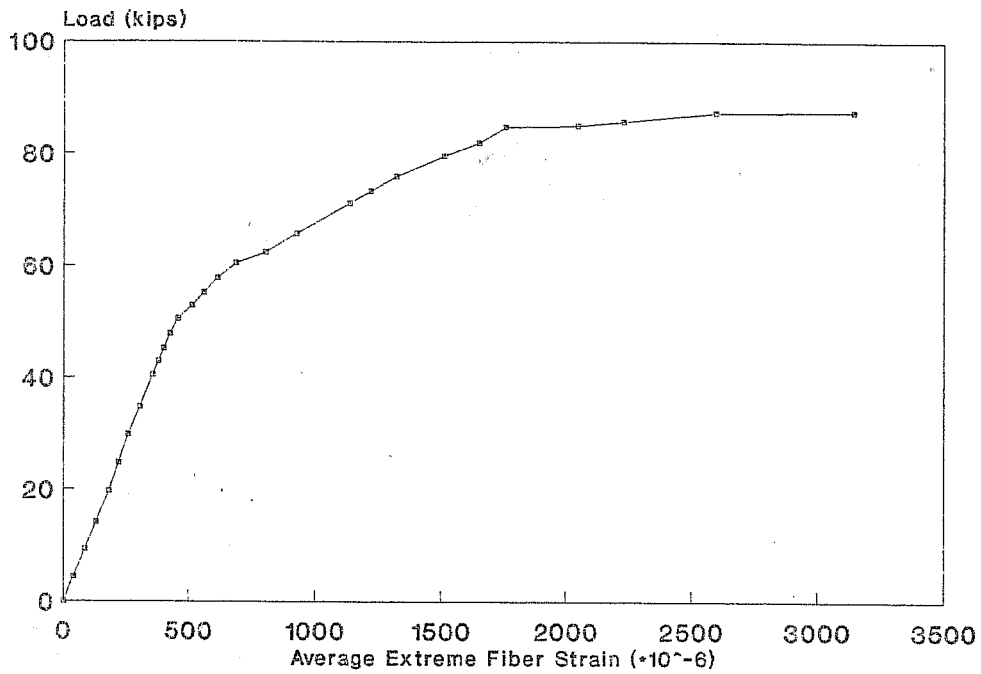


Figure D9: FA 550-4 Test B

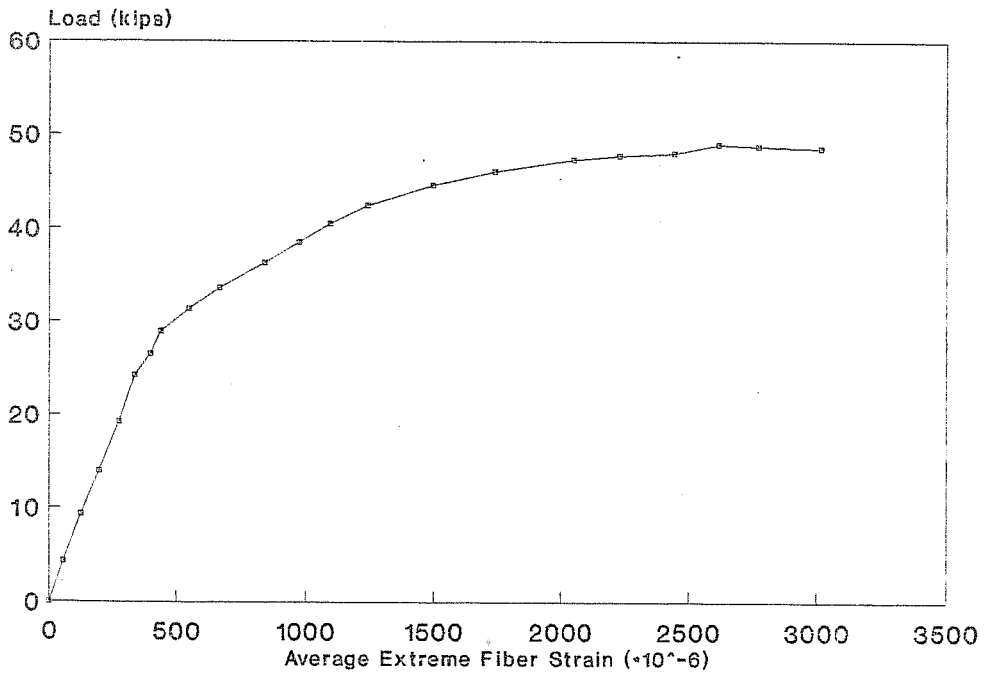


Figure D10: FA 460-1 Test A

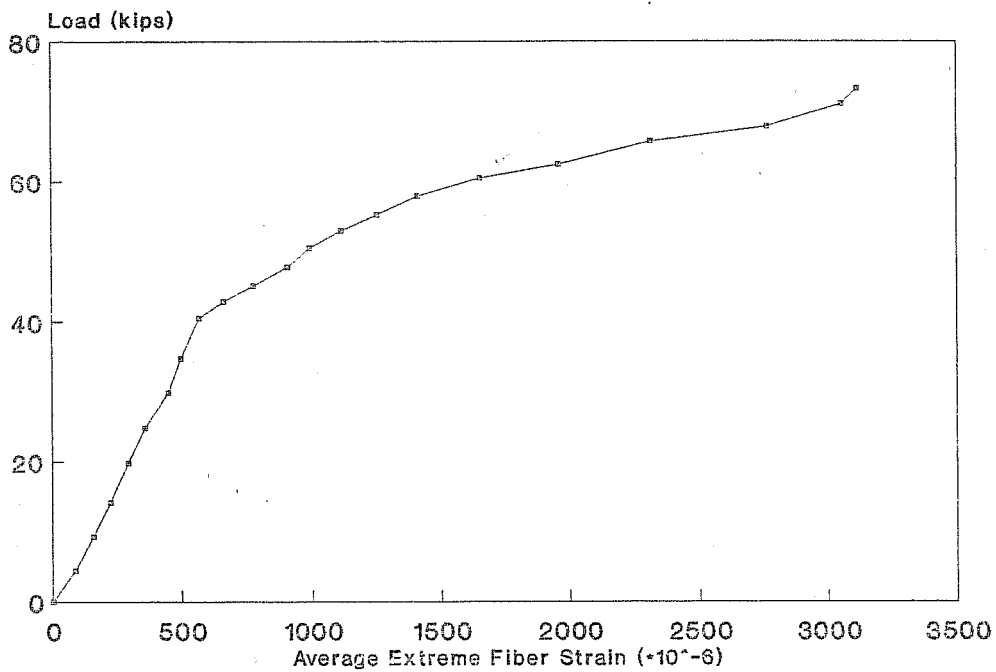


Figure D11: FA 460-1 Test B

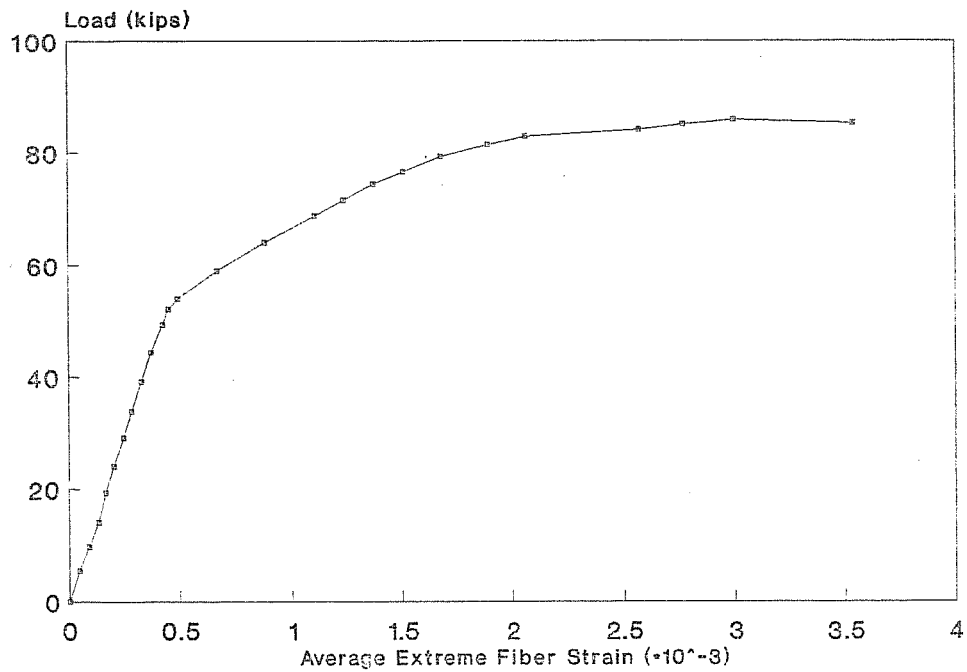


Figure D12: FA 460-2 Test A

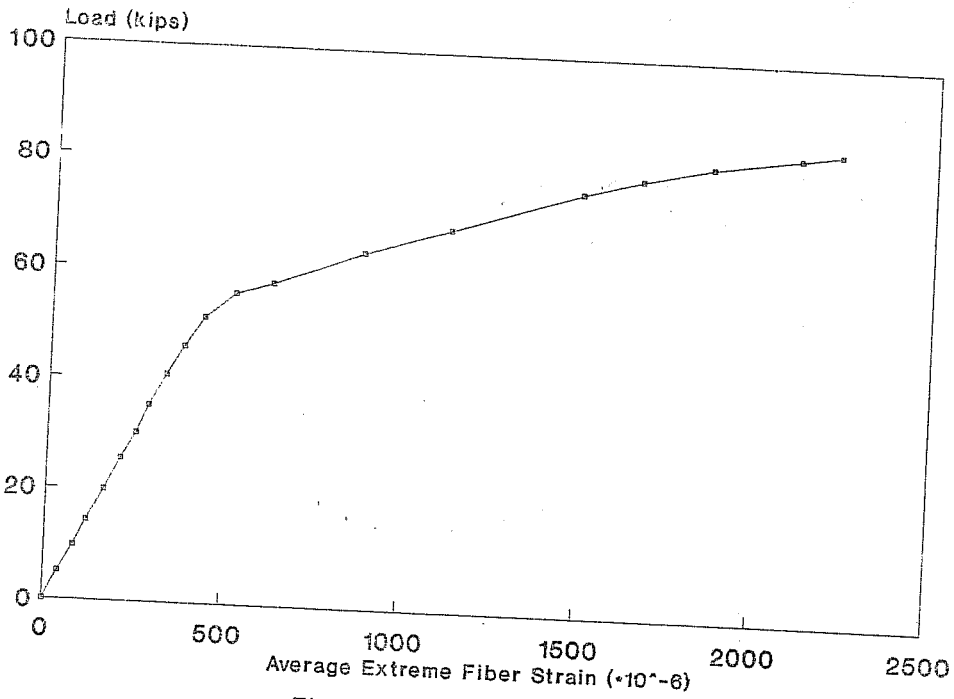


Figure D13: FA 460-2 Test B

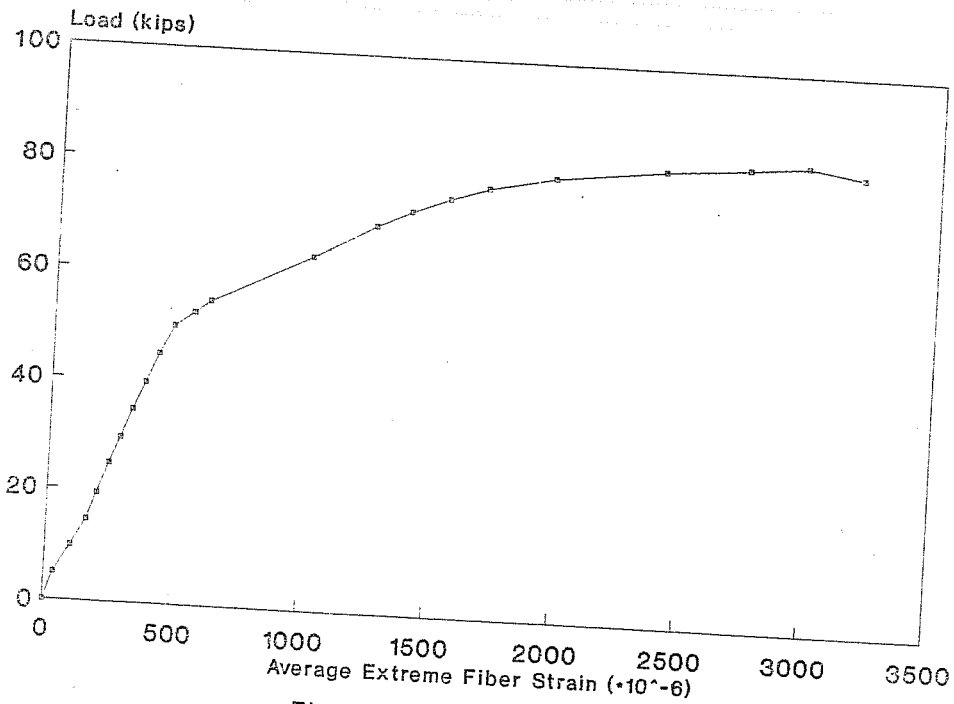


Figure D14: FA 460-3 Test A

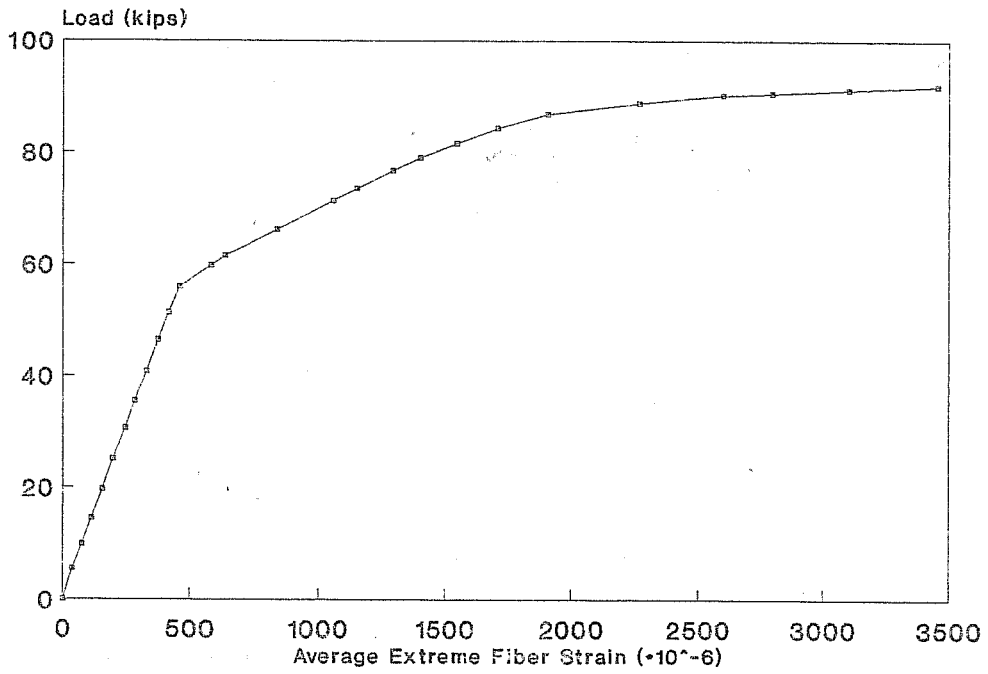


Figure D15: FA 460-3 Test B

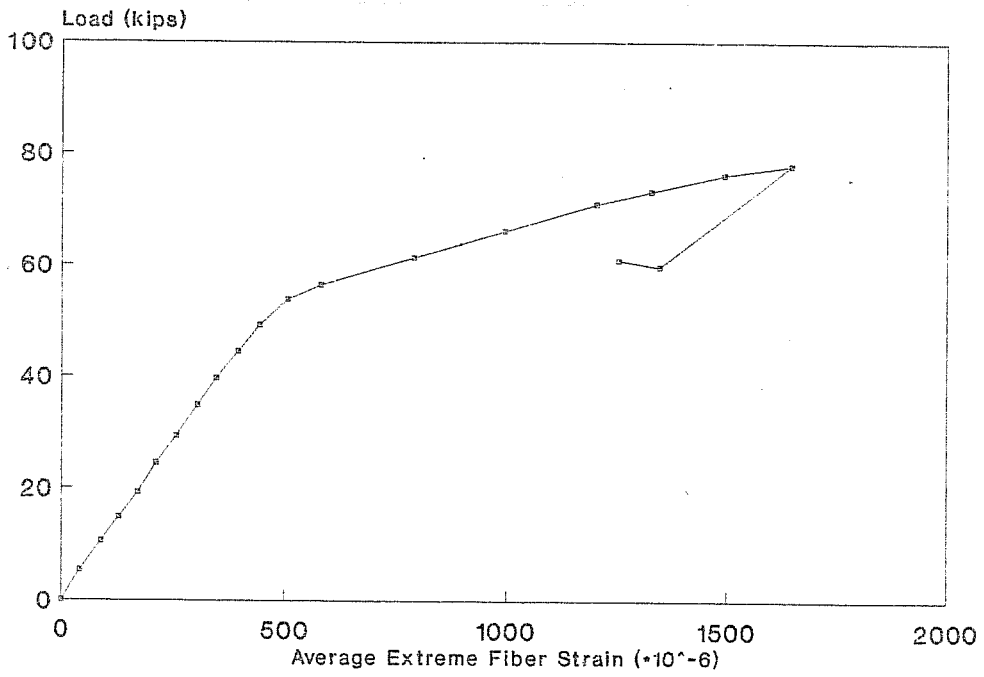


Figure D16: FA 460-5 Test A

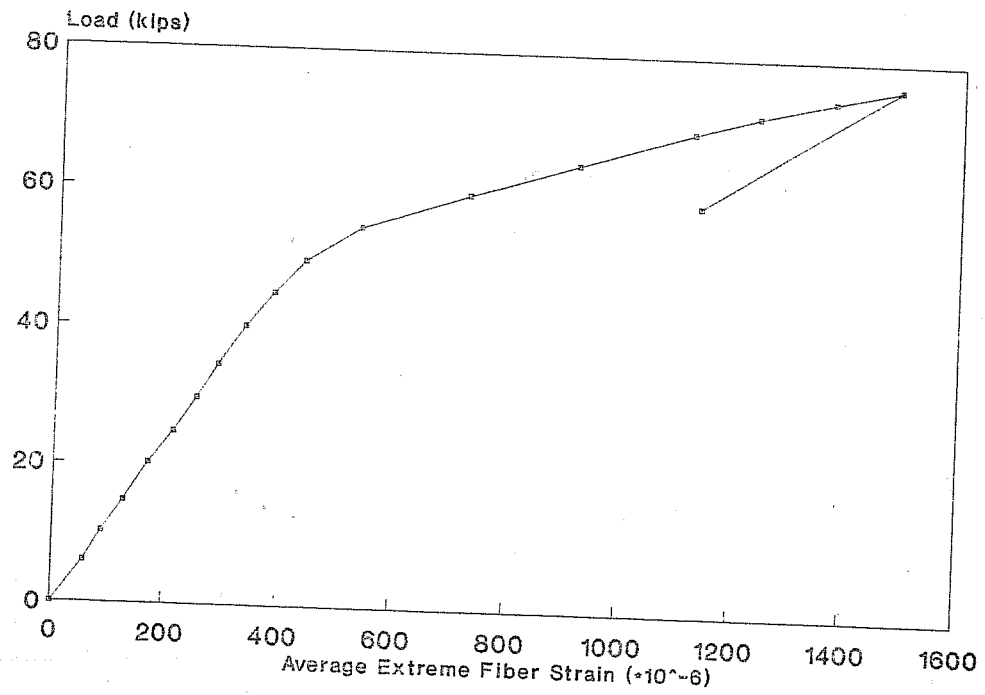


Figure D17: FA 460-5 Test B

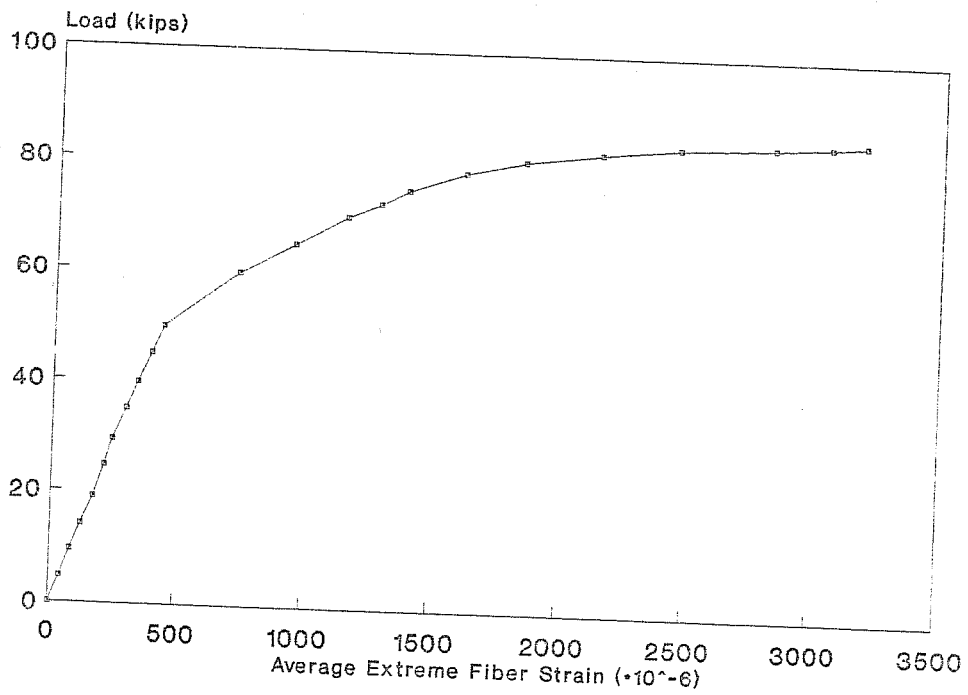


Figure D18: FA 460-6 Test A

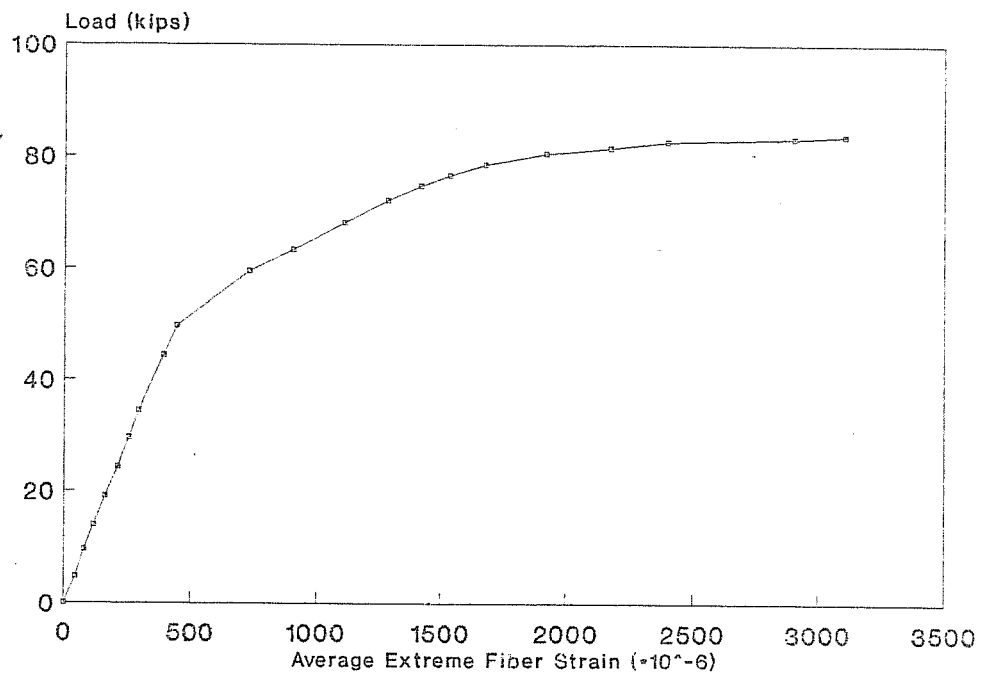


Figure D19: FA 460-6 Test B

APPENDIX E

MOMENT vs. CURVATURE RELATIONSHIPS

A moment vs. curvature relationship was derived for the $\frac{1}{2}$ inch and 0.6 inch specimens, based on strain compatibility. The moment vs. curvature plots are presented herein. The predicted load vs. deflection curves were calculated based on the moment vs. curvature graphs contained in this appendix.

Since all of the data points past cracking were calculated on a spreadsheet, the hand calculations are not presented. The following considerations were used for the strain compatibility:

- 1) $f'_c = 6000$ psi
- 2) The stress-strain curves provided in Appendix A were used for the prestressing strand.
- 3) The stress-strain curve for the concrete used the Secant Modulus approach:

$$\epsilon_o^2 - 4(\epsilon_{50} * \epsilon_o) + 2\epsilon_{50}^2 = 0$$

Solving for ϵ_o , the remaining calculated points were found using trial and error. A position for the neutral axis was assumed for a given concrete strain. The compressive concrete load was then found using:

$$C_c = bc^2(f'_c)(\Phi/\epsilon_o)[1-(\Phi c)/(3\epsilon_o)]$$

The tensile load in the steel was checked next. If the tensile load (T) did not equal the compressive load (C_c), a new position for the neutral axis was assumed. The trial and error procedure continued until $T=C_c$, and the corresponding moment was calculated. This procedure was repeated for all points past cracking. The ultimate moment corresponds to $\epsilon_c = 0.003$ in/in. The calculated

data points are also included on the respective moment vs. curvature graph.

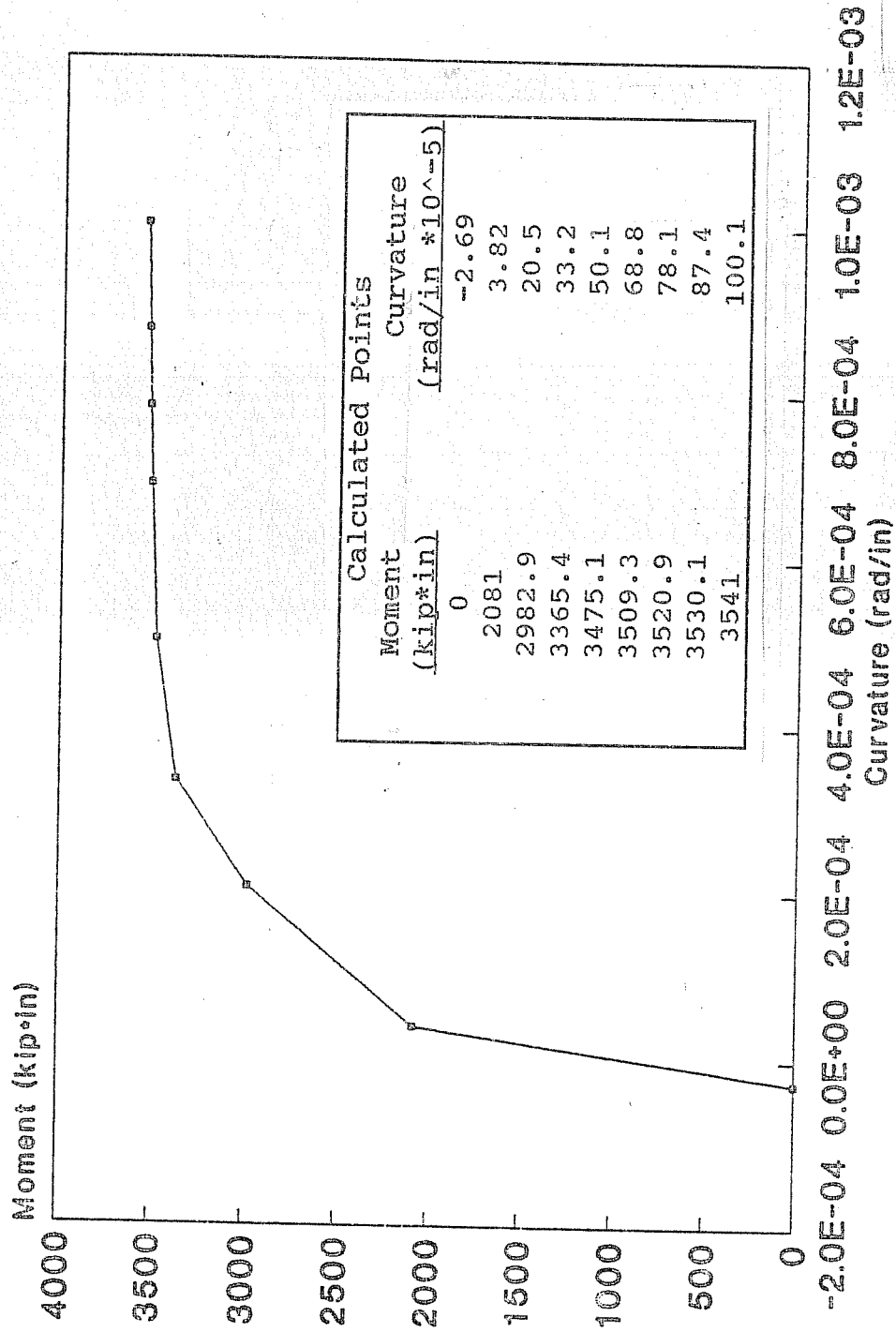


Figure E1: 0.5 inch strand

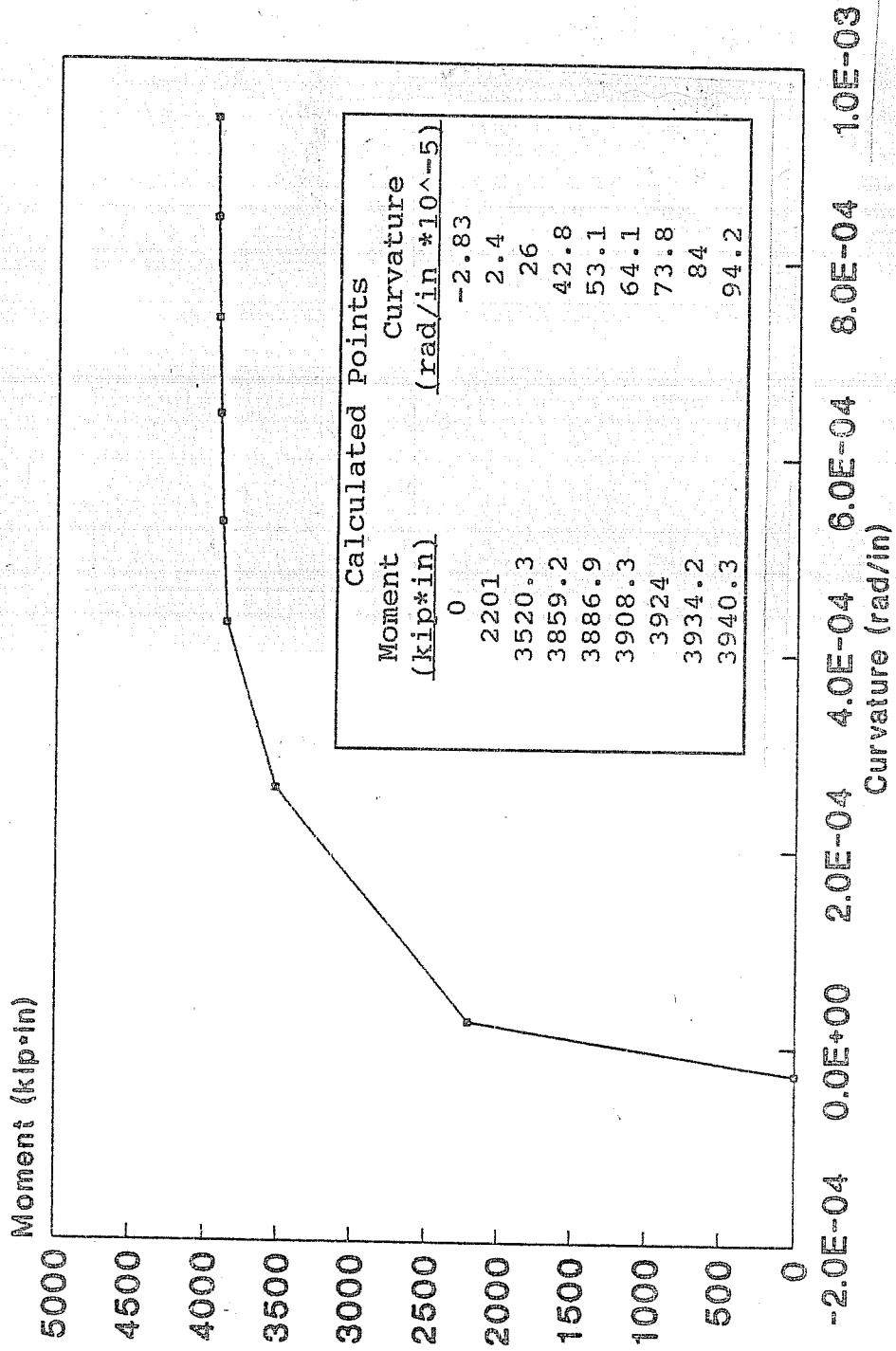


Figure E2: 0.6 inch strand

APPENDIX G

NOTATION

This appendix contains an explanation of the symbols used in this thesis.

ksi	---	kilopounds per square inch
psi	---	pounds per square inch
d_b	---	strand diameter (inches)
f_{pu}	---	ultimate tensile breaking stress of a strand
f_{ps}	---	stress in strands at nominal strength
f_{se}	---	effective stress in strands after prestress losses
f_{ci}	---	concrete strength at transfer of prestress
L_d	---	development length (defined in Sections 4.2.1 and 5.1)
M_{cr}	---	moment at cracking
M_{ult}	---	moment at ultimate load
M_{calc}	---	ultimate moment predicted by strain compatibility
f'_c	---	28 day concrete strength
L_t	---	transfer length
L_{flex}	---	flexural bond length
ϵ_{50}	---	concrete strain corresponding to 50% of 28 day concrete strength (f'_c)
ϵ_o	---	concrete strain corresponding to 28 day concrete strength (f'_c)
Φ	---	curvature
c	---	position of neutral axis (measured from top of section - inches)
b	---	width of top flange (inches)

APPENDIX F

TEST OBSERVATIONS

Important observations from all nineteen (19) tests are presented in this appendix. Detailed information about the test dimensions can be found in Figure 3.13 and Table 3.3. The results are also summarized in Tables 4.1-4.3 and Figures 4.1 and 4.2.

FA550-1A:

- First Flex. Crack @ 38 kips
- Unloaded @ 52 kips to replace leaking fitting
- Reload follows previous P-Delta
- Ultimate @ 61 kips - crushed concrete

FA550-1B:

- ** Honeycombing under load points
 poor consolidation @ placement
- First Flex. Crack @ 50 kips
- Audible Popping and Web Shear @ 69 kips
- End Slip @ 90 kips
- Bond Failure @ 100 kips - strands rotated
 as evident by slip gages

FA550-1C:

- ** Flex. cracks from FA550-1A under load points
- First Flex. Crack @ 40 kips
- Crushed concrete @ 75 kips
- No web shear cracking

FA550-2A:

- Web shear @ 68 kips
- Loss of hydraulic pressure @ 72 kips
- End slip/bond failure @ 62 kips
 (after pressure loss)

FA550-2B:

- First Flex. Crack @ 50 kips
- Audible popping @ 71 kips
- Web shear cracking/end slip @ 74.7 kips
- Failure followed web shear/bond slip @ 74.7 kips

FA550-3A:

- First Flex. Crack @ 51 kips
- Web shear crack @ 76.1 kips
- Flex. Failure @ 77 kips
- No end slip detected

FA 550-3B:

- First Flex. Crack @ 51 kips
- Audible popping @ 74.5 kips
- Flex. Failure @ 81 kips
- No end slip detected
- Reloaded - attained Mult again

FA550-4A:

- First Flex. Crack @ 54.6 kips
- Audible popping @ 60.4 kips
- Web shear cracking/end slip @ 69.4 kips
- Bond Failure @ 83.8 kips
- Max. Slip = 0.22 inches on bottom strands

FA550-4B:

- First Flex. Crack @ 50.5 kips
- Web shear cracking @ 78.4 kips
- End slip @ 81.9 kips (0.01 inches)
- Crushed concrete @ 83.9 kips
- Flex./Bond Failure

FA460-1A:

- First Flex. Crack @ 31.3 kips
- Flex failure @ 48.8 kips - crushed concrete
- No web shear
- No end slip

FA460-1B:

- First Flex. Crack @ 41.5 kips
- Flex failure @ 66.8 kips - crushed concrete
- No web shear
- No end slip

FA460-2A:

- First Flex. Crack @ 53.8 kips
- Web shear cracking/end slip @ 81.5 kips
- Crushed concrete @ 86.4 kips
- Flex./Bond failure - slip and crushing

FA460-2B:

- ** Inadequate Shear reinf. - originally designed for longer embedment length
- First Flex. Crack @ 55.7 kips
- Web shear cracking/end slip @ 78.5 kips
- Sudden failure @ 78.5 kips

FA460-3A:

- First Flex. Crack @ 52.4 kips
- Flex failure @ 83.7 kips - crushed concrete
- No web shear
- No end slip
- Reloaded - attained Mult again

FA460-3B:

- First Flex. Crack @ 59.7 kips
- Flex failure @ 92 kips - crushed concrete
- No web shear
- No end slip
- Reloaded - attained Mult again

FA460-5A:

- First Flex. Crack @ 56.5 kips
- Web shear cracking/end slip @ 76.3 kips
- Ult. @ 78.01 kips
- Bond failure @ 72.7 kips (loss of load from ult.)
- Web Shear cracks propagated towards load pts. as more load applied after ult.

FA460-5B:

- First Flex. Crack @ 54.6 kips
- Web shear cracking/end slip @ 74.3 kips
- Bond failure @ 58.6 kips (ult. load @ 76.3 kips)

FA460-6A:

- First Flex. Crack @ 54.3 kips
- End slip @ 82.6 kips
- Flex. Failure @ 84.2 kips - crushed concrete

FA460-6B:

- First Flex. Crack @ 54.3 kips
- Web shear cracking/end slip @ 80.6 kips
loss of load @ crack formation to 79.1 kips
- Crushing of concrete @ 83.8 kips
- Flex. failure @ 75.8 kips

BIBLIOGRAPHY

1. "Building Codes Requirements for Reinforced Concrete,"(1983). ACI 318-83, American Concrete Institute, Detroit, MI.
2. Burdette, Edwin G., and Deatherage, J.H. (1990). "Development Length And Lateral Spacing Requirements Of Prestressing Strand For Prestressed Concrete Bridge Products," The University of Tennessee at Knoxville.
3. Clark, C.R., and Johnston, D.W. (1983). "Early Loading Effects on Bond Strength," Journal of American Concrete Institute, 80(6), 532-539.
4. Cousins, T., Johnston, D., and Zia, P. (1986). "Bond of Epoxy Coated Prestressing Strand," Department of Civil Engineering, North Carolina State University at Raleigh.
5. Ghosh, D.K., and Fintel, M. (1986). "Development Length of Prestressing Strand, Including Debonded Strands, and Allowable Concrete Stresses in Pretensioned Members," Journal of Prestressed Concrete Institute, 31(5),38-57.
6. Hanson, N.W., and Kaar, P.H. (1959). "Flexural Bond Tests of Pretensioned Prestressed Beams," Journal of American Concrete Institute, 55(7), 783-803.
7. Janney, J.R. (1954). "Nature of Bond in Pre-Tensioned, Prestressed Concrete," Journal of American Concrete Institute, 50, 717_736.
8. Kaar, P.H., LaFraugh, R.W., and Mass, M.A. (1963). "Influence of Concrete Strength on Strand Transfer Length," Journal of Prestressed Concrete Institute, 8(5), 47-67.

9. Kaar, P.H., and Magura, D.D. (1965). "Effects of Strand Blanketing on Performance of Pretensioned Girders," *Journal of Prestressed Concrete Institute*, 10(6), 20-34.
10. Lin, T.Y., and Burns, N.H. (1981). *Design of Prestressed Concrete Structures*, John Wiley and Sons.
11. Malik, Raheel (1990). "Measurement Of Transfer Length Of 0.5 Inch and 0.6 Inch Diameter Prestressing Strand In Single Strand Specimens," Department of Civil Engineering, The University of Texas at Austin.
12. Martin, L.D., and Scott, N.L. (1976). "Development of Prestressing Strand in Pretensioned Members," *Journal of American Concrete Institute*, 73(8), 453-456.
13. "PCI Design Handbook," (1985). *Prestressed Concrete Institute*, Chicago, Illinois.
14. "Standard Specifications for Highway Bridges: (1983a). *American Association of State Highway Transportation Officials*, Washington, DC.
15. Unay, Ihsan Ozgür (1991). "Measurement of Transfer Length of Prestressing Strands in Prestressed Concrete Specimens," Department of Civil Engineering, The University of Texas at Austin.
16. Zia, P., and Mostafa, T. (1977). "Development Length of Prestressing Strands," *Journal of American Concrete Institute*, 22(5), 54-65.

VITA

Bruce A. Lutz was born in Skokie, IL on May 28, 1967, the son of Marshall G. Lutz. He attended high school at New Trier Township, in Winnetka, IL, and graduated in 1985. From 1985 to 1989, he attended The University of Kansas at Lawrence. In 1989 he graduated from the University of Kansas with a Bachelor's of Science in Civil Engineering. In August 1989, he entered the Graduate School at The University of Texas at Austin.

Permanent Address: 994 Coventry Lane
Highland Park, IL 60035

This thesis was typed by Bruce A. Lutz